SCHWARZ METHODS FOR FOURTH-ORDER PROBLEMS CONTAINING SINGULARITIES

by

Birce Palta

A dissertation submitted to the faculty of
The University of North Carolina at Charlotte
in partial fulfillment of the requirements
for the degree of Doctor of Philosophy in
Applied Mathematics

Charlotte

2019

Approved by:

_____
Dr. Hae-Soo Oh

_____
Dr. Joel Avrin

_____
Dr. Shaozhong Deng

_____
Dr. Ronald E. Smelser

ABSTRACT

BIRCE PALTA. Schwarz methods for fourth-order problems containing singularities. (Under the direction of DR. HAE-SOO OH)

We develop numerical methods for analysis of fourth-order partial differential equations on domains with angular corners. For the finite element analysis of fourth-order partial differential equations, we have to use smoother basis functions whose derivatives are continuous. Since the derivatives of Lagrange basis functions for the conventional finite element method are not contiuous, the complex Hermite basis functions are suggested. However, those existing exotic elements of Hermite type are complicate in construction and implementation. Whereas the approximation space for Isogeometric Analysis (IGA), developed recently, consists of B-spline basis functions with any desired regularity. However, IGA using single patch encounters difficulties in dealing with boundary value problems on irregular shaped polygonal domains. In this paper, in order to handle fourth-order problems with singularities, we introduce an Implicitly Enriched Galerkin method in which singular basis functions resembling the known point singularities are generated through a special geometric mapping and are combined with smooth basis functions through flat-top partition of unity (PU) functions. Unlike XFEM, this approach does not have singular integral problems. For the cases where multi-patches are necessary because of complex geometry of the problems, it is difficult to join two patches along their interface in IGA. To end this, we combine the Implicitly Enriched Galerkin method with Schwarz domain decomposition methods. Thanks to Schwarz methods, we are able to break down the problems

to smaller subproblems and are able to use different numerical techniques to solve each subproblem for localized treatment of complex geometries and singularities.

Our aim in this research is to develop effective numerical methods with less computational cost for the analysis of fourth-order problems on domains containing singularities. For this reason, we modify our method by applying different techniques such as Multicolor Schwarz and Supplemental Subdomain methods to reduce number of iterations for efficiency. Various numerical examples show the efficiency of our proposed method in dealing with fourth-order singular problems with crack singularities and/ or corner singularities.

ACKNOWLEDGMENTS

I am deeply indebted to my advisor, Dr. Hae- Soo Oh, for his expertise, assistance, guidance, and patience throughout my research period. I would also like to thank my dissertation committee members, Drs. Shaozhong Deng, Joel Avrin, and Ronald E. Smelser for their valuable contributions and comments on my dissertation. I also acknowledge all the faculty members who contributed to my doctoral study in our Mathematics and Statistics Department.

My deepest gratitude goes to my beloved husband, Emre, my son, Gokturk, and of course my daughter, who will be with us soon, for being in my life and giving me strength under any circumstances. I also would like to thank my family members, in particular, my sister and mother-in-law for their moral support and encourage.

TABLE OF CONTENTS

LIST OF FIGURES

LIST OF TABLES

CHAPTER 1: INTRODUCTION

1.1 Background

For numerical solutions of fourth-order partial differential equations (PDEs), it is necessary to construct $\mathcal{C}^1$-continuous basis functions due to the requirement of square integrable second derivatives of the basis functions in the variational formulation. In conventional Finite Element Analysis (FEA), Hermitian elements such as the Argyris triangle, the Bell's triangle, the Bogner-Fox-Schmit rectangle, and so on [**?**, 7] are suggested; however, their implementations and constructions are complicated. Isogeometric Analysis (IGA), introduced by Hughes, et al. [17], is a recently developed computational approach that aims to close the existing gap between Computed Aided Design (CAD) and FEA. Since IGA allows us to construct smooth B-spline basis functions with any order of regularity, it provides advantages in the numerical approximation of high order PDEs within the framework of the standard Galerkin formulation.

The Implicitly Enriched Galerkin method was introduced in [19] to have highly accurate solutions of fourth-order elliptic differential equations containing singularities in the framework of IGA. Singular functions in the physical domain that resemble the singularities are generated through a specially designed geometric mapping defined on the reference domain.

However, it is difficult to obtain a global mapping from the reference domain onto a non-convex physical domain containing crack or corner singularities. Furthermore, original designs of engineering structures do not have crack singularities since cracks occur later on, so design mappings are not acceptable for analysis of a cracked structures. To deal with singularities such as cracks and corners in fourth-order equations in the framework of IGA, adaptive refinements such as T-splines, and explicit enrichment methods are suggested in literature [2], [9], and [10]. However, these approaches are highly complex in implementing or are limited by high computational cost, elevated condition numbers, large degrees of freedom, and integration of singular enrichment functions. To alleviate these difficulties, we proposed Implicitly Enriched Schwarz methods. Combining the Implicitly Enriched Galerkin method with the domain decomposition method is a proper approach since the given physical domain is partitioned into several patches. By decomposing the physical domain so that each patch contains no more than one point singularity, one can construct a singular geometric mapping from the reference domain onto the patch containing a singularity that generate singular basis function resembling singular functions. Therefore, domain decomposition method allows a local treatment, which reduces computational complexity.

1.2 Problem Statement

Model Problem and its variational equation:

As a model problem, we consider the following fourth-order equation with non-

homogeneous clamped boundary conditions:

$$\begin{cases} \Delta^2 u &= f \; in \;\; \Omega \\ u &= g_1(x,y) \;\; on \;\; \partial\Omega \\ \nabla u \cdot \mathbf{n} &= g_2(x,y) \;\; on \;\; \partial\Omega \end{cases} \tag{1}$$

where $f \in L^2(\Omega)$, Δ stands for the Laplacian operator and n denotes the outward unit vector normal to the boundary. Let $u, v \in H^2(\Omega)$, then from Green's theorem, we have

$$\int_\Omega \Delta u \Delta v - \int_{\partial\Omega} \frac{\partial v}{\partial n} \Delta u + \int_{\partial\Omega} \frac{\partial \Delta u}{\partial n} v = \int_\Omega f v. \tag{2}$$

$$\begin{aligned} \mathcal{W} &= \{w \in H^2(\Omega) : w|_{\partial\Omega} = g_1, \nabla w \cdot \mathbf{n}|_{\partial\Omega} = g_2\}, \\ \mathcal{V} &= \{w \in H^2(\Omega) : w|_{\partial\Omega} = \nabla w \cdot \mathbf{n}|_{\partial\Omega} = 0\}. \end{aligned}$$

The variational formulation of (1) can be written as: Find $u \in \mathcal{W}$ such that

$$\mathcal{B}(u, v) = \mathcal{F}(v), \text{ for all } v \in \mathcal{V}, \tag{3}$$

where

$$\mathcal{B}(u, v) = \int_\Omega \Delta u \Delta v \text{ and } \mathcal{F}(v) = \int_\Omega f v$$

Weak solution in Sobolev space and the Galerkin Method:

Let Ω be a connected open subset of $\mathbb{R}^d$. We define the vector space $\mathcal{C}^m(\Omega)$ to consist of all those functions ϕ which, together with all their partial derivatives $\partial^\alpha \phi (= \partial_1^{\alpha_1} \cdots \partial_d^{\alpha_d} \phi)$ of orders $|\alpha| = \alpha_1 + \cdots + \alpha_d \leq m$, are continuous on Ω. A function

$\phi \in \mathcal{C}^m(\Omega)$ is said to be a $\mathcal{C}^m$-continuous function. If Ψ is a function defined on Ω, we define the **support** of Ψ as.

$$\text{supp } \Psi = \overline{\{x \in \Omega | \Psi(x) \neq 0\}}.$$

For an integer $k \geq 0$, we also use the usual Sobolev space denoted by $H^k(\Omega)$. For $u \in H^k(\Omega)$, the norm and the semi-norm, respectively, are

$$\|u\|_{k,\Omega} = \left(\sum_{|\alpha| \leq k} \int_\Omega |\partial^\alpha u|^2 dx \right)^{1/2}, \quad \|u\|_{k,\infty,\Omega} = \max_{|\alpha| \leq k} \left\{ \text{ess.sup} |\partial^\alpha u(x)| : x \in \Omega \right\};$$

$$|u|_{k,\Omega} = \left(\sum_{|\alpha| = k} \int_\Omega |\partial^\alpha u|^2 dx \right)^{1/2}, \quad |u|_{k,\infty,\Omega} = \max_{|\alpha| = k} \left\{ \text{ess.sup} |\partial^\alpha u(x)| : x \in \Omega \right\}.$$

The variational formulation of the boundary value problem (1) can be written as: Find $u \in \mathcal{W}$ such that

$$\mathcal{B}(u, v) = \mathcal{F}(v), \text{ for all } v \in \mathcal{V}, \tag{4}$$

Here $\mathcal{B}$ is a continuous bilinear form that is $\mathcal{V}$-elliptic [7] and $\mathcal{F}$ is a continuous linear functional. The solution to (4) is called a **weak solution** which is equivalent to the strong (classical) solution corresponding the fourth-order PDE whenever u is smooth enough. Let $\mathcal{W}^h \subset \mathcal{W}$, $\mathcal{V}^h \subset \mathcal{V}$ be finite dimensional subspaces. Since B-spline basis functions do not satisfy the Kronecker delta property, in this paper we approximate the non-homogenuous clamped boundary condition by the least squares method as follows: $g_1^h, g_2^h \in \mathcal{W}^h$ such that

$$\int_{\partial\Omega} |g_1 - g_1^h|^2 d\gamma \text{ and } \int_{\partial\Omega} |g_2 - g_2^h|^2 d\gamma$$

become minimum. We can write the Galerkin approximation method (a discrete

variational equation) of (1) as follows: Given g_1^h, g_2^h, find $u^h = w^h + g_1^h + g_2^h$, where $w^h \in \mathcal{V}^h$, such that

$$\mathcal{B}(u^h, v^h) = \mathcal{F}(v^h), \text{ for all } v^h \in \mathcal{V}^h,$$

which can be rewritten as: Find the trial function $w^h \in \mathcal{V}^h$ such that

$$\mathcal{B}(w^h, v^h) = \mathcal{F}(v^h) - \mathcal{B}(g_1^h + g_2^h, v^h), \text{ for all test functions } v^h \in \mathcal{V}^h. \tag{5}$$

The energy norm of the trial function u is defined by

$$\|u\|_{\text{Eng}} = \left[\frac{1}{2}\mathcal{B}(u,u)\right]^{1/2}.$$

The relative error in the energy norm in percentage is

$$\|u - U\|^2_{Eng,rel}(\%) = \left|\frac{\|u\|^2_{Eng} - \|U\|^2_{Eng}}{\|u\|^2_{Eng}}\right| \times 100 \tag{6}$$

The relative error in the maximum norm in percentage is

$$\|u - U\|_{\infty,rel}(\%) = \frac{\|u - U\|_\infty}{\|u\|_\infty} \times 100. \tag{7}$$

1.3 Outline of Dissertation

The dissertation is divided into six chapters. After this introduction and problem formulation, this dissertation is organized as follows: in Chapter 2, we review definitions and terminologies that are needed to understand this paper. We give a brief review of B-splines, refinement methods, and constructions of smooth flat-top PU functions. Borden [4], Cottrell [8], Rogers [32], Piegl and Tiller [30] are suggested for detailed information.

In Chapter 3, the basic Schwarz Alternating and Additive (Parallel) Schwarz meth-

ods are discussed in detail. In Chapter 3.2, we present Implicitly Enriched Galerkin method and pullback of the bilinear form for fourth-order problems onto the reference domain. In Chapter 3.3, we explain modification of the basis functions with assigning homogeneous and non-homogeneous boundary conditions. In Chapter 3.4, we present how overlapping size between subdomains affects the convergence rate.

In Chapter 4, several non-singular numerical problems that demonstrate the accuracy and efficiency of the proposed method are presented. In Chapter 4.1, we test our method to one dimensional fourth-order problems with polynomial true solution and exponential true solution with different overlapping sizes. Thereafter, in Chapter 4.2, we extend testing our method to two dimensional fourth-order problem in a rectangular domain with vertical interface, and we compare convergence rate for different overlapping sizes. In Chapter 4.3, we solve two dimensional fourth-order problem in a rectangular domain with slanted interface by using both Schwarz Alternating method and the Schwarz Additive (Parallel) methods to compare the number of iterations required for the expected accuracy for each method. In Chapter 4.4, we also test our method for two dimensional fourth-order problem in a triangular domain divided into three overlapping quadrilateral subdomains.

In Chapter 5, Implicitly Enriched Schwarz method is applied to fourth-order problems containing singularities. In Chapter 5.1, we first test our method in one dimensional problem with monotone singularity. In Chapter 5.2, we solve two dimensional fourth-order problem in a circular domain with crack singularity. In Chapters 5.3 and 5.4, we extend our method to two dimensional problems in a cracked rectangular domain and L-shaped domain, respectively. These problems require more subdivision

as well as more computational time. To reduce the computational complexity, we solve these problems by using three different techniques named Implicitly Enriched Schwarz methods (IESM), IESM with increased overlapping parts of subdomains, and Supplemental Subdomain method. The techniques are compared to each other in terms of the total number of iterations for the desired accuracy of the approximate solution.

Finally, we state the concluding remarks and future work in Chapter 6 of this dissertation.

CHAPTER 2: PRELIMINARIES

2.1 Isogeometric Analysis

Engineers use Computer Aided Design (CAD) software for designing systems. The main aim of CAD software is to produce accurate visual representation of physical objects. For analysis of a practical problem, it is necessary to convert software data into the geometry which is suitable for FEA. However, analysis-suitable models are not automatically created or readily meshed from CAD geometry, and there are many time consuming steps involved. Transfering information between CAD and numerical computation of solutions as well as processing transferred data to fit the respective requirements can be a very costly procedure in practical applications. IGA aims at breaking down the barriers between engineering design and analysis. By directly using the geometry representation from CAD, IGA integrates methods for analysis and CAD into a single, unified process.

2.1.1 Knot Vector

A *Knot vector* in one dimension is a non-decreasing set of coordinates in the parameter space, written $\Xi = \{\xi_1, \xi_2, ..., \xi_{n+p+1}\}$, where $\xi_i \in \mathbb{R}$ is the i^{th} knot, i is the knot index, $i = 1, 2, ..., n + p + 1$, p is the polynomial degree, $k = p + 1$ is the order of basis functions, and n is the number of basis functions used to construct the B-spline curve. The knot vector represents the parameterization of the curve, determining the

domain of the spline and the joins between the polynomial segments of the curve. The knots partition the parameter space into elements. They are tied to the order of the spline k, and the number of control points $n + 1$, but they also represent the parameterization of the spline curve and the parameterization of each of the polynomial segments of the spline. We can manipulate the knot vector in a number of ways. In the case of B-splines, the functions are piecewise polynomials where the different pieces join along knot lines. In this way the functions are $\mathcal{C}^{\infty}$-continuous within an element.

Knot vectors may be *uniform* if the knots are equally space in the parameter space. If they are unequally space, the knot vector is *non-uniform*. Knot values may be repeated, that is, more than one knot may take on the same value. The multiplicities of knot values have important implications for the continuity of the basis function across knots.

A knot vector is said to be *open* if its first and last knot values appear $p + 1$ times. Open knot vectors are the standard in the CAD literature. In one dimension, basis functions formed from open knot vectors are interpolatory at the ends of the parameter space.

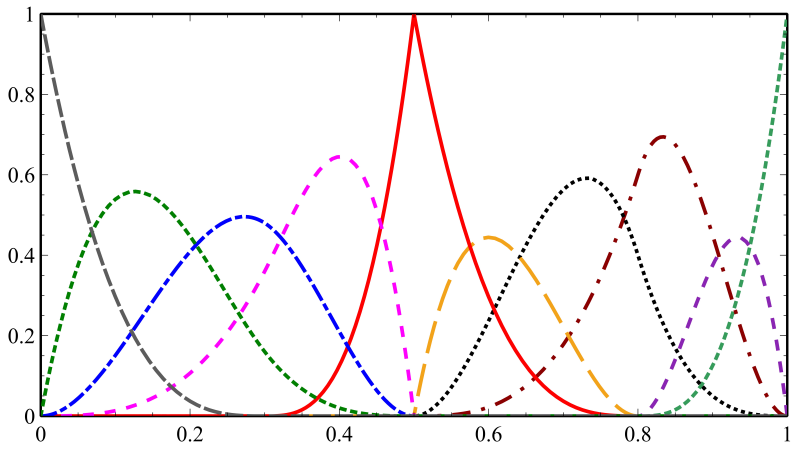

Figure 1: B-Spline functions $N_{i,4}(u)$; i = 1, 2, $\cdots$, 10 of order k = 4 for knot vector $N_{i,4}(\xi)$, $\Xi = \{0, 0, 0, 0, 0.3, 0.5, 0.5, 0.5, 0.8, 0.8, 1, 1, 1, 1\}$

2.1.2 B-splines

With a knot vector, the B-spline basis functions are defined recursively starting with piecewise constants($p = 0$):

$$N_{i,1} = \begin{cases} 1 & \text{if } \xi_i \leq \xi < \xi_{i+1} \\ 0 & \text{otherwise} \end{cases} \tag{8}$$

For $p = 1, 2, 3, ...$, they are defined by

$$N_{i,p+1}(\xi) = \frac{\xi - \xi_i}{\xi_{i+p} - \xi_i} N_{i,p}(\xi) + \frac{\xi_{i+p+1} - \xi}{\xi_{i+p+1} - \xi_{i+1}} N_{i+1,p}(\xi) \tag{9}$$

This is referred to as the *Cox-de Boor recursion formula*[Cox, 1971; de Boor, 1972]. The results of applying (8) and (9) to an open knot vector

$\Xi = \{0, 0, 0, 0, 0.3, 0.5, 0.5, 0.5, 0.8, 0.8, 1, 1, 1, 1\}$ are presented in Figure 1.

The B-spline basis functions are useful in design as well as in the Galerkin approximation for the higher-order equations since they have the following important

properties:

- $N_{i,k}(\xi)$ is non-negative for all i, k and u.
- Each polynomial $N_{i,k}(\xi)$ has local support on $[\xi_i, \xi_{i+k})$.
- On any span $[\xi_i, \xi_{i+1})$, at most $p+1$ basis functions of degree p are non-zero, i.e, $N_{i-p,k}(\xi), N_{i-p+1,k}(\xi), N_{i-p+2,k}(\xi), \cdots, N_{i,k}(\xi)$.
- The sum of all non-zero degree p basis functions on span $[\xi_i, \xi_{i+1})$ is 1.
- B-spline functions are linearly independent.
- $N_{i,k}(0) = N_{n+p,k} = 1$.
- Basis function $N_{i,k}(\xi)$ is a composite curve of degree p polynomials with joining points at knots in $[\xi_i.\xi_{i+p+1})$.
- Partition of Unity property, that is $\sum N_{i,k}(\xi) = 1$ for all $\xi \in [0, 1]$

B-spline Geometries Given n basis functions, $N_{i,p}, i = 1, 2, ..., n$ and corresponding control points $B_i \in \mathbb{R}^d, i = 1, 2, ..., n$ (vector-valued coefficients), a piecewise-polynomial *B-spline curve* is given by

$$C(\xi) = \sum_{i=1}^{n} N_{i,p}(\xi) B_i$$

Given a *control net* $B_{i,j}, i = 1, 2, ..., n, j = 1, 2, ..., m$, polynomial order p and q, and knot vectors $\Xi = \{\xi_1, \xi_2, ..., \xi_{n+p+1}\}$, and $\Im = \{\eta_1, \eta_2, ..., \eta_{m+q+1}\}$, a tensor product *B-spline surface* is defined by

$$S(\xi, \eta) = \sum_{i=1}^{n} \sum_{j=1}^{m} N_{i,p}(\xi) M_{j,q}(\eta) B_{i,j}$$

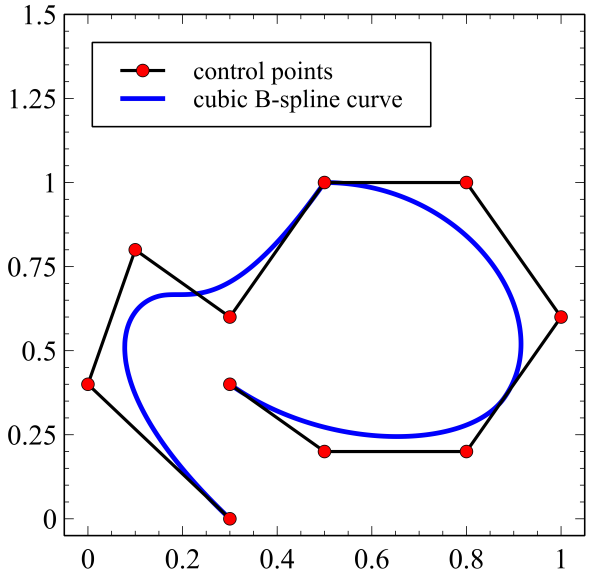

Figure 2: B-spline curve and control points

where $N_{i,p}(\xi)$ and $M_{j,q}(\eta)$ are univariate B-spline basis functions of order p and q, corresponding to knot vectors Ξ and $\aleph$, respectively.

B-spline geometries have following properties:

- *Affine covariance*, the ability to apply an affine transformation to a curve by applying it directly to the control points
- A curve will have at least as many continuous derivatives across an element boundary as its basis functions have across the corresponding knot value.
- Moving a single control point can affect the geometry of no more than $p + 1$ elements of the curve.
- B-spline curve is completely contained within the convex hull defined by its control points.

- As the polynomial order increases, the curve become smoother and the effect of each individual control point is diminished.

- B-spline curves also possess a variation diminishing property.(no variation diminishing property for surface)

2.1.3 NURBS

Non-Uniform Rational B-Splines (NURBS) are powerful extension of B-splines. They are also defined by their order, a knot vector, and a set of control points, but unlike simple B-splines, each of the control points has a weight. When the weights are equal to 1, NURBS are simply B-splines. NURBS are the standard for surface modeling in much of computer graphics and computer aided design. Non-uniform rational B-spline surfaces, which have additional degrees of freedom, are much more flexible than B-spline surfaces. NURBS can exactly reproduce the conic surfaces, whereas B-spline surfaces can only approximate them. NURBS allow modeling systems to use a single internal representation for a wide range of curves and surfaces, from straight lines and flat planes to precise circles and spheres. [32]

Define *weighting function*

$$W(\xi) = \sum_{i=1}^{n} N_{i,p}(\xi) w_i$$

where w_i is the i^{th} *weight*. NURBS basis is given by

$$R_i^p(\xi) = \frac{N_{i,p}(\xi) w_i}{W(\xi)} = \frac{N_{i,p}(\xi) w_i}{\sum_{\hat{i}=1}^{n} N_{\hat{i},p}(\xi) w_{\hat{i}}}$$

which is clearly a piecewise rational function. A NURBS curve is defined by

$$C(\xi) = \sum_{i=1}^{n} R_i^p(\xi) B_i$$

Rational surfaces and solids are defined analogously in terms of the rational basis functions

$$R_{i,j}^{p,q}(\xi,\eta) = \frac{N_{i,p}(\xi) M_{j,q}(\eta) w_{i,j}}{\sum_{\hat{i}=1}^{n} \sum_{\hat{j}=1}^{m} N_{\hat{i},p}(\xi) M_{\hat{j},q}(\eta) w_{\hat{i},\hat{j}}}$$

$$R_{i,j,k}^{p,q,r}(\xi,\eta,\zeta) = \frac{N_{i,p}(\xi) M_{j,q}(\eta) L_{k,r}(\zeta) w_{i,j,k}}{\sum_{\hat{i}=1}^{n} \sum_{\hat{j}=1}^{m} \sum_{\hat{k}=1}^{l} N_{\hat{i},p}(\xi) M_{\hat{j},q}(\eta) L_{\hat{k},r}(\zeta) w_{\hat{i},\hat{j},\hat{k}}}$$

The NURBS functions have the same properties as B-splines, and are capable of representing a wider class of geometries.

2.2 Refinements

The B-spline basis functions can be enriched by three types of refinements: knot insertion, degree elevation or degree and continuity elevation. We have control over the element size, the order of the basis, and the continuity of the basis.

2.2.1 Knot Insertion

Given a knot vector $\Xi = \{\xi_i, \xi_2, ..., \xi_{n+p+1}\}$, a new knot may be added into the existing knot vector without changing the geometry of the curve. We have an *extended* knot vector $\bar{\Xi} = \{\bar{\xi}_1 = \xi_1, \bar{\xi}_2, ..., \bar{\xi}_{n+m+p+1} = \xi_{n+p+1}\}$, such that $\Xi \subset \bar{\Xi}$ as shown in Figure 3. This new knot can be equal to an existing one and in this case the multiplicity of that knot is increased by one. The new $n + m$ basis functions are formed by applying the Cox-de Boor recursion formula and the new $n + m$ control

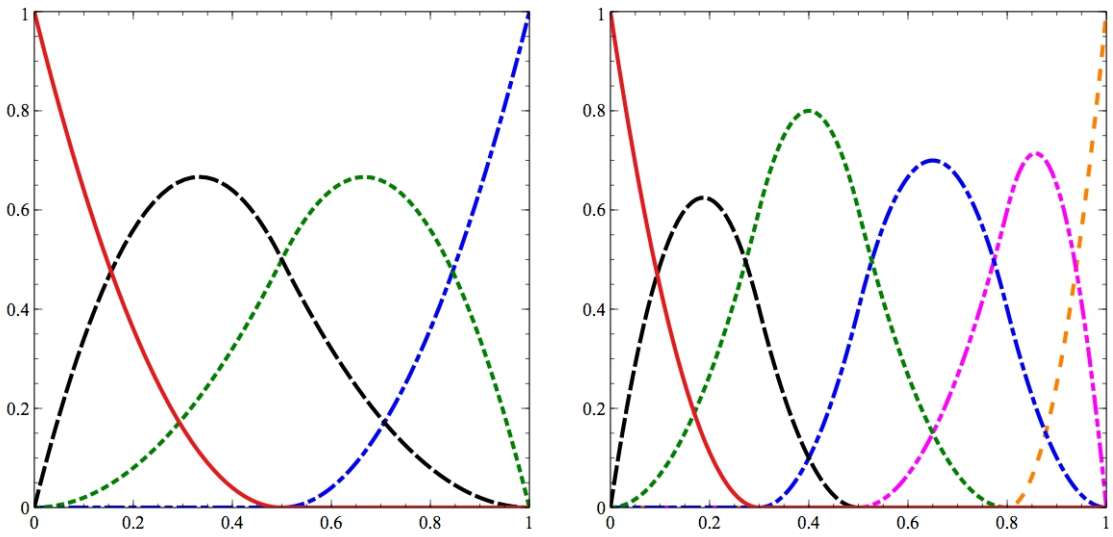

(a) (b)

Figure 3: Knot Insertion (a) Initial B-Spline basis functions $N_{i,3}(\xi)$; i = 1, $\cdots$, 4 of order k = 3 for knot vector $\Xi = \{0, 0, 0, 0.5, 1, 1, 1\}$ (b) B-Spline basis functions $N_{i,3}(\xi)$; i = 1, $\cdots$, 6 of order k = 3 after knot insertion with knot vector $\Xi = \{0, 0, 0, 0.3, 0.5, 0.8, 1, 1, 1\}$

points are formed from linear combinations of the original control points by

$$\bar{B} = T^p B$$

where

$$T_{ij}^0 = \begin{cases} 1 & \bar{\xi}_i \in [\xi_j, \xi_{j+1}) \\ 0 & \text{otherwise} \end{cases}$$

$$T_{ij}^{q+1} = \frac{\bar{\xi}_{i+q} - \xi_j}{\xi_{j+q} - \xi_j} T_{ij}^q + \frac{\xi_{j+q+1} - \bar{\xi}_{i+q}}{\xi_{j+q+1} - \xi_{j+1}} T_{ij+1}^q \qquad \text{for } q = 0, 1, 2, ..., p-1$$

This process may be repeated to enrich the solution space by adding more basis functions of the same order while leaving the curve unchanged. This results in a new spline space with more B-splines and therefore more flexibility than the original spline space. The control polygon will also have moved closer to the spline itself. By

inserting sufficiently many knots, we can make the distance between the spline and its control polygon as small as we wish, which has obvious advantages for practical computations.

Insertion of new knot values has similarities with the classical h-refinement strategy in finite element analysis [1]. However, it differs in the number of new functions and in the continuity of the basis across the newly created element boundaries. To perfectly replicate h-refinement, one would need to insert each of the new knot values p times so that the functions will be $\mathcal{C}^0$-continuous across the new boundary.

2.2.2 Degree Elevation

Degree elevation increases the degree of a curve without changing the geometry of the curve as seen in the Figure 4 . Although higher degree basis functions require longer time to process, they do have higher flexibility for designing shapes. This flexibility leads us to a new higher-order technique that is unique to isogeometric analysis. Therefore, it would be very helpful to increase the degree of a basis function without changing its shape. The basis functions of order p have $p - m_i$ continuous derivatives across knot ξ_i , where m_i is the multiplicity of the value of ξ_i in the knot vector. When p is increased, m_i must also be increased if we are to preserve the discontinuities in the various derivatives already existing in the original curve. During order elevation, the multiplicity of each knot value is increased by one, but no new knot values are added. As with knot insertion, neither the geometry nor the parameterization are changed.

Degree elevation can be used repeatedly as long as the system permits. As the

degree increases, the number of control points increases. Moreover, the shape of the curve is not changed as its degree increases, and the control polygon moves closer and closer to the curve. Eventually, as the degree keeps increasing to infinity, the control polygon approaches to the curve and has it as a limiting position.

Degree elevation clearly has much in common with the classical p-refinement strategy in finite element analysis as it increases the polynomial order of the basis. The major difference is that p-refinement always begins with a basis that is $\mathcal{C}^0$-continuous everywhere, while degree elevation is compatible with any combination of continuities that exist in the unrefined B-spline mesh.

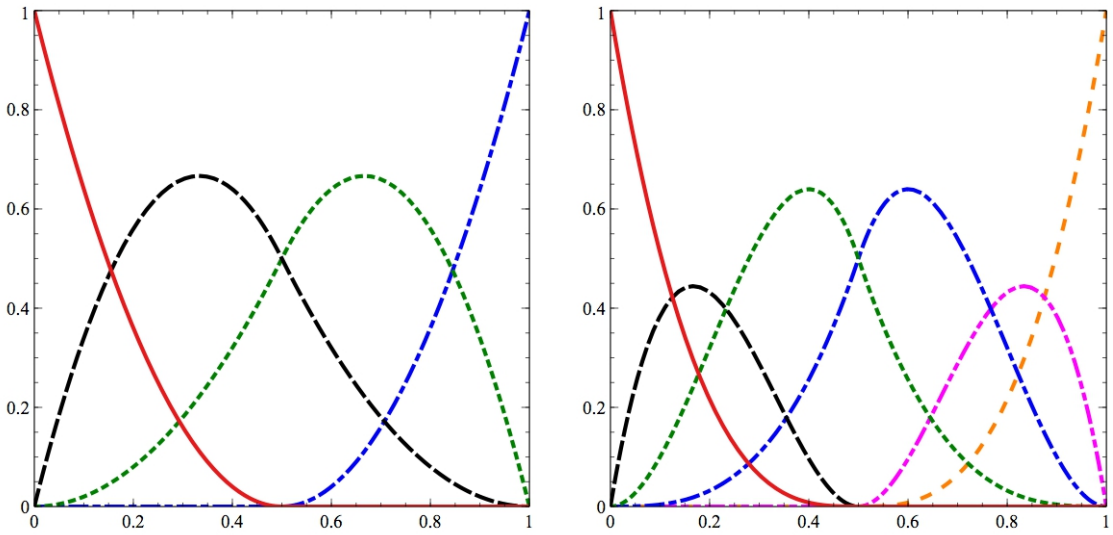

(a) (b)

Figure 4: Degree Elevation (a) Initial B-Spline basis functions $N_{i,3}(\xi)$; i = 1, $\cdots$, 4 of order k = 3 for knot vector $\Xi = \{0, 0, 0, 0.5, 1, 1, 1\}$ (b) B-Spline basis functions $N_{i,4}(\xi)$; i = 1, $\cdots$, 6 of order k = 4 after degree elevation with knot vector $\Xi = \{0, 0, 0, 0, 0.5, 0.5, 1, 1, 1, 1\}$

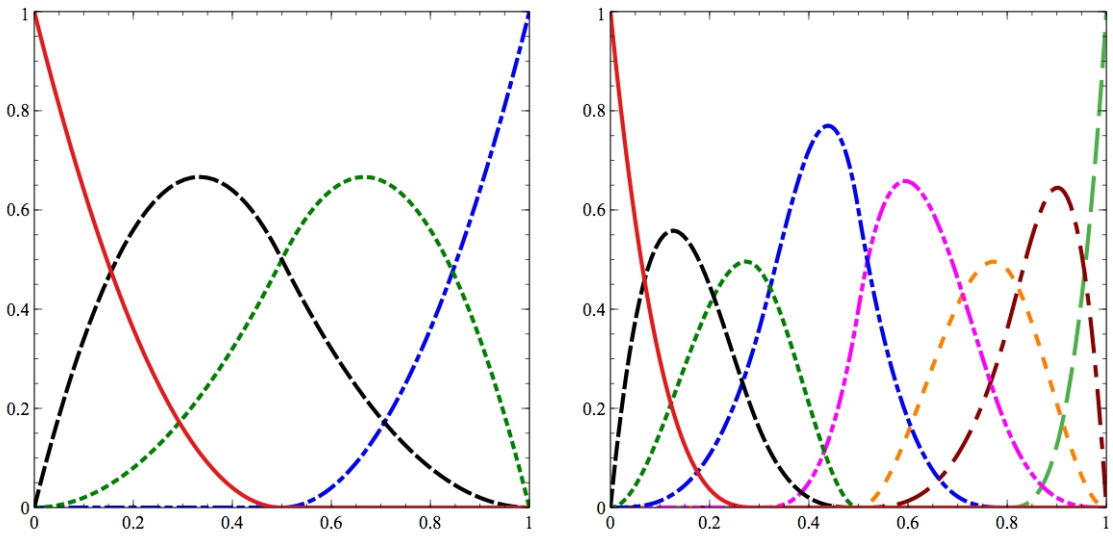

(a) (b)

Figure 5: k-refinement (a) Initial B-Spline basis functions $N_{i,3}(\xi)$; i = 1, $\cdots$, 4 of order k = 3 for knot vector $\Xi = \{0, 0, 0, 0.5, 1, 1, 1\}$ (b) B-Spline basis functions $N_{i,4}(\xi)$; i = 1, $\cdots$, 8 of order k = 4 after k-refinement with knot vector $\Xi = \{0, 0, 0, 0, 0.3, 0.5, 0.5, 0.8, 1, 1, 1, 1\}$

2.2.3 k-refinement

We can insert new knot values with multiplicities equal to one to define new elements across whose boundaries functions will be $\mathcal{C}^{p-1}$-continuous. We can also repeat existing knot values to lower the continuity of the basis across existing element boundaries. This makes knot insertion a more flexible process than simple h-refinement, Similarly, we have a more flexible higher-order refinement as well.

In the k-refinement, we elevate the degree as well as we insert a new knot without changing the shape of the curve. This has no equivalent refinement in the standard FEA. First we increase the degree of the curve and also increase the multiplicity of all intermediate knot values so the continuity of the curve does not change at these specific knots, and then we insert a new knot as shown in the Figure 5.

Note that pure $k-$refinement, where all functions maintain maximal $\mathcal{C}^{p-1}$-continuity across element boundaries, is only possible if the coarsest mesh is comprised of a single element. If the initial mesh places constraints on the continuity across certain element boundaries, these constraints will exist on all meshes. In general, though some such constraints will exist, the number of elements desired for analysis will be much higher than the number needed for modeling the geometry. Refinements may be performed such that the functions have $p-1$ continuous derivatives across these new element boundaries and the benefits of k-refinement will still be significant.

2.3 Partition of Unity

2.3.1 Partition of Unity Functions

Let $\bar{\Omega}$ is the closure of $\Omega \subset \mathbb{R}^d$. The vector space $\mathcal{C}(\bar{\Omega})$ is defined by

$$\begin{aligned}\mathcal{C}(\bar{\Omega}) &= \{\phi \in C^m(\Omega) \mid D^\alpha \phi : \text{bounded and uniformly continuous on } \Omega \\ &\quad \text{for } |\alpha| = \alpha_1 + ... + \alpha_d \leq m\}\end{aligned}$$

A function $\phi \in \mathcal{C}^m(\Omega)$ is said to be a $\mathcal{C}^m$ -continuous function. If Ψ is a function defined on Ω, the *support* of Ψ is defined as

$$supp\Psi = \overline{\{x \in \Omega \mid \Psi(x) \neq 0\}}$$

For an integer $k \geq 0$, the *Sobolev space* $H^k(\Omega)$ is defined by

$$H^k(\Omega) = \{v \in L_2 \mid D^\alpha v \in L_2, \ \forall |\alpha| \leq k\}$$

The *norm* and *semi-norm* are defined for $u \in H^k(\Omega)$ as followings:

$$\|u\|_{k,\Omega} = (\sum_{|\alpha|\leq k} \int_\Omega |\partial^\alpha u|^2 dx)^{1/2}$$

$$\|u\|_{k,\infty,\Omega} = max_{|\alpha|\leq k}\{ess.sup|\partial^\alpha u(x),\ \ x \in \Omega\}$$

$$|u|_{k,\Omega} = (\sum_{|\alpha|=k} \int_\Omega |\partial^\alpha u|^2 dx)^{1/2}$$

$$|u|_{k,\infty,\Omega} = max_{|\alpha|=k}\{ess.sup|\partial^\alpha u(x),\ \ x \in \Omega\}$$

A family $\{U_k :$ open subsets of $\mathbb{R}^d \mid k \in \mathcal{D}\}$ is said to be *a point finite open covering* of $\Omega \subset \mathbb{R}^d$ if there is M such that any $x \in \Omega$ lies in at most M of the open sets U_k and $\Omega \subseteq \bigcup_{k\in\mathcal{D}} U_k$.

For a point finite open covering $\{U_k \mid k \in \mathcal{D}\}$ of a domain, suppose there is a family of Lipschitz functions $\{\phi_k \mid k \in \mathcal{D}\}$ on Ω satisfying the following conditions:

- For $k \in \mathcal{D},\ 0 \leq \phi_k(x) \leq 1, \quad x \in \mathbb{R}^d$
- The support of ϕ_i is contained in $\bar{U_k}$, for each $k \in \mathcal{D}$
- $\sum_{k\in\mathcal{D}} \phi_k(x) = 1$ for each $x \in \Omega$

Then $\{\phi_k \mid k \in \mathcal{D}\}$ is called *a partition of unity (PU)* subordinate to the covering $\{U_k \mid k \in \mathcal{D}\}$. The covering sets $\{U_k\}$ are called *patches*.

A weight function, or window function, is a non-negative continuous function with compact support and is denoted by $w(x)$. Consider the following conical window function: For $x \in \mathbb{R}$,

$$w(x) = \begin{cases} (1-x^2)^l, & |x| \leq 1 \\ 0, & |x| > 1 \end{cases}$$

where l is an integer. $w(x)$ is z $\mathcal{C}^{l-1}$-continuous function. In $\mathbb{R}^d$ the weight function $w(x)$ can be constructed from a one dimensional weight function as $w(x) = \prod_{i=1}^{d} w(x_i)$, where $x = (x_1, ..., x_d)$. We use the normalized window function defined by

$$w_\delta^l(x) = Aw(\frac{x}{\delta}), \qquad A = \frac{(2l+1)!}{2^{2l+1}(l!)^2\delta} \tag{10}$$

where A is the constant such that $\int_{\mathbb{R}} w_\delta^l(x)dx = 1$; refer to [16].

2.3.2 Flat-top Partition of Unity Functions

We first review one dimensional flat-top partition of unity functions; refer to [25] and [27]. For any positive integer n, $\mathcal{C}^{n-1}$-continuous piecewise polynomial basic PU functions were constructed as follows: For integers $n \geq 1$, we define a piecewise polynomial function by

$$\phi_{g_n}^{(pp)}(x) = \begin{cases} \phi_{g_n}^L(x) = (1+x)^n g_n(x), & x \in [-1, 0] \\ \phi_{g_n}^R(x) = (1-x)^n g_n(-x), & x \in [0, 1] \\ 0, & |x| \geq 1 \end{cases} \tag{11}$$

where $g_n(x) = a_0^{(n)} + a_1^{(n)}(-x) + a_2^{(n)}(-x)^2 + ..., +a_{n-1}^{(n)}(-x)^{n-1}$ whose coefficients are inductively constructed by the following recursion formula:

$$a_k^{(n)} = \begin{cases} 1, & k = 0 \\ \sum_{j=0}^{k} a_j^{(n-1)}, & 0 < k \leq n-2 \\ 2(a_{n-2}^{(n)}), & k = n-1 \end{cases}$$

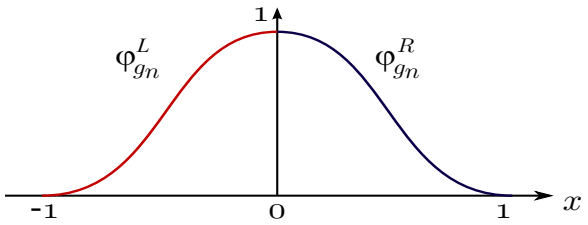

Figure 6: Reference PU functions $\phi_{g_n}^{(pp)}$ with respect to various regularities

$\phi_{g_n}^{(pp)}$ is depicted in Figure 6 for various regularities.

The $\phi_{g_n}^{(pp)}$ has the following properties; refer to [16]

- $$\phi_{g_n}^{(pp)}(x) + \phi_{g_n}^{(pp)}(x-1) = 1, \quad \forall x \in [0,1] \tag{12}$$

  Hence $\{\phi_{g_n}^{(pp)}(x-j) \mid j \in \mathbb{Z}\}$ is a partition of unity on $\mathbb{R}$.

- $\phi_{g_n}^{(pp)}$ is a $\mathcal{C}^{n-1}$-continuous function.

We can construct $\mathcal{C}^{n-1}$-continuous flat-top PU function whose support is $[a-\delta, b+\delta]$ with $a+\delta < b-\delta$ by the basic PU function $\phi_{g_n}^{(pp)}$.

$$\psi_{[a,b]}^{(\delta,n-1)}(x) = \begin{cases} \phi_{g_n}^L(\dfrac{x-(a+\delta)}{2\delta}), & x \in [a-\delta, a+\delta] \\ 1, & x \in [a+\delta, b-\delta] \\ \phi_{g_n}^R(\dfrac{x-(b-\delta)}{2\delta}), & x \in [b-\delta, b+\delta] \\ 0, & x \notin [a-\delta, b+\delta] \end{cases} \tag{13}$$

In order to make a PU function a flat-top, we assume $\delta \leq \dfrac{b-a}{3}$. See the Figure 7.

This flat-top PU function $\psi_{[a,b]}^{(\delta,n-1)}$ is the convolution of the characteristic function

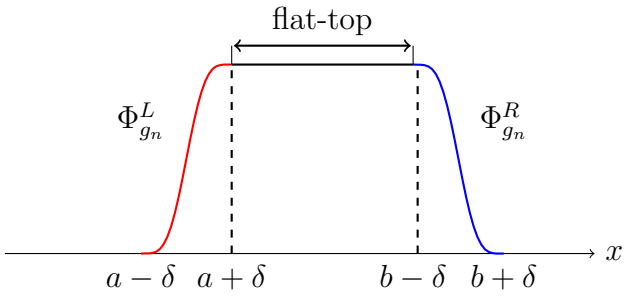

Figure 7: Flat-top PU function $\psi^{(\delta,n-1)}_{[a,b]}(x)$

$\chi_{[a,b]}$ and the scaled window function w^n_δ, that is,

$$\psi^{(\delta,n-1)}_{[a,b]} = \chi_{[a,b]}(x) * w^n_\delta(x)$$

By the first property of PU function $\phi^{(pp)}_{g_n}$,

$$\phi^R_{g_n}(\xi) + \phi^L_{g_n}(\xi - 1) = 1, \quad \xi \in [0,1]$$

If $\varphi : [-\delta, \delta] \to [0,1]$ is defined by

$$\varphi(x) = \frac{x+\delta}{2\delta}$$

then we have

$$\phi^R_{g_n}(\varphi(x)) + \phi^L_{g_n}(\varphi(x) - 1) = 1, \quad \xi \in [-\delta, \delta]$$

Construction of flat-top partition of unity functions

The flat-top PU function (13) can be constructed by either convolution or B-spline functions as follows:

- **PU functions constructed by convolutions:** The flat-top PU function (13) can be constructed by convolution, $\psi^{(\delta,n-1)}_{[a,b]}(x) = \chi_{[a,b]}(x) * w^n_\delta(x)$, the convolution of the characteristic function $\chi_{[a,b]}$ and the scaled window function w^n_δ

defined by (10). The characteristic function is defined by

$$\chi_{[a,b]}(x) = \begin{cases} 1 & \text{if } x \in [a,b], \\ 0 & \text{if } x \notin [a,b]. \end{cases}$$

- **PU functions constructed by B-splines:** Using the partition of unity property of the B-splines,

  the PU function (13) can also be constructed by B-spline functions.

  1. For $\mathcal{C}^1$-continuous piecewise polynomial flat-top PU functions, let $N_{i,4}(x), i = 1, \ldots, 12$ be B-splines of degree 3 that correspond to the open knot vector:

  $$\Big\{ \underbrace{0,..,0}_{4}, \underbrace{a-\delta, a-\delta}_{2}, \underbrace{a+\delta, a+\delta}_{2}, \underbrace{b-\delta, b-\delta}_{2}, \underbrace{b+\delta, b+\delta}_{2}, \underbrace{1,..,1}_{4} \Big\}$$

  A polynomial $P_3(x)$ of degree 3 defined on $[a-\delta, a+\delta]$ is uniquely determined by four constraints:

  $$P_3(a-\delta) = 0, \quad P_3(a+\delta) = 1$$
  $$\frac{d}{dx}P_3(a-\delta) = \frac{d}{dx}P_3(a+\delta) = 0$$

  $\phi^L_{g_2}(\dfrac{x-(a+\delta)}{2\delta})$ satisfies the four constraints and also $N_{5,4}(x) + N_{6,4}(x)$ satisfies the four constraints. Therefore, we have

  $$\phi^L_{g_2}(\frac{x-(a+\delta)}{2\delta}) = N_{5,4}(x) + N_{6,4}(x), \text{ for } x \in [a-\delta, a+\delta].$$

  Similarly, we have

  $$\phi^R_{g_2}(\frac{x-(b-\delta)}{2\delta}) = N_{7,4}(x) + N_{8,4}(x), \text{ for } x \in [b-\delta, b+\delta].$$

Using the partition of unity property of B-splines, we have

$$N_{5,4}(x) + N_{6,4}(x) + N_{7,4}(x) + N_{8,4}(x) = 1, \text{ for } x \in [a+\delta, b-\delta].$$

2. For $\mathcal{C}^2$-continuous piecewise polynomial flat-top PU functions, let $N_{i,6}(x), i = 1, \ldots, 18$, be B-splines of degree 5 corresponding to the open knot vector,

$$\Big\{\underbrace{0,..,0}_{6},\underbrace{a-\delta,..,a-\delta}_{3},\underbrace{a+\delta,..,a+\delta}_{3},\underbrace{b-\delta,..,b-\delta}_{3},\underbrace{b+\delta,..,b+\delta}_{3},\underbrace{1,..,1}_{6}\Big\}.$$

A polynomial $P_5(x)$ of degree 5 defined on $[a-\delta, a+\delta]$ is uniquely determined by six constraints: three at $a-\delta$ and three at $a+\delta$,

$$P_5(a-\delta) = 0, \quad P_5(a+\delta) = 1$$
$$\frac{d}{dx}P_5(a-\delta) = \frac{d}{dx}P_5(a+\delta) = 0$$
$$\frac{d^2}{dx^2}P_5(a-\delta) = \frac{d^2}{dx^2}P_5(a+\delta) = 0$$

$\phi^L_{g_3}(\frac{x-(a+\delta)}{2\delta})$ satisfies the six constraints and $N_{7,6}(x)+N_{8,6}(x)+N_{9,6}(x)$ also satisfies the six constraints. Therefore, we have

$$\phi^L_{g_3}(\frac{x-(a+\delta)}{2\delta}) \;=\; N_{7,6}(x) + N_{8,6}(x) + N_{9,6}(x), \text{ for } x \in [a-\delta, a+\delta]$$

Similarly, we have

$$\phi^R_{g_3}(\frac{x-(b-\delta)}{2\delta}) \;=\; N_{10,6}(x) + N_{11,6}(x) + N_{12,6}, \text{ for } x \in [b-\delta, b+\delta]$$

Moreover, we have

$$N_{7,6}(x)+N_{8,6}(x)+N_{9,6}(x)+N_{10,6}(x)+N_{11,6}(x)+N_{12,6} = 1, \text{ for } x \in [a+\delta, b-\delta].$$

3. In general, for each n, the $\mathcal{C}^{n-1}$-continuous piecewise polynomial flat-top PU function can be constructed by the B-splines of degree $2n-1$, $N_{i,2n}(x), i = 1, \ldots, 6n$, corresponding to the open knot vector:

$$\Big\{ \underbrace{0,..,0}_{2n}, \underbrace{a-\delta,..,a-\delta}_{n}, \underbrace{a+\delta,..,a+\delta}_{n}, \underbrace{b-\delta,..,b-\delta}_{n}, \underbrace{b+\delta,..,b+\delta}_{n}, \underbrace{1,..,1}_{2n} \Big\}.$$

We have

$$\psi_{[a,b]}^{(\delta,n-1)}(x) = \begin{cases} \sum_{k=1}^{n} N_{2n+k,2n}(x) & \text{if} \quad x \in [a-\delta, a+\delta] \\ \sum_{k=1}^{2n} N_{2n+k,2n}(x) = 1 & \text{if} \quad x \in [a+\delta, b-\delta] \\ \sum_{k=1}^{n} N_{3n+k,2n}(x) & \text{if} \quad x \in [b-\delta, b+\delta] \\ 0 & \text{if} \quad x \notin [a-\delta, b+\delta] \end{cases} \tag{14}$$

Since the two functions $\phi_{g_n}^R$ and $\phi_{g_n}^L$ defined by (11), satisfy the following relation:

$$\phi_{g_n}^R(\xi) + \phi_{g_n}^L(\xi - 1) = 1, \text{ for } \xi \in [0, 1],$$

if $\varphi : [-\delta, \delta] \to [0, 1]$ is defined by

$$\varphi(x) = (x + \delta)/(2\delta),$$

then we have

$$\phi_{g_n}^R(\varphi(x)) + \phi_{g_n}^L(\varphi(x) - 1) = 1, \text{ for } x \in [-\delta, \delta].$$

The gradient of the flat-top PU function $\psi_{[a,b]}^{(\delta,n-1)}$ is bounded as follows:

$$\Big| \frac{d}{dx} \Big[\psi_{[a,b]}^{(\delta,n-1)}(x) \Big] \Big| \leq \frac{C}{2\delta} \tag{15}$$

CHAPTER 3: IMPLICITLY ENRICHED SCHWARZ METHODS

3.1 Domain Decomposition

We will concentrate on one special group of domain decomposition methods, namely iterative domain decomposition methods using overlapping subdomains. The overlapping domain decomposition methods operate by an iterative procedure, where the fourth-order problem is repeatedly solved within every subdomain. For each subdomain, the artificial internal boundary condition is provided by its neighboring subdomains. The convergence of the solution on these internal boundaries ensures the convergence of the solution in the entire solution domain.

The alternating method was originally proposed by H. A. Schwarz [33] in 1870 as a technique to prove the existence of a solution to the Laplace equation on a domain which is a combination of a rectangle and a circle. The idea was then used and extendedby P. L. Lions [21], [22], [23] to parallel algorithms for solving partial differential equations. Since then, many kind of domain decomposition methods have been developed, to improve the performance of the classical domain decomposition method. A modification of this method is known as Parallel Schwarz method.

In Schwarz Alternating method, the domain is divided into two overlapping subdomains and the iterative procedure starts by taking one initial guess for the boundary of the first subproblem. This method involves solving the boundary value problem on

each of the two subdomains in turn, taking always the last values of the approximate solution as the next boundary conditions. It is important to note that in Schwarz Alternating method, the solution of the first problem is required before the second problem can be solved. In Parallel Schwarz method, the domain is divided into two overlapping subdomains and the iterative procedure starts by taking initial guesses on each subdomain. In this case, the subproblems can be solved independently in each iteration.

3.1.1 Schwarz Alternating Method

The Schwarz Alternating method is an iterative method based on solving alternatively sub-problems in overlaying subdomains Ω_1 and Ω_2. It is sequential by nature since the solution of the first problem is required to solve the second problem in each iteration.

Consider the fourth-order problem

$$\begin{cases} \Delta^2 u = f \quad \text{in} \quad \Omega \\ u = \dfrac{\partial u}{\partial n} = 0 \quad \text{on} \quad \partial\Omega \end{cases} \tag{16}$$

on a bounded Lipschitz region Ω with homogeneous clamped boundary conditions on boundary $\partial\Omega$. This domain is divided into two subdomains Ω_1 and Ω_2 with artificial boundaries Γ_1 and Γ_2 respectively, as shown in Figure 8.

The Schwarz Alternating method gives us two subproblems:

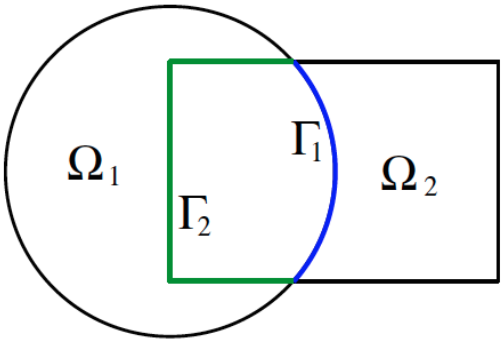

Figure 8: Overlapping subdomains with artificial boundaries

$$\begin{cases} \Delta^2 u_1^{k+1} = f \quad \text{in} \quad \Omega_1 \\ u_1^{k+1} = \frac{\partial u_1^{k+1}}{\partial n} = 0 \quad \text{on} \quad \partial\Omega_1 \setminus \Gamma_1 \\ u_1^{k+1} = u_2^k \quad \text{on} \quad \Gamma_1 \\ \frac{\partial u_1^{k+1}}{\partial n} = \frac{\partial u_2^k}{\partial n} \quad \text{on} \quad \Gamma_1 \end{cases} \tag{17}$$

$$\begin{cases} \Delta^2 u_2^{k+1} = f \quad \text{in} \quad \Omega_2 \\ u_2^{k+1} = \frac{\partial u_2^{k+1}}{\partial n} = 0 \quad \text{on} \quad \partial\Omega_2 \setminus \Gamma_2 \\ u_2^{k+1} = u_1^{k+1} \quad \text{on} \quad \Gamma_2 \\ \frac{\partial u_2^{k+1}}{\partial n} = \frac{\partial u_1^{k+1}}{\partial n} \quad \text{on} \quad \Gamma_2 \end{cases} \tag{18}$$

where k denotes the number of iterations. To start the iterative process, subproblem (18) is first solve for $k = 0$ with some initial guess u_2^0 on artificial boundary Γ_1. The iterations (17) and (18) are performed by updating $u_1^{k+1}(x, y)$ and $u_2^{k+1}(x, y)$, which are most updated values of $u_1(x, y)$ and $u_2(x, y)$ respectively, until certain convergence conditions are met.

3.1.2 Additive(Parallel) Schwarz Method

Pierre-Louis Lions [22] proposed Parallel Schwarz method by doing small but essential modification in Schwarz Alternating method which made the problem perfect for parallel computing. The difference between the Alternating Schwarz and the Additive(Parallel) methods is the way how the artificial boundary condition is updated on Γ_1 and Γ_2. The Additive(Parallel) Schwarz method solves the fourth-order problem(30) concurrently in subdomains Ω_1 and Ω_2 as follows:

$$\begin{cases} \Delta^2 u_1^{k+1} = f \qquad \text{in} \quad \Omega_1 \\ u_1^{k+1} = \frac{\partial u_1^{k+1}}{\partial n} = 0 \quad \text{on} \quad \partial\Omega_1 \setminus \Gamma_1 \\ u_1^{k+1} = u_2^k \quad \text{on} \quad \Gamma_1 \\ \frac{\partial u_1^{k+1}}{\partial n} = \frac{\partial u_2^k}{\partial n} \quad \text{on} \quad \Gamma_1 \end{cases} \tag{19}$$

$$\begin{cases} \Delta^2 u_2^{k+1} = f \qquad \text{in} \quad \Omega_2 \\ u_2^{k+1} = \frac{\partial u_2^{k+1}}{\partial n} = 0 \quad \text{on} \quad \partial\Omega_2 \setminus \Gamma_2 \\ u_2^{k+1} = u_1^k \quad \text{on} \quad \Gamma_2 \\ \frac{\partial u_2^{k+1}}{\partial n} = \frac{\partial u_1^k}{\partial n} \quad \text{on} \quad \Gamma_2 \end{cases} \tag{20}$$

To start this parallel process, subproblems (19) and (20) are solved together for n = 0 step with two initial guesses u_1^0 and u_2^0 on artificial boundaries Γ_1 and Γ_2 respectively.

It should be noted that convergence property of Additive Schwarz method falls behind that of the Schwarz Alternating method. Although the Additive Schwarz

method suits well for parallel computing, its convergence property is inferior to that of the Alternating Schwarz method. In case of convergence, the Additive Schwarz method uses roughly twice as many iterations as that of the standard Alternating Schwarz method. This is not surprising when the Schwarz methods are compared with their linear system solver analogues; Alternating Schwarz is a block Gauss-Seidel approach, whereas Additive Schwarz is a block Jacobi approach [6]. We will extend the classical Alternating Schwarz method to more than two subdomains by combining Alternating Schwarz method and Additive Schwarz method to keep the required number of iterations small.

3.2 Implicitly Enriched Galerkin Method

Implicitly Enriched Galerkin method generates singular B-spline basis functions through a geometric mapping from the reference domain onto the singular zone of the physical domain. In other words, the pullback of the singularity into the reference domain by the geometric mapping becomes highly smooth. Since the proposed method eliminates influence of singularity without using external singular basis functions in the approximation space, singular integrals do not appear in computation of stiffness matrices and load vectors. It also overcomes large condition number and additional degrees of freedom caused by directly added enrichment functions.

For analysis of the fourth-order problems on irregular shaped domains, it is necessary to use multipatches to reduce the problem on a complicated domain to a sequence of problems on simple domains. However, it is hard to join two patches along their interfaces. To avoid the difficulties in multi-pathes approaches, we combine Implicitly

Enriched Galerkin method with Schwarz domain decomposition methods.

We applied our proposed Implicitly Enriched Schwarz methods to deal with two dimensional fourth-order equations on non-convex domains such as square domain with crack singularity and L-shaped domain.

In view of Grisvard's results [15], the solution of fourth-order equation in cracked domain with clamped boundary condition along the crack faces as follows:

If $f \in P_2^k(\Omega)$, i.e $r^{-k+|\alpha|}D^\alpha f \in L_2(\Omega)$, $|\alpha| \leq k$, then the solution of $\Delta^2 u = f$ in cracked domain Ω is

$$u(r,\theta) = \sum_{1\leq m<k+5/2} r^{m+1/2}\Big(\lambda_m s_m^1 + \nu_m s_m^2\Big) + u_{reg}(r,\theta) \tag{21}$$

where

$$\begin{aligned} s_m^1 &= \sin(m+1/2)\theta - \frac{2m+1}{2m-3}\sin(m-3/2)\theta, \\ s_m^2 &= \cos(m+1/2)\theta - \cos(m-3/2)\theta, \quad u_{reg} \in P_2^{k+4}(\Omega). \end{aligned}$$

Here λ_m, ν_m are constants. We construct test problems from this solution.

Pullback of the bilinear form for fourth-order problems onto the reference domain

We calculate the pullback of the Laplacian on the physical domain onto the reference domain for calculations of the stiffness matrix and the load vector of the fourth-order problem.

Let $\Phi : \hat{\Omega} \longrightarrow \Omega$ be a mapping from the parameter space to the physical space

defined by

$$\Phi(\xi,\eta) = (x(\xi,\eta), y(\xi,\eta)),$$

and let

$$\hat{u} = u \circ \Phi, \quad \nabla_x = (\partial_x, \partial_y)^T, \quad \nabla_\xi = (\partial_\xi, \partial_\eta)^T,$$

where u is a differentiable function defined on Ω. Then we have

$$(\nabla_x u) \circ \Phi = J(\Phi)^{-1} \nabla_\xi \hat{u} \quad \text{or} \tag{22}$$

$$\begin{bmatrix} u_x \circ \Phi \\ u_y \circ \Phi \end{bmatrix} = \frac{1}{|J(\Phi)|} \begin{bmatrix} y_\eta & -y_\xi \\ -x_\eta & x_\xi \end{bmatrix} \begin{bmatrix} \hat{u}_\xi \\ \hat{u}_\eta \end{bmatrix} = \begin{bmatrix} J_{11}^{-1} & J_{12}^{-1} \\ J_{21}^{-1} & J_{22}^{-1} \end{bmatrix} \begin{bmatrix} \hat{u}_\xi \\ \hat{u}_\eta \end{bmatrix}.$$

Using (22), we have

$$\begin{aligned} (\nabla_x u_x) \circ \Phi &= J(\Phi)^{-1} \nabla_\xi (u_x \circ \Phi) \\ &= J(\Phi)^{-1} \nabla_\xi (J_{11}^{-1} \hat{u}_\xi + J_{12}^{-1} \hat{u}_\eta) \end{aligned} \tag{23}$$

$$\begin{bmatrix} u_{xx} \circ \Phi \\ u_{xy} \circ \Phi \end{bmatrix} = J(\Phi)^{-1} \begin{bmatrix} (J_{11}^{-1} \hat{u}_\xi + J_{12}^{-1} \hat{u}_\eta)_\xi \\ (J_{11}^{-1} \hat{u}_\xi + J_{12}^{-1} \hat{u}_\eta)_\eta \end{bmatrix}$$

Similarly, we have

$$\begin{aligned} (\nabla_x u_y) \circ \Phi &= J(\Phi)^{-1} \nabla_\xi (u_y \circ \Phi) \\ &= J(\Phi)^{-1} \nabla_\xi (J_{21}^{-1} \hat{u}_\xi + J_{22}^{-1} \hat{u}_\eta) \end{aligned} \tag{24}$$

$$\begin{bmatrix} u_{yx} \circ \Phi \\ u_{yy} \circ \Phi \end{bmatrix} = J(\Phi)^{-1} \begin{bmatrix} (J_{21}^{-1} \hat{u}_\xi + J_{22}^{-1} \hat{u}_\eta)_\xi \\ (J_{21}^{-1} \hat{u}_\xi + J_{22}^{-1} \hat{u}_\eta)_\eta \end{bmatrix}$$

Let $\varphi(x,y) = \hat{\varphi} \circ \Phi^{-1}(x,y)$. Then

$$\begin{aligned}
(\partial_{xx}\varphi)\circ\Phi &= J_{11}^{-1}\frac{\partial}{\partial\xi}(J_{11}^{-1}\frac{\partial}{\partial\xi}\hat{\varphi} + J_{12}^{-1}\frac{\partial}{\partial\eta}\hat{\varphi}) + J_{12}^{-1}\frac{\partial}{\partial\eta}(J_{11}^{-1}\frac{\partial}{\partial\xi}\hat{\varphi} + J_{12}^{-1}\frac{\partial}{\partial\eta}\hat{\varphi}) \\
(\partial_{yy}\varphi)\circ\Phi &= J_{21}^{-1}\frac{\partial}{\partial\xi}(J_{21}^{-1}\frac{\partial}{\partial\xi}\hat{\varphi} + J_{22}^{-1}\frac{\partial}{\partial\eta}\hat{\varphi}) + J_{22}^{-1}\frac{\partial}{\partial\eta}(J_{21}^{-1}\frac{\partial}{\partial\xi}\hat{\varphi} + J_{22}^{-1}\frac{\partial}{\partial\eta}\hat{\varphi}) \\
(\partial_{xy}\varphi)\circ\Phi &= J_{21}^{-1}\frac{\partial}{\partial\xi}(J_{11}^{-1}\frac{\partial}{\partial\xi}\hat{\varphi} + J_{12}^{-1}\frac{\partial}{\partial\eta}\hat{\varphi}) + J_{22}^{-1}\frac{\partial}{\partial\eta}(J_{11}^{-1}\frac{\partial}{\partial\xi}\hat{\varphi} + J_{12}^{-1}\frac{\partial}{\partial\eta}\hat{\varphi}) \\
(\partial_{yx}\varphi)\circ\Phi &= J_{11}^{-1}\frac{\partial}{\partial\xi}(J_{21}^{-1}\frac{\partial}{\partial\xi}\hat{\varphi} + J_{22}^{-1}\frac{\partial}{\partial\eta}\hat{\varphi}) + J_{12}^{-1}\frac{\partial}{\partial\eta}(J_{21}^{-1}\frac{\partial}{\partial\xi}\hat{\varphi} + J_{22}^{-1}\frac{\partial}{\partial\eta}\hat{\varphi})
\end{aligned} \tag{25}$$

It is worthwhile to note that $\Delta\varphi \circ \Phi$ of (25) is different from the simplified form shown in [34] that does not hold for general cases.

For $u, v \in \mathcal{V}_\Omega$, we can calculate the entries in stiffness matrix $\mathcal{B}_i(u,v)$ and load vector $\mathcal{F}_i(v)$ for each subdomain Ω_i with corresponding geometric mapping $F_i : \hat{\Omega} \to \Omega_i$ as follows:

Let $\triangle_{xy} = \dfrac{\partial^2}{\partial x^2} + \dfrac{\partial^2}{\partial y^2}$ and $f(x,y) = \Delta^2 u$, then $\forall u, v \in \mathcal{V}_{F_i}$

$$\begin{aligned}
\mathcal{B}(u,v) &= \int_0^1\int_0^1 (\Delta_{xy}u)\circ F_i \cdot (\Delta_{xy}v)\circ F_i \cdot |J(F_i)| d\xi d\eta \\
\mathcal{F}(v) &= \int_0^1\int_0^1 f(F_i(\xi,\eta))\cdot\hat{v}\cdot|J(F_i)|d\xi d\eta.
\end{aligned}$$

3.3 Modification of Basis Functions and Assigning Boundary Conditions

In case we divide physical domain into several patches and assemble B-spline functions constructed on each patch in a patchwise manner, then the derivatives of assembled B-spline functions could be discontinuous along the patch boundaries. So some modifications are required in order to make them continuous. These modified B-spline basis functions are linearly independent and their first derivatives are zero at both ends except for the second and the second last basis functions. Since $\mathcal{C}^1$-continuous B-spline functions are not interpolant, assigning homogeneous and non-homogeneous

clamped boundary conditions for fourth-order equation has some limitations. To impose the homogeneous boundary conditions, we discard first two and last two basis functions. To impose the non-homogeneous boundary conditions, we modify first two basis functions $\hat{N}_{f_1,p+1}(\xi)$,$\hat{N}_{f_2,p+1}(\xi)$ and last two basis functions $\hat{N}_{l_1,p+1}(\xi)$,$\hat{N}_{l_2,p+1}(\xi)$ in the following way:

Let $N_{i,p+1}(\xi), i = 1, \ldots, m$, be $\mathcal{C}^{p-1}$-continuous B-spline functions of degree p corresponding to the knot vectors. In what follows, we denote the first, the second, the second last, and the last of basis functions $N_{i,p+1}(\xi), i = 1, \ldots, m$, respectively, as follows:

$$N_{f_1,p+1}(\xi), N_{f_2,p+1}(\xi), N_{l_2,p+1}(\xi), N_{l_1,p+1}(\xi)$$

$$\begin{cases} N^*_{f_1,p+1}(\xi) &= N_{f_1,p+1}(\xi) + N_{f_2,p+1}(\xi) = [(1-\xi)^{p-1}(1+(p-1)\xi)] \\ N^*_{f_2,p+1}(\xi) &= N_{f_2,p+1}(\xi)/(\dfrac{d}{d\xi}N_{f_2,p+1})(0) \\ N^*_{l1,p+1}(\xi) &= N_{l_1,p+1}(\xi) + N_{l_2,p+1}(\xi) = [\xi^{p-1}(p-(p-1)\xi)] \\ N^*_{l_2,p+1}(\xi) &= N_{l_2,p+1}(\xi)/(\dfrac{d}{d\xi}N_{l_2,p+1})(1) \end{cases} \tag{26}$$

Then, the modified B-spline functions have the following properties at the end points 0 and 1:

$$\begin{cases} N^*_{f_1,p+1}(0) = 1 \quad , \quad (\dfrac{d}{d\xi}N^*_{f_1,p+1})(0) = 0 \\ N^*_{f_2,p+1}(0) = 0 \quad , \quad (\dfrac{d}{d\xi}N^*_{f_2,p+1})(0) = 1 \\ N^*_{l_1,p+1}(1) = 1 \quad , \quad (\dfrac{d}{d\xi}N^*_{l_1,p+1})(1) = 0 \\ N^*_{l_2,p+1}(1) = 0 \quad , \quad (\dfrac{d}{d\xi}N^*_{l_2,p+1})(1) = 1 \end{cases} \tag{27}$$

After B-spline basis functions are modified, non-homogenuous Dirichlet and Neu-

mann boundary conditions are externally imposed by using the Least Squares Method.

3.4 Affect of Overlapping Size

The numerical Schwarz algorithm is essentially same as the block Gauss-Seidel method for a modified matrix equation which has the same solution as the original finite element and finite difference equations of the elliptic partial differential equation. The relationship between the convergence of Schwarz Alternating Method and the area of overlap has been observed previously. An attempt to derive the theoretical convergence rate of the method for linear elliptic problems was made by Evans et al. [11] , Evans et al. [12], and Li-Shan and Evans [13]. It was shown analytically as well as numerically that the convergence rate of the Schwarz Alternating method increases with the size of the overlap region. In [24], it was proven that the method converges geometrically, and the numerical convergence of the method as a function of overlap size was also investigated. In [29], they showed how overlapping affects the convergence of the Schwarz Alternating Method for model problems in p-dimensional case. The convergence rate was also found to be exponential in both the amount of overlap and in the number of regions.

CHAPTER 4: NON-SINGULAR FOURTH-ORDER ELLIPTIC EQUATIONS

4.1 1D Non-singular Elliptic Problems

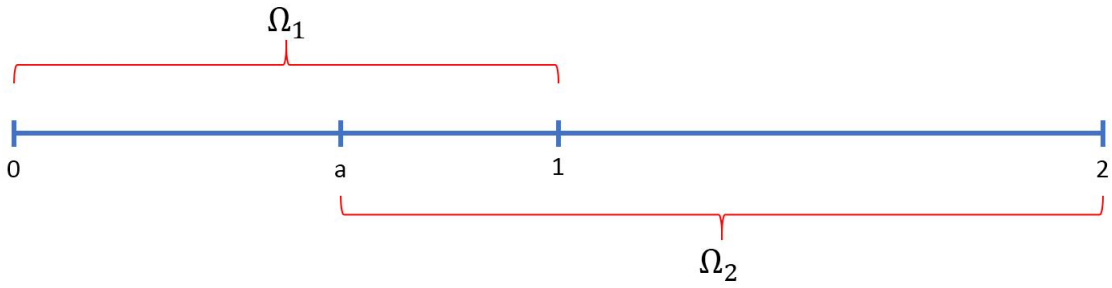

Figure 9: 1D physical domain Ω

Example 1. Consider 1D non-singular fourth-order problem on domain $\Omega = [0, 2]$

$$\begin{cases} u^{(4)}(x) & = f(x) \ \ in \ \ (0,2) \\ u(0) & = u^{'}(0) = 0 \\ u(2) & = u^{'}(2) = 0 \end{cases}$$

with the exact solution $u(x) = (2-x)^2 x^2$.

Domain $\Omega = [0, 2]$ is subdivided into $\Omega_1 = [0, 1]$ and $\Omega_2 = [a, 2]$ for $0 < a < 1$. We define the following smooth linear mappings F_1 and F_2 which map parameter space to physical subspaces Ω_1 and Ω_2, respectively:

$$F_1 : \hat{\Omega} = [0,1] \to \Omega_1 = [0,1] \quad \text{such that} \quad F_1(\xi) = \xi \tag{28}$$

$$F_2 : \hat{\Omega} = [0,1] \to \Omega_2 = [a,2] \quad \text{such that} \quad F_2(\xi) = (2-a)\xi + a \tag{29}$$

$$\text{Modified approximation spaces:} \quad \hat{\mathcal{V}}_{F_1} = \{\hat{M}_k(\xi) : k = 3, \ldots, 2q+1\},$$
$$\hat{\mathcal{V}}_{F_2} = \{\hat{N}_k(\xi) : k = 1, \ldots, 2q-1\},$$

where $\hat{M}_{k,q+1}$ and $\hat{N}_{k,q+1}$ are B-splines corresponding to the following knot vector:

$$\{\underbrace{0\ldots0}_{q+1}, \underbrace{1/(q+1)}_{1}, \underbrace{2/(q+1)}_{1}, \ldots, \underbrace{q/(q+1)}_{1} \underbrace{1\ldots1}_{q+1}\}.$$

To satisfy homogeneous clamped BC, **the first two** of $\hat{M}_{k,q+1}$ and **the last two** of $\hat{N}_{k,q+1}$ B-spline functions are discarded.

To satisfy artificial BC, **the last two** of $\hat{M}_{k,q+1}$ and **the first two** of $\hat{N}_{k,q+1}$ B-spline functions are modified such that

$$\begin{aligned}
\hat{M}^*_{2q+1,q+1}(\xi) &= \xi^5(6-5\xi) \\
\hat{M}^*_{2q,q+1}(\xi) &= \frac{\hat{M}_{2q,q+1}(\xi)}{\hat{M}'_{2q,q+1}(1)} \\
\hat{N}^*_{1,q+1}(\xi) &= (1-\xi)^5(1+6\xi) \\
\hat{N}^*_{2,q+1}(\xi) &= \frac{\hat{N}_{2,q+1}(\xi)}{\hat{N}'_{2,q+1}(0)}
\end{aligned}$$

This problem is solved for different overlapping sizes to verify the affect of overlapping size on the required number of iterations for desired accuracy. As we expected, Figure 10(b) shows that larger overlapping domain region requires smaller number of iterations to converge.

Example 2. Consider 1D non-singular problem on domain $\Omega = [0, 2]$

$$\begin{cases}
u^{(4)}(x) = f(x) \ \ in \ \ (0,2) \\
u(0) = u'(0) = 0 \\
u(2) = u'(2) = 0
\end{cases}$$

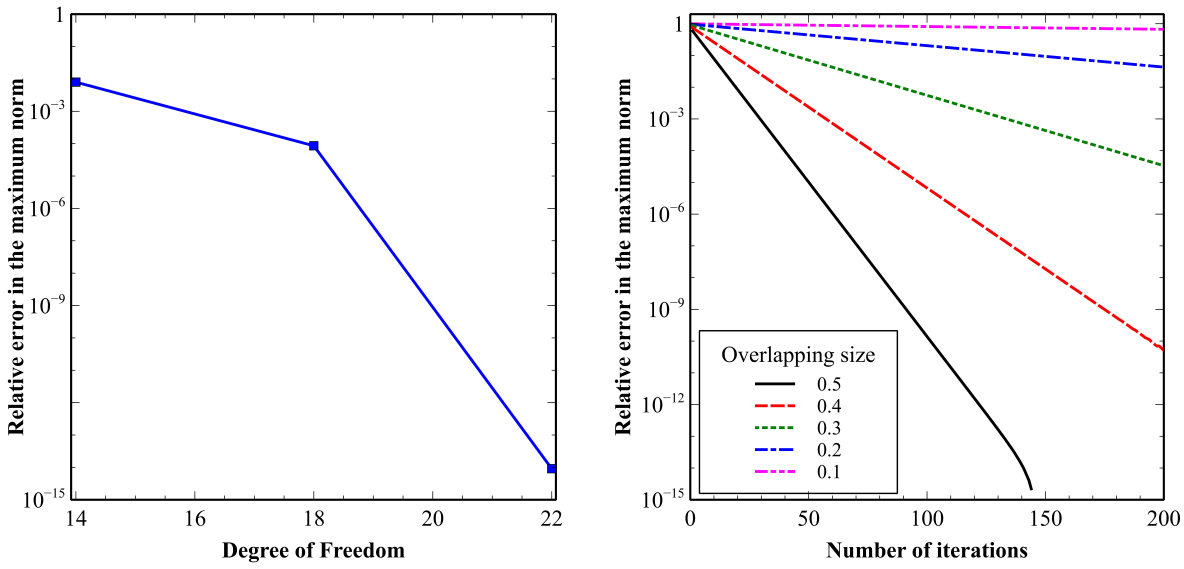

(a) (b)

Figure 10: 1D fourth-order problem whose true solution is a polynomial function (a)Relative Error in the maximum norm with fixed overlapping size a=0.5 for basis functions with different degrees p=4,5, and 6, (b)Relation betwen number of iterations and overlapping size between subdomains for the fixed degree p=8

with the exact solution $u(x) = e^x(2-x)^2x^2$.

We consider same smooth linear mappings F_1 and F_2, defined in the previous example, which map the parameter space to physical subspaces Ω_1 and Ω_2, respectively where $\Omega_1 = [0, 1]$ and $\Omega_2 = [a, 2]$ for $0 < a < 1$. Example 2 is solved with respect to various sizes of the overlapping subdomains with initial guess 0 on artificial boundary

Table 1: Relative errors in the maximum norm of numerical solutions of 1D fourth-order problem whose true solution is a polynomial function for basis functions with different degrees for the fixed overlapping size a=0.5

Degree	DOF	Iterations	$\|RelErr\|_{Max}$
4	14	22	7.9547E-003
5	18	41	8.6046E-005
6	22	141	9.1039E-015

$x = a$. Relative errors in the maximum norm versus basis functions of various degrees are depicted in Figure 11(a) and in Table 2.

If the size of the overlapping region is increased, then the solution acquired in the first step was very close to the true solution. Hence it required a small number of iterations and thus had smaller convergence rate as shown in Figure 11(b).

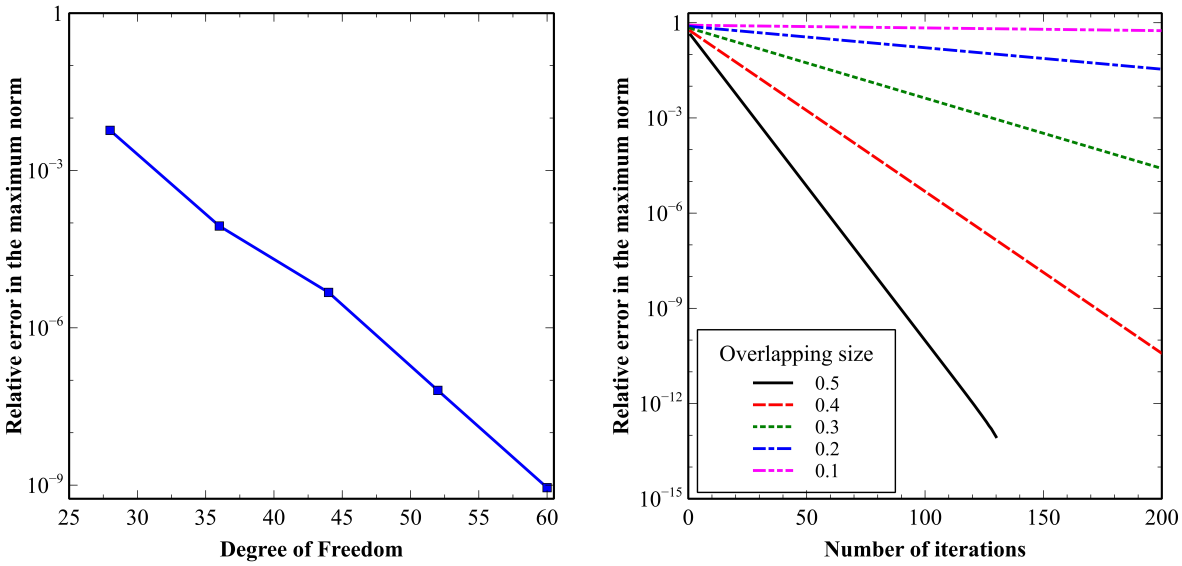

(a) (b)

Figure 11: 1D fourth-order problem whose true solution is an exponential function (a)Relative Error in the maximum norm with fixed overlapping size a=0.5 for basis functions with different degrees p=4,5,6,7, and 8 (b)Relation betwen number of iterations and overlapping size between subdomains for the fixed degree p=8

4.2 2D Fourth-order Problem on a Rectangular Domain with Vertical Interface

Example 3. Consider the test problem on the domain $\Omega = [0, 2] \times [0, 1]$

$$\begin{cases} \Delta^2 u = f \quad \text{in} \quad \Omega \\ u = \dfrac{\partial u}{\partial n} = 0 \quad \text{on} \quad \partial\Omega \end{cases}$$

whose true solution is $u(x, y) = (2x - x^2)^2.(y^2 - y)^2$.

Table 2: Relative errors in the maximum norm of numerical solutions of 1D fourth-order problem whose true solution is an exponential function for basis functions with different degrees for the fixed overlapping size a=0.5

Degree	DOF	Iterations	$\|RelErr\|_{Max}$
4	28	22	5.8153E-003
5	36	43	8.7332E-005
6	44	52	4.7264E-006
7	52	77	6.4140E-008
8	60	106	8.9628E-010

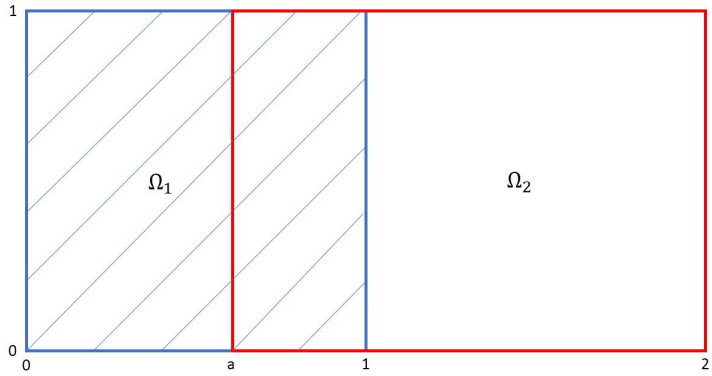

Figure 12: Rectangular domain with vertical interface

Suppose Ω is decomposed into $\Omega_1 = [0,1] \times [0,1]$, $\Omega_2 = [a,2] \times [0,1]$, $0 < a < 1$. Then, the linear patch mappings $F_1 : \hat{\Omega} \to \Omega_1$ and $F_2 : \hat{\Omega} \to \Omega_2$ where $\hat{\Omega} = [0,1] \times [0,1]$, are defined as follows:

$F_1 : \hat{\Omega} \to \Omega_1$ and $F_1(\xi,\eta) = (x(\xi,\eta), y(\xi,\eta))$ where

$$F_1(\xi,\eta) = \begin{cases} x(\xi,\eta) = \xi \\ \\ y(\xi,\eta) = \eta \end{cases}$$

$F_2 : \hat{\Omega} \to \Omega_2$ and $F_2(\xi,\eta) = (x(\xi,\eta), y(\xi,\eta))$ where

$$F_2(\xi,\eta) = \begin{cases} x(\xi,\eta) = (2-a)\xi + a \\ \\ y(\xi,\eta) = \eta \end{cases}$$

Modified approximation space:

$$\hat{\mathcal{V}}_{F_1} = \{\hat{N}_{i,q+1}(\xi) \cdot \hat{M}_{j,q+1}(\eta) : i = 3, \ldots, 2q+1; j = 3, \cdots, 2q-1\}.$$

where $\hat{M}_{k,q+1}$ and $\hat{N}_{k,q+1}$ are B-splines corresponding to the following knot vector:

$$\{\underbrace{0 \ldots 0}_{q+1}, \underbrace{1/(q+1)}_{1}, \underbrace{2/(q+1)}_{1}, \ldots, \underbrace{q/(q+1)}_{1} \underbrace{1 \ldots 1}_{q+1}\}.$$

- To satisfy homogeneous clamped BC, **the first two** of $\hat{N}_{k,q+1}(\xi)$ and **the first and last two** of $\hat{M}_{k,q+1}(\eta)$ B-spline functions were discarded.

- To assign non-homogeneous artificial BC, **the last two** of $\hat{N}_{k,q+1}(\xi)$ were modified.

$$\hat{\mathcal{V}}_{F_2} = \{\hat{N}_{i,p+1}(\xi) \cdot \hat{M}_{j,q+1}(\eta) : i = 1, \ldots, 2q-1; j = 3, \cdots, 2q-1\}.$$

where $\hat{M}_{k,q+1}$ and $\hat{N}_{k,q+1}$ are B-splines corresponding to the following knot vector:

$$\{\underbrace{0 \ldots 0}_{q+1}, \underbrace{1/(q+1)}_{1}, \underbrace{2/(q+1)}_{1}, \ldots, \underbrace{q/(q+1)}_{1} \underbrace{1 \ldots 1}_{q+1}\}.$$

- To satisfy homogeneous clamped BC, **the last two** of $\hat{N}_{k,q+1}(\xi)$ and **the first and last two** of $\hat{M}_{k,q+1}(\eta)$ B-spline functions were discarded.

- To assign non-homogeneous artificial BC, **the first two** of $\hat{N}_{k,q+1}(\xi)$ were modified.

Applying the Schwarz Alternating method with Mapping Method to Example 3, we have the numerical results obtained by using basis functions of different degrees in Table 3 and Figure 13(a). This probem is solved for different overlapping regions. Like in one-dimensional case, the number of iterations required to get the solution

of desired accuracy is dependent upon the size of the overlapping region but not on the location of artificial boundaries. The relative errors in the maximum norm for different overlapping sizes are shown in Figure 13(b). Note that for results in Figure 13(b), the degree of the basis functions are fixed. Therefore, no extra cost is required.

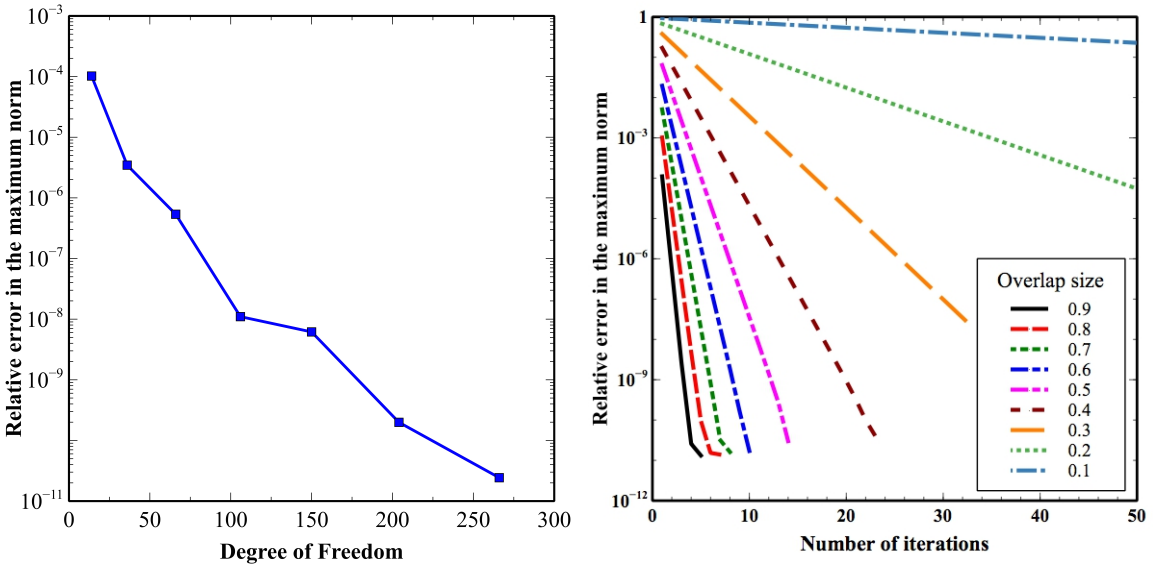

(a) (b)

Figure 13: 2D fourth-order problem on a rectangular domain with vertical interface (a)Relative errors in the maximum norm for basis functions with degrees p=4,5,..., and 10 for fixed overlapping size a=0.5.(Table 3), (b)Relation between number of iterations and overlapping size between subdomains for the fixed degree p=8.

4.3 2D Fourth-order Problem on a Rectangular Domain with Slanted Interface

Example 4. This test problem is on the domain $\Omega = [0, 2] \times [0, 1]$

$$\begin{cases} \Delta^2 u = f \quad \text{in} \quad \Omega \\ u = \dfrac{\partial u}{\partial n} = 0 \quad \text{on} \quad \partial\Omega \end{cases}$$

with the exact solution: $u(x, y) = (x^2 - 2x)^2(y^2 - y)^2$.

The linear patch mappings F_1 and F_2 onto two patches are defined as follows:

Table 3: Relative errors in the maximum norm of numerical solutions of 2D fourth-order problem on a rectangular domain with vertical interface for basis functions with different degrees p=4,5,..., and 10 for the fixed overlapping size a=0.5

Degree	DOF	Iterations	$\|RelErr\|_{Max}$
4	14	8	1.02E-004
5	36	10	3.46E-006
6	66	10	5.37E-007
7	106	13	1.10E-008
8	150	15	6.19E-009
9	204	17	1.99E-010
10	266	15	2.43E-011

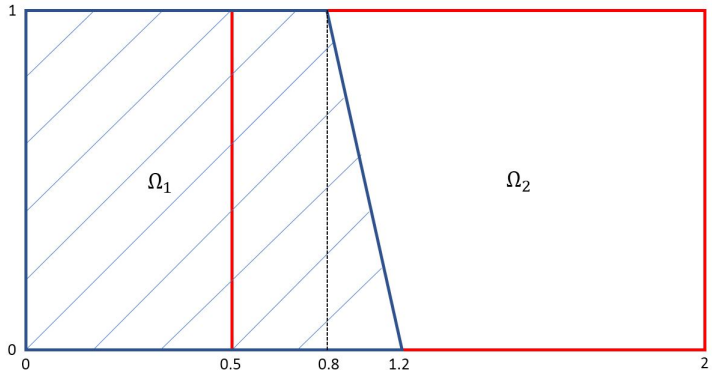

Figure 14: Rectangular domain with slanted interface

$F_1 : \hat{\Omega} \to \Omega_1$ and $F_1(\xi, \eta) = (x(\xi, \eta), y(\xi, \eta))$ where

$$F_1(\xi, \eta) = \begin{cases} x(\xi, \eta) = 1.2\xi - 0.4\xi\eta \\ y(\xi, \eta) = \eta \end{cases}$$

$F_2 : \hat{\Omega} \to \Omega_2$ and $F_2(\xi, \eta) = (x(\xi, \eta), y(\xi, \eta))$ where

$$F_2(\xi, \eta) = \begin{cases} x(\xi, \eta) = (2 - a)\xi + a \\ y(\xi, \eta) = \eta \end{cases}$$

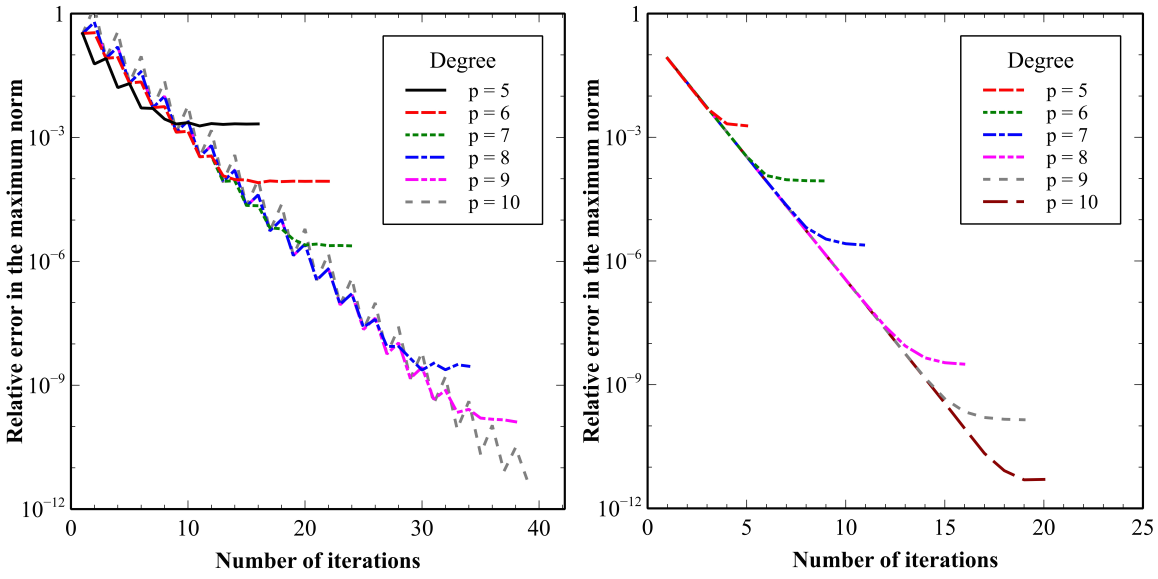

(a) (b)

Figure 15: 2D fourth-order problem on a rectangular domain with slanted interface (a)Relative Errors obtained by using Additive Schwarz Method for basis functions with different degrees, (b)Relative Errors obtained by using Schwarz Alternating Method for basis functions with different degrees

Modified approximation space:

$$\hat{\mathcal{V}}_{F_1} = \{\hat{N}_{i,q+1}(\xi) \cdot \hat{M}_{j,q+1}(\eta) : i = 3, \ldots, 2q+1; j = 3, \cdots, 2q-1\}.$$

where $\hat{M}_{k,q+1}$ and $\hat{N}_{k,q+1}$ are B-splines corresponding to the following knot vector:

$$\{\underbrace{0 \ldots 0}_{q+1}, \underbrace{1/(q+1)}_{1}, \underbrace{2/(q+1)}_{1}, \ldots, \underbrace{q/(q+1)}_{1} \underbrace{1 \ldots 1}_{q+1}\}.$$

- To satisfy homogeneous clamped BC, **the first two** of $\hat{N}_{k,q+1}(\xi)$ and **the first and last two** of $\hat{M}_{k,q+1}(\eta)$ B-spline functions were discarded.

- To satisfy non-homogeneous artificial BC, **the last two** of $\hat{N}_{k,q+1}(\xi)$ were modified.

$$\hat{\mathcal{V}}_{F_2} = \{\hat{N}_{i,p+1}(\xi) \cdot \hat{M}_{j,q+1}(\eta) : i = 1, \ldots, 2q-1; j = 3, \cdots, 2q-1\}.$$

Table 4: Relative errors of numerical solutions obtained by using Additive Schwarz Method and Schwarz Alternating Method for 2D fourth-order problem on a rectangular domain with slanted interface. The size of overlapping part of two subdomains is fixed

		Additive(Parallel) Schwarz		Schwarz Alternating	
DEG	DOF	Iterations	$\|RelErr\|_{Max}$	Iterations	$\|RelErr\|_{Max}$
5	36	16	2.13E-003	4	2.12E-003
6	66	22	8.69E-005	11	8.70E-005
7	104	24	2.37E-006	12	2.36E-006
8	150	34	2.88E-009	17	3.07E-009
9	204	38	1.30E-010	18	1.41E-010
10	266	39	4.39E-012	19	4.93E-012

where $\hat{M}_{k,q+1}$ and $\hat{N}_{k,q+1}$ are B-splines corresponding to the following knot vector:

$$\{\underbrace{0\ldots0}_{q+1},\underbrace{1/(q+1)}_{1},\underbrace{2/(q+1)}_{1},\ldots,\underbrace{q/(q+1)}_{1}\underbrace{1\ldots1}_{q+1}\}.$$

- To satisfy homogeneous clamped BC, **the last two** of $\hat{N}_{k,q+1}(\xi)$ and **the first and last two** of $\hat{M}_{k,q+1}(\eta)$ B-spline functions were discarded.

- To satisfy non-homogeneous artificial BC, **the first two** of $\hat{N}_{k,q+1}(\xi)$ were modified.

We solve the same problem with respect to the Schwarz Alternating method and the Additive Schwarz method. Both of the methods give same results, but the number of iterations required to reach solution of accuracy 4.9E-012 for the Schwarz Alternating method is much less compared with the Additive(Parallel) Schwarz Method as we expected. The convergence rates for these two methods are compared in Table 4 and Figure 15.

4.4 2D Fourth-order Problem on a Triangular Domain

Example 5. Consider fourth-order equation $\Delta^2 u = f$ in the triangular domain Ω with non-homogeneous clamped boundary conditions whose solution is

$$\begin{aligned} u(x,y) &= (xy)^4 \\ \text{Then,} \quad f(x,y) &= \Delta^2 u = 24(x^4+y^4) + 288x^2y^2 \end{aligned}$$

Domain Decomposition and Geometric Mappings

We partition the physical domain into three overlapping subdomains as shown in Figure 16 and construct three patch mappings F_1, F_2, and F_3 from the reference domain $\hat{\Omega}$ onto the subdomains Ω_1, Ω_2, and Ω_3 respectively.

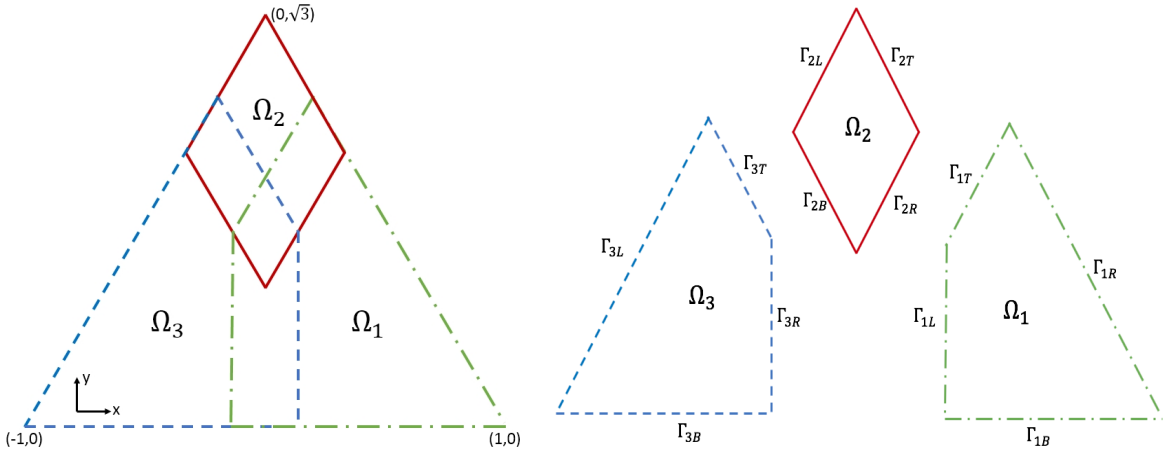

Figure 16: Decomposition of a triangular domain

[F_1-mapping]: $F_1 : \hat{\Omega} = [0,1] \times [0,1] \to \Omega_1$

$$F_1(\xi,\eta) = \begin{cases} x(\xi,\eta) = \dfrac{9}{8}\xi - \dfrac{19}{24}\xi\eta - \dfrac{1}{8}, \\ y(\xi,\eta) = \dfrac{\sqrt{3}}{24}\eta(8\xi+11). \end{cases}$$

where

$$J(F_1) \;=\; \begin{bmatrix} \frac{9}{8}-\frac{19}{24}\eta & \frac{8\sqrt{3}}{24}\eta \\ -\frac{19}{24}\xi & \frac{\sqrt{3}(8\xi+11)}{24} \end{bmatrix}, \quad |J(F_1)| = \frac{3\sqrt{3}(8\xi+11)}{64} - \frac{209\sqrt{3}\eta}{576}$$

[F_2-mapping]: $F_2 : \hat{\Omega} = [0,1]\times[0,1] \to \Omega_2$

$$F_2(\xi,\eta) = \begin{cases} x(\xi,\eta) = \dfrac{(\xi+\eta)}{3} - \dfrac{1}{3}, \\ y(\xi,\eta) = \dfrac{\sqrt{3}}{3}(\eta-\xi+2). \end{cases}$$

where

$$J(F_2) \;=\; \begin{bmatrix} \frac{1}{3} & \frac{-\sqrt{3}}{3} \\ \frac{1}{3} & \frac{\sqrt{3}}{3} \end{bmatrix}, \quad |J(F_2)| = \frac{2\sqrt{3}}{9}$$

[F_3-mapping]: $F_3 : \hat{\Omega} = [0,1]\times[0,1] \to \Omega_3$

$$F_3(\xi,\eta) = \begin{cases} x(\xi,\eta) = \dfrac{19}{24}\eta + \dfrac{9}{8}\xi - \dfrac{19}{24}\xi\eta - 1, \\ y(\xi,\eta) = -\dfrac{\sqrt{3}}{24}\eta(8\xi-19). \end{cases}$$

where

$$J(F_3) \;=\; \begin{bmatrix} \frac{9}{8}-\frac{19}{24} & \frac{-\sqrt{3}}{3}\eta \\ \frac{19}{24}-\frac{19}{24}\xi & \frac{-\sqrt{3}}{24}(8\xi-19) \end{bmatrix}, \quad |J(F_3)| = \frac{209\sqrt{3}\eta}{576} - \frac{3\sqrt{3}(8\xi-19)}{64}$$

Construction of basis functions: We assume $p, q \geq 4$. Let $\hat{N}_{k,p+1}(\xi)$ and $\hat{M}_{l,q+1}(\eta), k = 1,2,\ldots,p+5, l = 1,2,\ldots,q+5$ be $\mathcal{C}^{p-1}$-continuous B-splines of degree

p and q, respectively, corresponding to open knot vectors

$$S_\xi = \{\underbrace{0\ldots0}_{p+1}, \underbrace{0.2}_{1}, \underbrace{0.4}_{1}, \underbrace{0.6}_{1}, \underbrace{0.8}_{1}, \underbrace{1\ldots1}_{p+1}\}. \tag{30}$$

$$S_\eta = \{\underbrace{0\ldots0}_{q+1}, \underbrace{0.2}_{1}, \underbrace{0.4}_{1}, \underbrace{0.6}_{1}, \underbrace{0.8}_{1}, \underbrace{1\ldots1}_{q+1}\}. \tag{31}$$

To satisfy non-homogeneous clamped boundary conditions as well as non-homogeneous artificial boundary conditions along interfaces, we modify **the first and the last two** of $\hat{N}_{k,q+1}(\xi)$ and $\hat{M}_{k,q+1}(\eta)$ B-spline basis functions as defined in Equation (26). We define basis functions on the reference domain for the mappings F_1, F_2, and F_3 as follows:

$$\hat{\mathcal{V}}_{F_i} = \{\hat{N}_{k,p+1}(\xi)\cdot\hat{M}_{l,q+1}(\eta) : k = 1,\ldots,p+5; l = 1,\cdots,q+5\} \quad \text{for} \quad i = 1,2,3.$$

The corresponding approximation functions on the physical subdomains Ω_i are

$$\mathcal{V}_{F_i} = \{\Big(\hat{N}_{k,p+1}(\xi)\cdot\hat{M}_{l,q+1}(\eta)\Big)\circ F_i^{-1} : k = 1,\ldots,p+5; l = 1,\cdots,q+5\} \quad \text{for} \quad i = 1,2,3.$$

Our approximation space to deal with fourth-order partial differential equation on a triangular domain Ω is

$$\mathcal{V}_\Omega = \mathcal{V}_{F_1} \cup \mathcal{V}_{F_2} \cup \mathcal{V}_{F_3} \tag{32}$$

The total number of the degree of freedom is

$$\begin{aligned} \text{card}(\mathcal{V}_\Omega) &= \text{card}(\mathcal{V}_{F_1}) + \text{card}(\mathcal{V}_{F_2}) + \text{card}(\mathcal{V}_{F_3}) \\ &= 3\Big((p+5)(q+5)\Big) \end{aligned}$$

Table 5: Relative errors of numerical solutions obtained by using Mapping Method with Schwarz Methods for 2D fourth-order problem whose true solution is smooth on a triangular domain

Degree	DOF	Iterations	$\|RelErr\|_{Max}$
4	243	6	2.79E-003
5	300	21	3.79E-004
6	363	27	1.41E-004
7	432	54	5.88E-006
8	507	165	9.55E-012

Iteration Algorithm

Since we partition the triangular domain into three subdomains, we extend the classical Alternating Schwarz method introduced for two subdomains by combining classical Alternating Schwarz method and Additive Schwarz method. We reduced the required number of iterations by superior convergence property of the Alternatig Schwarz method since the Additive Schwarz method uses roughly twice as many iterations as that of the standard Alternating Schwarz method.

The iterative procedures are as follows:

1. Assignning zero clamped BC along the artificial boundaries Γ_{1L} and Γ_{1T} (shown in Figure 16), we obtain the solution u_1^0 on Ω_1.

2. Assigning zero clamped BC along the artificial boundary Γ_{3R} and Γ_{3T} (shown in Figure 16), we obtain the solution u_3^0 on Ω_1.

3. With $u_2^0|_{\Gamma_{23}} = \Omega_3 \cap \Gamma_{2B}$ and $u_2^0|_{\Gamma_{2R}} = \Omega_3 \cap \Gamma_{2R}$, we have the solution u_2^0 on Ω_2.

These steps are represented by the following three fourth-order problems with non-

homogeneous clamped BC:

$$\begin{cases} \Delta^2 u_1^{k+1} = f \qquad \text{in} \quad \Omega_1 \\ u_1^{k+1} = u \quad \text{on} \quad \partial\Omega_1 \setminus (\Gamma_{1L} \cup \Gamma_{1T}) \\ \frac{\partial u_1^{k+1}}{\partial n} = \frac{\partial u_1}{\partial n} \quad \text{on} \quad \partial\Omega_1 \setminus (\Gamma_{1L} \cup \Gamma_{1T}) \\ u_1^{k+1} = u_2^k \quad \text{on} \quad \Gamma_{1T} \\ u_1^{k+1} = u_3^k \quad \text{on} \quad \Gamma_{1L} \\ \frac{\partial u_1^{k+1}}{\partial n} = \frac{\partial u_2^k}{\partial n} \quad \text{on} \quad \Gamma_{1T} \\ \frac{\partial u_1^{k+1}}{\partial n} = \frac{\partial u_3^k}{\partial n} \quad \text{on} \quad \Gamma_{1L} \end{cases} \tag{33}$$

$$\begin{cases} \Delta^2 u_3^{k+1} = f \qquad \text{in} \quad \Omega_3 \\ u_3^{k+1} = u \quad \text{on} \quad \partial\Omega_3 \setminus (\Gamma_{3R} \cup \Gamma_{3T}) \\ \frac{\partial u_3^{k+1}}{\partial n} = \frac{\partial u}{\partial n} \quad \text{on} \quad \partial\Omega_3 \setminus (\Gamma_{3R} \cup \Gamma_{3T}) \\ u_3^{k+1} = u_2^k \quad \text{on} \quad \Gamma_{3T} \\ u_3^{k+1} = u_1^k \quad \text{on} \quad \Gamma_{3R} \\ \frac{\partial u_3^{k+1}}{\partial n} = \frac{\partial u_2^k}{\partial n} \quad \text{on} \quad \Gamma_{3T} \\ \frac{\partial u_3^{k+1}}{\partial n} = \frac{\partial u_1^k}{\partial n} \quad \text{on} \quad \Gamma_{3R} \end{cases} \tag{34}$$

$$
\begin{cases}
\Delta^2 u_2^{k+1} = f \qquad \text{in} \quad \Omega_3 \\
\quad u_2^{k+1} = u \quad \text{on} \quad \partial\Omega_2 \setminus (\Gamma_{2B} \cup \Gamma_{2R}) \\
\frac{\partial u_2^{k+1}}{\partial n} = \frac{\partial u}{\partial n} \quad \text{on} \quad \partial\Omega_2 \setminus (\Gamma_{2B} \cup \Gamma_{2R}) \\
\quad u_2^{k+1} = u_3^{k+1} \quad \text{on} \quad \Gamma_{2B} \\
\quad u_2^{k+1} = u_1^{k+1} \quad \text{on} \quad \Gamma_{2R} \\
\quad \frac{\partial u_2^{k+1}}{\partial n} = \frac{\partial u_3^{k+1}}{\partial n} \quad \text{on} \quad \Gamma_{2B} \\
\quad \frac{\partial u_2^{k+1}}{\partial n} = \frac{\partial u_1^{k+1}}{\partial n} \quad \text{on} \quad \Gamma_{2R}
\end{cases} \tag{35}
$$

Asigning Boundary Conditions

A discrete solution u_1^h of (33) at the k^{th}-iteration, can be expressed as

$$
\begin{aligned}
(u_1^h)^{(k)}(x,y) \;=\; & \sum_{i=3}^{p+3}\sum_{j=3}^{q+3} c_{i,j}\Big(\hat{N}_{i,p+1} \times \hat{M}_{j,q+1}\Big) \circ F_1^{-1}(x,y) \\
& + \sum_{j=3}^{q+3}\Big[c_{f_1,j}\Big(\hat{N}_{f_1,p+1} \times \hat{M}^*_{j,q+1}\Big) + c_{f_2,j}\Big(\hat{N}_{f_2,p+1} \times \hat{M}^*_{j,q+1}\Big)\Big] \circ F_1^{-1}(x,y) \\
& + \sum_{j=3}^{q+3}\Big[c_{l_2,j}\Big(\hat{N}_{l_2,p+1} \times \hat{M}^*_{j,q+1}\Big) + c_{l_1,j}\Big(\hat{N}_{l_1,p+1} \times \hat{M}^*_{j,q+1}\Big)\Big] \circ F_1^{-1}(x,y) \\
& + \sum_{i=3}^{p+3}\Big[c_{i,f_1}\Big(\hat{N}_{i,p+1} \times \hat{M}^*_{f_1,q+1}\Big) + c_{i,f_2}\Big(\hat{N}_{i,p+1} \times \hat{M}^*_{f_2,q+1}\Big)\Big] \circ F_1^{-1}(x,y) \\
& + \sum_{i=3}^{p+3}\Big[c_{i,l_2}\Big(\hat{N}_{i,p+1} \times \hat{M}^*_{l_2,q+1}\Big) + c_{i,l_1}\Big(\hat{N}_{i,p+1} \times \hat{M}^*_{l_1,q+1}\Big)\Big] \circ F_1^{-1}(x,y).
\end{aligned}
$$

The unknowns $c_{f_1,j}, c_{f_2,j}, c_{l_1,j}, c_{l_2,j}, c_{i,f_1}, c_{i,f_2}, c_{i,l_1}, c_{i,l_2}, 3 \le i \le (p+3), 3 \le j \le (q+3)$, which are amplitudes of basis functions along the boundary, can be decided by non-homogeneous clamped BC:

1. $c_{f_1,j}, 3 \le j \le (q+3)$, can be determined by $u_1^k = u_3^{k-1}$ on Γ_{1L}

2. $c_{f_2,j}, 3 \le j \le (q+3)$, can be determined by $\nabla_x(u_1^k)\cdot\mathbf{n} = \nabla_x(u_3^{k-1})\cdot\mathbf{n}$ on Γ_{1L}

3. $c_{l_1,j}, 3 \le j \le (q+3)$, can be determined by $u_1^k = u$ on Γ_{1R}

4. $c_{l_2,j}, 3 \le j \le (q+3)$, can be determined by $\nabla_x(u_1^k)\cdot\mathbf{n} = \nabla_x(u)\cdot\mathbf{n}$ on Γ_{1R}

5. $c_{i,f_1}, 3 \le i \le (p+3)$, can be determined by $u_1^k = u$ on Γ_{1B}

6. $c_{i,f_2}, 3 \le i \le (p+3)$, can be determined by $\nabla_x(u_1^k)\cdot\mathbf{n} = \nabla_x(u)\cdot\mathbf{n}$ on Γ_{1B}

7. $c_{i,l_1}, 3 \le i \le (p+3)$, can be determined by $u_1^k = u_2^{k-1}$ on Γ_{1T}

8. $c_{i,l_2}, 3 \le i \le (p+3)$, can be determined by $\nabla_x(u_1^k)\cdot\mathbf{n} = \nabla_x(u_2^{k-1})\cdot\mathbf{n}$ on Γ_{1T}

where $\nabla_x(u)\cdot\mathbf{n}$ denotes the normal derivative with respect to the outward unit normal vector $\mathbf{n}$ to the corresponding boundary.

Imposing essential BC of u_1 along the boundary Γ_{1T} . By (27), we have

$$(u_1^h)^{(k)} \circ F_1(\xi,1) = \sum_{i=3}^{p+3} c_{i,l_1}\Big(\hat{N}_{i,p+1}\times \hat{M}^*_{l_1,q+1}\Big)(\xi,1) = \sum_{i=3}^{p+3} c_{i,l_1}\hat{N}_{i,p+1}(\xi). \tag{36}$$

Using the least squares method to determine $c_{i,l_1}, 3 \le i \le (p+3)$, we solve the following linear system: for $3 \le j \le p+3$,

$$\sum_{i=3}^{p+3} c_{i,l_1}\int_0^1 \hat{N}_{i,p+1}(\xi)\hat{N}_{j,p+1}(\xi) = -\int_0^1 \hat{N}_{j,p+1}(\xi)(u_2^{k-1})\circ F_1(\xi,1) \tag{37}$$

Imposing the natural BC, $\nabla u_1\cdot\mathbf{n}$, along the boundary Γ_{1T}: We use the following notations in what follows.

$$J(F_1)^{-1}(\xi,1) \;=\; \begin{bmatrix} J(F_1)^{-1}_{11}, & J(F_1)^{-1}_{12} \\ J(F_1)^{-1}_{21}, & J(F_1)^{-1}_{22} \end{bmatrix}. \tag{38}$$

Under a parameterization of the boundary Γ_{1T}, we have $\mathbf{n} \circ F_1(\xi, 1) =< -1, 0 >$.

Using (27) and (38), we have

$$
\begin{aligned}
&(\nabla_x(u_1^{(k)}) \cdot \mathbf{n}) \circ F_1(\xi, 1) = \Big((-1)\frac{\partial}{\partial x}(u_1^{(k)}) + (0)\frac{\partial}{\partial y}(u_1^{(k)})\Big) \circ F_1(\xi, 1) \\
&= \Big\langle J(F_1)_{11}^{-1}(\xi, 1) \sum_{i=3}^{p+3} c_{i,l_1} \frac{d}{d\xi}\hat{N}_{i,p+1}(\xi) + J(F_1)_{12}^{-1}(\xi, 1) \sum_{i=3}^{p+3} c_{i,l_2}\hat{N}_{i,p+1}, \\
&J(F_1)_{21}^{-1}(\xi, 1) \sum_{i=3}^{p+3} c_{i,l_1} \frac{d}{d\xi}\hat{N}_{i,p+1}(\xi) + J(F_1)_{22}^{-1}(\xi, 1) \sum_{i=3}^{p+3} c_{i,l_2}\hat{N}_{i,p+1}\Big\rangle \cdot \Big\langle -\frac{\sqrt{3}}{2}, \frac{1}{2}\Big\rangle
\end{aligned}
$$

Then, the unknown $c_{i,l_1}, c_{i,l_2}, 3 \le i \le p+3$, are those which minimize the following:

$$
\int_0^1 \Big(\frac{1}{2}\sum_{i=3}^{p+n-1} (\nabla_x(u_1^{(k)}) \cdot \mathbf{n}) \circ F_1(\xi, 1) + (\nabla_x(u_2^{(k-1)}) \cdot \mathbf{n}) \circ F_1(\xi, 1)\Big)^2 \| \frac{d}{d\xi} F_1(\xi, 1)\|.
$$

Hence we solve the following system: for $3 \le j \le p+3$

$$
\begin{aligned}
&\int_0^1 \sum_{i=3}^{p+3} \Big[A \cdot B \cdot c_{i,l_1} \frac{\partial}{\partial \xi}\hat{N}_{i,p+1}(\xi)\hat{N}_{j,p+1}(\xi) + B^2 \cdot c_{i,l_2}\hat{N}_{i,p+1}(\xi)\hat{N}_{j,p+1}(\xi)\Big] \quad (39) \\
= &\int_0^1 (\nabla_x(u_2^{(k-1)}) \cdot \mathbf{n}) \circ F_1(\xi, 1) \cdot B \cdot \hat{N}_{j,p+1}(\xi) d\xi.
\end{aligned}
$$

where $c_{i,l_1}, 3 \le i \le p+3$ are derived from (37). We use the same technique for imposing homogeneous and non-homogeneous boundary conditions to the other subproblems.

Applying the extended Schwarz methods combined with Mapping Method, the percentage relative errors in the maximum norm with respect to a k-refinement are listed in Table 5. Our method yield highly accurate numerical solutions by selecting proper geometric mappings for subdomains. In the next section, we extend the proposed method to fourth-order problems on non-convex domains.

CHAPTER 5: FOURTH-ORDER PROBLEMS ON NON-CONVEX DOMAINS

In this section, we consider numerical solutions of fourth-order problems on non-convex domain, especially a polygonal domain with cracks and the L-shaped domain. In the frame of IGA, a mapping method and enriched isogeometric analysis for second order and fourth order PDEs with singularities was introduced in [18], [28], [19], and [20]. In the engineering literature, extended isogeometric analysis (XIGA) were introduced to solve the singularity problems, whereas, in [19], we introduced Implicitly Enriched Galerkin method (IXFEM) to handle the crack singularities. Our method has advantages over XIGA since it is not involved in singular integrals, and hence does not use the Duffy transformation [26]. However, for simplicity, we present it for fourth-order problems on cracked circular domain. In order to extend the proposed enrichment method to non-convex polygonal domains, we can use either partition of unity method or Schwarz Alternating method. In this paper we use the latter approach to extend IXFEM for fourth-order singularity problems on polygonal domains.

5.1 1D Fourth-order Problem with Monotone Singulatity

Example 6. Consider 1D-singular problem on $\Omega = [0, 2]$ shown in the Figure 9.

$$\begin{cases} u^{(4)}(x) & = f(x) \ \ in \ \ (0,2) \\ u(0) & = u^{'}(0) = 0 \\ u(2) & = u^{'}(2) = 0 \end{cases}$$

with the exact solution:

$$u(x) = x^{1.6}(2-x)^2$$

u has a singularity $x^{1.6}$ at the left end of the physical subdomain Ω_1. We construct an example of a fourth-order equation containing singularity of the type x^α. To determine how strong the intensity of singularity α is allowed, we use the following lemma proved in [19]:

Lemma: Suppose $v \in H_0^2(a,b)$ with $0 \le a \le b$. Then

$$(1)\ \ |v(x)| < Cx^{1.5}$$

$$(2)\ \ |\int_a^b x^{\alpha-4} v(x)dx| < \infty, \quad \text{if } \alpha > \mathbf{1.5}$$

(I) Partition of the physical subdomain Ω_1 into a singular zone and a regular zone: To build singular basis functions on a singular zone $\Omega_{sing} = [0, 0.5]$ and regular basis functions on a regular zone $\Omega_{reg} = [0.4, 1]$, two mappings

$$F_s : \hat{\Omega} = [0,1] \longrightarrow \Omega_{sing}, \quad F_r : \hat{\Omega} = [0,1] \longrightarrow \Omega_{reg},$$

defined by

$$x = F_s(\xi) \ = \ 0.5\xi^5$$

$$x = F_r(\xi) \ = \ 0.6\xi + 0.4$$

- The selection of mappings depend on the strength of singularity $\alpha = 1.6$.
- The inverse mapping $\xi = F_s^{-1}(x)$ brings $\xi^8, \xi^{13}, \xi^{18}$ in $\hat{\Omega}$ to $(2x)^{1.6}, (2x)^{2.6}, (2x)^{3.6}$ in Ω.
- These functions satisfy the clamped boundary conditions at $x = 0$.

(II) $\mathcal{C}^1$-continuous flat-top PU functions: Let us define two PU functions on the physical domain as follows:

$$\begin{aligned}
\psi(x) &= \begin{cases} 1 & \text{if } 0 \le x \le 0.4 \\ (5-10x)^2(20x-7) & \text{if } 0.4 \le x \le 0.5 \\ 0 & \text{if } 0.5 \le x \le 1 \end{cases} \\
\psi^*(x) &= 1 - \psi(x), \\
\hat{\psi}(\xi) &= \psi \circ F_s, \quad \hat{\psi}^*(\xi) = \psi^* \circ F_r.
\end{aligned}$$

(III) Basis functions on $\hat{\Omega}$ whose push-forwards resemble the singularities:

$$\begin{aligned}
\hat{\mathcal{V}}_{F_s} &= \hat{\psi}(\xi) \times \{\hat{M}_1 = \xi^8, \hat{M}_2 = \xi^{13}, \hat{M}_3 = \xi^{18}\}, \\
\hat{\mathcal{V}}_{F_r} &= \hat{\psi}^*(\xi) \times \{\hat{N}_k(\xi) : k = 1, \ldots, 2p-1\},
\end{aligned}$$

where $\hat{N}_{k,p+1}$ are B-splines corresponding to the following knot vector:

$$\{\underbrace{0 \ldots 0}_{p+1}, \underbrace{1/(p+1)}_{1}, \underbrace{2/(p+1)}_{1}, \ldots, \underbrace{p/(p+1)}_{1} \underbrace{1 \ldots 1}_{p+1}\}.$$

For the non-homogeneous artificial BC, last two B-spline functions were modified

$$\begin{aligned}
\hat{N}^*_{2p,p+1}(\xi) &= \xi^9(10 - 9\xi) \\
\hat{N}^*_{2p+1,p+1}(\xi) &= 0.6(\xi^{10} - \xi^9)
\end{aligned}$$

Computing Bilinear forms and load vectors in Ω_1:

Case 1: (Bilinear form for two basis functions in $\mathcal{V}_{F_s}$)

Suppose $u = \hat{u} \circ F_s^{-1}, v = \hat{v} \circ F_s^{-1}$, where $\hat{u} = \hat{\psi}(\xi) \cdot \hat{M}_k$ and $\hat{v} = \hat{\psi}(\xi) \cdot \hat{M}_l$ are in

$\hat{\mathcal{V}}_{F_s}$. Then, we have

$$\mathcal{B}(u,v) = \Big(\int_0^{F_s^{-1}(0.4)} + \int_{F_s^{-1}(0.4)}^1\Big)(u_{xx}\circ F_s)(v_{xx}\circ F_s)|J(F_s)|d\xi$$

$$\mathcal{F}(v) = \Big(\int_0^{F_s^{-1}(0.4)} + \int_{F_s^{-1}(0.4)}^1\Big)(f\circ F_s)(v\circ F_s)|J(F_s)|d\xi$$

Let $\hat{u}(\xi) = (u\circ F)(\xi)$. Then,

$$u_{xx}\circ F_s = \hat{u}_{\xi\xi}\Big((\frac{dF_s}{d\xi})^{-1}\Big)^2 + \hat{u}_{\xi}\Big((\frac{dF_s}{d\xi})^{-1}\Big)_{\xi}(\frac{dF_s}{d\xi})^{-1}$$

If $\hat{u} = \hat{\psi}(\xi)\cdot\hat{M}(\xi)$, and $\hat{M} = \xi^k$ with $k \geq 8$, then we have

$$\begin{aligned}\hat{u}_{\xi} &= (\hat{\psi})_{\xi}\hat{M} + \hat{\psi}\hat{M}_{\xi}\\ \hat{u}_{\xi\xi} &= (\hat{\psi})_{\xi\xi}\hat{M} + 2(\hat{\psi})_{\xi}\hat{M}_{\xi} + \hat{\psi}\hat{M}_{\xi\xi},\end{aligned}$$

where

$$\begin{aligned}(\hat{\psi})_{\xi} &= \psi(F_s(\xi))_{\xi} = (\psi)_x(F_s(\xi))\frac{dF_s}{d\xi},\\ (\hat{\psi})_{\xi\xi} &= \psi(F_s(\xi))_{\xi\xi} = (\psi)_{xx}(F_s(\xi))(\frac{dF_s}{d\xi})^2 + (\psi)_x(F_s(\xi))\frac{d^2F_s}{d\xi^2}.\end{aligned}$$

Case 2: (Bilinear form for two basis functions in $\hat{\mathcal{V}}_{F_r}$)

Suppose $u = \hat{u}\circ F_r^{-1}, v = \hat{v}\circ F_r^{-1}$, where $\hat{u} = \hat{\psi}^*(\xi)\cdot\hat{N}_k(\xi)$ and $\hat{v} = \hat{\psi}^*(\xi)\cdot\hat{N}_l(\xi)$ are in $\hat{\mathcal{V}}_{F_r}$.

$$\begin{aligned}\mathcal{B}(u,v) &= \int_0^1 u_{xx}v_{xx}dx = \Big(\int_0^{F_r^{-1}(0.5)} + \int_{F_r^{-1}(0.5)}^1\Big)(u_{xx}\circ F_r)(v_{xx}\circ F_r).|J(F_r)|d\xi\\ \mathcal{F}(v) &= \Big(\int_0^{F_r^{-1}(0.5)} + \int_{F_r^{-1}(0.5)}^1\Big)(f\circ F_r)\cdot(\hat{v}).|J(F_r)|d\xi\end{aligned}$$

Let $\hat{w}(\xi) = (w \circ F_r)(\xi)$.Then

$$w_{xx} \circ F_r = \hat{w}_{\xi\xi}\Big((\frac{dF_r}{d\xi})^{-1}\Big)^2 + \hat{w}_{\xi}\Big((\frac{dF_r}{d\xi})^{-1}\Big)_{\xi}(\frac{dF_r}{d\xi})^{-1}$$

Now, if $w = \Big(\hat{\psi}^*(\xi) \cdot \hat{N}(\xi)\Big) \circ F_r^{-1} = \Big(\hat{\psi}^*(\xi) \cdot \hat{N}(\xi)\Big) \circ F_r^{-1}$, we have

$$\begin{aligned}
\hat{w} &= w \circ F_r = \Big(\hat{\psi}^*(\xi) \cdot \hat{N}(\xi)\Big), \\
\hat{w}_{\xi} &= (\hat{\psi}^*)_{\xi}\hat{N} + \hat{\psi}^*\hat{N}_{\xi}, \\
\hat{w}_{\xi\xi} &= (\hat{\psi}^*)_{\xi\xi}\hat{N}(\xi) + 2(\hat{\psi}^*)_{\xi}\hat{N}_{\xi}(\xi) + \hat{\psi}^*\hat{N}_{\xi\xi}(\xi).
\end{aligned}$$

where $(\hat{\psi}^*)_{\xi}$ and $(\hat{\psi}^*)_{\xi\xi}$, respectively, are as follows:

$$\begin{aligned}
(\hat{\psi}^*)_{\xi} &= \Big(\psi^*(F_r(\xi))\Big)_{\xi} = (\psi^*)_x(F_r(\xi))\frac{dF_r}{d\xi}, \\
(\hat{\psi}^*)_{\xi\xi} &= \psi^*(F_r(\xi))_{\xi\xi} = (\psi^*)_{xx}(F_r(\xi))(\frac{dF_r}{d\xi})^2
\end{aligned}$$

Case 3: (Bilinear form for mixed type:one in $\hat{\mathcal{V}}_{F_s}$ and the other in $\hat{\mathcal{V}}_{F_r}$)

For $\hat{u} \in \hat{\mathcal{V}}_{F_s}$ and $\hat{v} \in \hat{\mathcal{V}}_{F_r}$, domains of $\hat{u} \circ {F_s}^{-1}$ and $\hat{v} \circ {F_r}^{-1}$ have non-void intersections only on $[0.4, 0.5]$. Specifically, the product of two basis functions

$$u = \hat{u} \circ F_s^{-1} = \psi(x)(\hat{M} \circ F_s^{-1}) \text{ and } v = \hat{v} \circ F_r^{-1} = \psi^*(x)(\hat{N} \circ F_r^{-1})$$

vanish except for points in $[0.4, 0.5]$. That is, let $\hat{u} = \hat{\psi}\hat{M}$ and $\hat{v} = \hat{\psi}^*\hat{N}$.

$$
\begin{aligned}
\mathcal{B}(u,v) &= \int_0^1 \Big((\hat{u}\circ F_s^{-1})_{xx}(\hat{v}\circ F_r^{-1})_{xx}\Big)dx \\
&= \int_{0.4}^{0.5} \Big((\hat{u}\circ F_s^{-1})_{xx}(\hat{v}\circ F_r^{-1})_{xx}\Big)\circ F_r\circ F_r^{-1}dx \\
&= \int_{0.4}^{0.5} \Big[\Big((\hat{\psi}\cdot\hat{M}\circ F_s^{-1})_{xx}\circ F_r\Big)\cdot \\
&\quad \Big((\hat{\psi}^*\cdot\hat{N}\circ F_r^{-1})_{xx}\circ F_r\Big)\Big]\circ F_r^{-1}dx \\
&= \int_{F_s^{-1}(0.4)}^{1} \Big[\Big((\hat{\psi}\cdot\hat{M}\circ F_s^{-1})_{xx}\circ F_r\Big)\cdot \\
&\quad \Big((\hat{\psi}^*\cdot\hat{N}\circ F_r^{-1})_{xx}\circ F_r\Big)\Big]\circ(F_r^{-1}\circ F_s)|J(F_s)|d\xi \\
&= \int_{F_s^{-1}(0.4)}^{1} \Big((\hat{\psi}\cdot\hat{M}\circ F_s^{-1})_{xx}\circ F_s\Big)\cdot \\
&\quad \Big((\hat{\psi}^*\cdot\hat{N}\circ F_r^{-1})_{xx}\circ F_r\Big)\circ(F_r^{-1}\circ F_s)\cdot|J(F_s)|d\xi \\
&\text{where} \quad (F_r^{-1}\circ F_s)(\xi) = \frac{5}{6}(\xi^5 - 0.8).
\end{aligned}
$$

$$
\begin{aligned}
\mathcal{F}(v) &= \int_{F_s^{-1}(0.4)}^{1} (f\circ F_s)(v\circ F_s)\cdot|J(F_s)|d\xi \\
&= \int_{F_s^{-1}(0.4)}^{1} (f\circ F_s)(\xi)\cdot\psi^*(F_s(\xi))\cdot(\hat{N}\circ F_r^{-1}\circ F_s)\cdot|J(F_s)|d\xi
\end{aligned}
$$

(IV) Basis functions and mapping for Ω_2:

$$
G:\hat{\Omega}=[0,1]\to\Omega_2=[a,2] \quad \text{such that} \quad G(\xi) = (2-a)\xi + a
$$

$$
\text{Modified approximation space} \quad \hat{\mathcal{V}}_G = \{\hat{M}_k(\xi) : k = 3,\ldots,2q+1\},
$$

where $\hat{M}_{k,q+1}$ are B-splines corresponding to the following knot vector:

$$
\{\underbrace{0\ldots0}_{q+1},\underbrace{1/(q+1)}_{1},\underbrace{2/(q+1)}_{1},\ldots,\underbrace{q/(q+1)}_{1}\underbrace{1\ldots1}_{q+1}\}.
$$

To satisfy artificial BC, the first two B-spline functions were modified such that

$$\hat{M}^*_{1,q+1}(\xi) = (1-\xi)^9(1+9\xi)$$

$$\hat{M}^*_{2,q+1}(\xi) = (2-a)\hat{M}_{2,q+1}(\xi)/\hat{M}'_{2,q+1}(0)$$

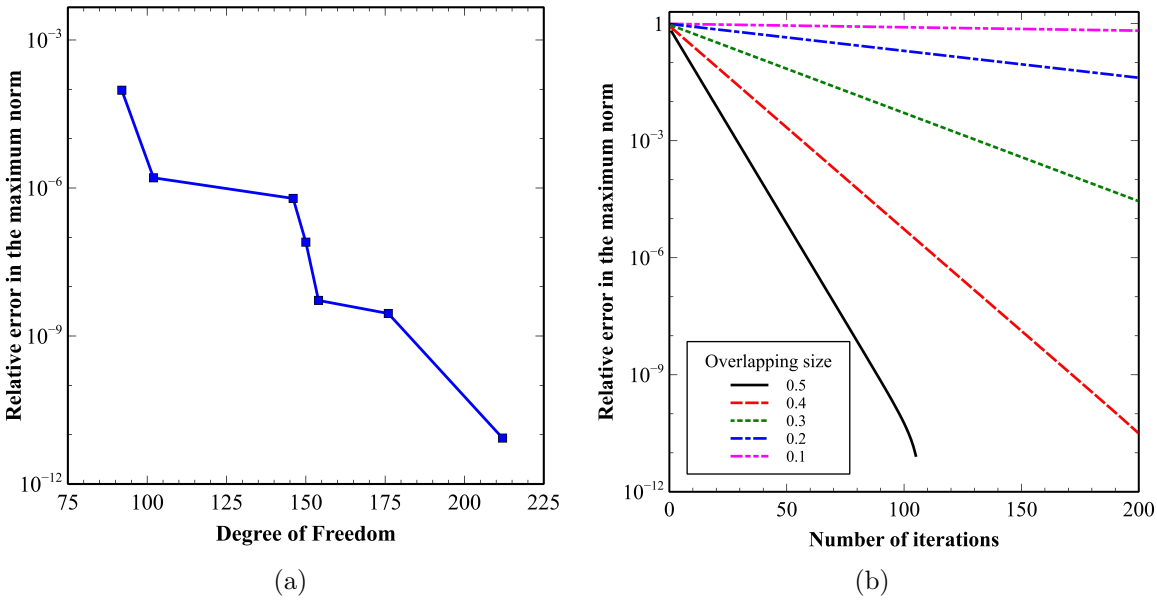

(a) (b)

Figure 17: 1D fourth-order problem containing singularity (a)Relative errors in the maximum norm for basis functions with different degrees for the fixed overlapping size a=0.5, (b)Relation between number of iterations and overlapping size between subdomains for the fixed degree p=8

5.2 2D Fourth-order Problem on a Cracked Circular Domain

Example 7. Consider $\Delta^2 u = f$ in the cracked circular domain Ω with clamped boundary conditions whose true solution is

$$u(r,\theta) = (2-r)^2 r^{1.5}\Big(\sin(1.5\theta) - 3\sin(0.5\theta) + \cos(1.5\theta) - \cos(0.5\theta)\Big).$$

Mappings from the reference domain into subdomains:

Table 6: Relative Errors in the maximum norm obtained by using Implicitly Enriched Schwarz Method for 1D fourth-order problem whose true solution contains singularity

Degree	DOF	Iteration	$\|RelErr\|_{Max}$
4	24	46	9.58E-005
5	27	51	1.61E-006
6	30	73	6.14E-007
7	33	75	7.98E-008
8	36	77	5.26E-009
9	39	88	2.86E-009
10	42	106	8.53E-012

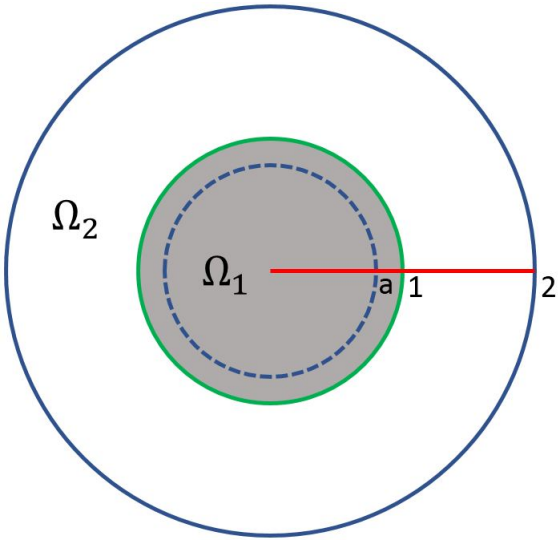

Figure 18: 2D cracked circular domain

- Geometric mapping onto Ω_1:

$$F : \hat{\Omega} = [0,1] \times [0,1] \longrightarrow \Omega_1 = \{(x,y) : 0 \leq x^2 + y^2 \leq 1\}$$

- Geometric mapping onto Ω_2:

$$G : \hat{\Omega} = [0,1] \times [0,1] \longrightarrow \Omega_2 = \{(x,y) : a^2 \leq x^2 + y^2 \leq 2^2\}$$

[**F-mapping:**] Define a mapping to deal with singularities as follows:

$$F(\xi,\eta) = (x(\xi,\eta), y(\xi,\eta)) = \eta^2\Big(\cos 2\pi(1-\xi), \sin 2\pi(1-\xi)\Big)$$

Then we have

$$\begin{aligned} J(F) &= \begin{bmatrix} 2\pi\eta^2 \sin 2\pi(1-\xi), & -2\pi\eta^2 \cos 2\pi(1-\xi) \\ 2\eta \cos 2\pi(1-\xi), & 2\eta \sin 2\pi(1-\xi) \end{bmatrix}, \quad |J(F)| = 4\pi\eta^3, \\ F^{-1}(x,y) &= (\xi(x,y), \eta(x,y)), \text{ where} \\ & \xi(x,y) = \begin{cases} 1 - \frac{1}{2\pi}\cos^{-1}\frac{x}{r} & \text{if } y \geq 0, \\ \frac{1}{2\pi}\cos^{-1}\frac{x}{r} & \text{if } y < 0, \end{cases} ; \quad \eta(x,y) = r^{1/2}. \end{aligned}$$

Flat-top PU functions on the physical domain:

$$\begin{aligned} \psi_R(r,\theta) &= \begin{cases} 1 & \text{if } 0 \leq r \leq 0.49 \\ \frac{1}{15^3}\Big(64-100r\Big)^2\Big(200r-83\Big) & \text{if } 0.49 \leq r \leq 0.64 \\ 0 & \text{if } 0.64 \leq r \leq 1 \end{cases} \\ \psi_L(r,\theta) &= 1 - \psi_R(r,\theta) \\ \hat{\psi}_R(\xi,\eta) &= \psi_R \circ F = \begin{cases} 1 & \text{if } 0 \leq \eta \leq 0.7 \\ \frac{1}{15^3}\Big(64-100\eta^2\Big)^2\Big(200\eta^2-83\Big) & \text{if } 0.7 \leq \eta \leq 0.8 \\ 0 & \text{if } 0.8 \leq \eta \leq 1 \end{cases} \\ \hat{\psi}_L(\xi,\eta) &= \psi_L \circ F = \begin{cases} 0 & \text{if } 0 \leq \eta \leq 0.7 \\ \frac{1}{15^3}\Big(100\eta^2-49\Big)^2\Big(143-200\eta^2\Big) & \text{if } 0.7 \leq \eta \leq 0.8 \\ 1 & \text{if } 0.8 \leq \eta \leq 1 \end{cases} \end{aligned}$$

Remark:

- $\psi_L(r,\theta) + \psi_R(r,\theta) = 1$ for all $(r,\theta) \in \Omega$, but $\hat{\psi}_L(\xi,\eta) + \hat{\psi}_R(\xi,\eta) \neq 1$.

Construction of $\mathcal{C}^1$-continuous basis functions satisfying clamped boundary conditions:

[I] Basis functions on Ω_{sing} : $\hat{N}_{k,p+1}(\xi), k = 1, 2, \ldots, p+10$, are $\mathcal{C}^{p-1}$-continuous B-splines of degree p, corresponding to an open knot vector

$$S_\xi = \{\underbrace{0 \ldots 0}_{p+1}, \frac{1}{10}, \frac{2}{10}, \ldots, \frac{8}{10}, \frac{9}{10}, \underbrace{1 \cdots 1}_{p+1}\}.$$

- To satisfy clamped boundary conditions along the crack, we remove the first two and the last two B-spline functions among $\hat{N}_{i,p+1}(\xi), 1 \leq i \leq p+10$.

- We define basis function on the reference domain for the mapping F as follows:

$$\hat{\mathcal{V}}_F^{sing} = \{\hat{N}_{i,p+1}(\xi)(\eta)^l : i = 3, \ldots, p+8; l = 3, 5, 7\}$$

The set $\hat{\mathcal{V}}_F^{sing} \circ F^{-1}$ generates the crack singularity in the radial direction:

$$r^{1.5}, r^{2.5}, r^{3.5} \quad \text{where} \quad r^2 = x^2 + y^2.$$

Using the PU function ψ_R, we construct basis functions defined on Ω_{sing} as follows:

$$\begin{aligned} \mathcal{V}_F^{sing} &= (\hat{\mathcal{V}}_F^{sing} \circ F^{-1}) \cdot \psi_R \\ &= \Big\{ \Big(\hat{N}_{i,p+1}(\xi) \cdot (\eta)^l \cdot \hat{\psi}_R(\xi, \eta) \Big) \circ F^{-1} : i = 3, \ldots, p+8; l = 3, 5, 7 \Big\}. \end{aligned}$$

[II] Basis functions on Ω_{reg} : $\hat{M}_{k,q+1}(\eta), k = 1, 2, \ldots, q+13$: B-splines corresponding to an open knot vector

$$S_\eta = \{\underbrace{0 \ldots 0}_{q+1}, 0.7, 0.7, 0.725, 0.725, 0.75, 0.75, 0.775, 0.775, 0.8, 0.8, 0.9, 0.9, \underbrace{1 \ldots 1}_{q+1}\}.$$

We choose approximation functions on the subdomain Ω_{reg} as follows:

$$\hat{\mathcal{V}}_F^{reg} = \{\hat{N}_{i,p+1}(\xi) \cdot \hat{M}_{j,q+1}(\eta) : i = 3, \ldots, p+8; j = 1, \cdots, q+13\}.$$

$$\begin{aligned} \mathcal{V}_F^{reg} &= (\hat{\mathcal{V}}_F^{reg} \circ F^{-1}) \cdot \psi_L \\ &= \Big\{\psi_L(x,y) \times \Big(\hat{N}_{i,p+1}(\xi) \cdot \hat{M}_{j,q+1}(\eta)\Big) \circ F^{-1} : \\ &\qquad\qquad 3 \le i \le p+8; 1 \le j \le q+13\Big\} \end{aligned}$$

The last two basis functions on the η direction are modified as follow:

$$\begin{aligned} \hat{M}^*_{2q,q+1}(\eta) &= \frac{\hat{M}_{2q,q+1}(\eta)}{\hat{M}'_{2q,q+1}(1)} \\ \hat{M}^*_{2q+1,q+1}(\eta) &= (0.3\eta + 0.7)^{10}(11 - 10(0.3\eta + 0.7)) \end{aligned}$$

[G-mapping:] Define a geometric mapping $G : \hat{\Omega} = [0,1]\times[0,1] \longrightarrow \Omega_2 = \{(x,y) : a^2 \le x^2 + y^2 \le 2^2\}$ by

$$G(\xi,\eta) = (a + (2-a)\eta)\Big(\cos 2\pi(1-\xi), \sin 2\pi(1-\xi)\Big)$$

where Ω_2 has a crack along the positive x-axis and $0.3 \le a < 1$. Then we have

$$G^{-1}(x,y) = (\xi(x,y), \eta(x,y))$$

where

$$\xi(x,y) = \begin{cases} \frac{1}{2\pi}\cos^{-1}(\frac{x}{r}), & \text{if } y < 0 \\ (1 - \frac{1}{2\pi}\cos^{-1}(\frac{x}{r})), & \text{if } 0 \le y \end{cases}; \quad \eta(x,y) = \frac{(r-a)}{(2-a)}.$$

$$r = \sqrt{x^2+y^2}; \quad |J(G)| = 2(2-a)\pi\Big(a + (2-a)\eta\Big).$$

We choose approximation space on the subdomain Ω_2 as follows:

$$\hat{\mathcal{V}}_G = \{\hat{N}_{i,p+1}(\xi) \cdot \hat{M}_{j,q+1}(\eta) : i = 3, \ldots, p+8; j = 1, \cdots, q+8\}.$$

where the last two basis functions are discarded to satisfy homogeneous clamped boundary conditions, and the first two basis functions are modified to satisfy non-homogeneous artificial boundary conditions such that

$$\begin{aligned} \hat{M}^*_{1,q+1}(\eta) &= (1-\eta)^{10}(1+10\eta) \\ \hat{M}^*_{2,q+1}(\eta) &= \frac{\hat{M}_{2,q+1}(\eta)}{\hat{M}'_{2,q+1}(0)} \end{aligned}$$

Approximation Space on Ω

Our approximation space to deal with fourth-order partial differential equation on a cracked circular domain Ω is

$$\mathcal{V}_\Omega = \mathcal{V}_G \cup \mathcal{V}_F^{reg} \cup \mathcal{V}_F^{sing} \tag{40}$$

We observe the following:

- The total number of the degree of freedom is

$$\begin{aligned} \text{card}(\mathcal{V}_\Omega) &= \text{card}(\mathcal{V}_F^{reg}) + \text{card}(\mathcal{V}_F^{sing}) + \text{card}(\mathcal{V}_G) \\ &= (p+6)(q+13) + (p+6)(3) + (p+6)(q+8) \\ &= (p+6)\Big(2q+24\Big) \end{aligned}$$

- The intersections of basis functions in $\mathcal{V}_F^{sing}$ and those in $\mathcal{V}_F^{reg}$ occur only in the

Table 7: Relative errors in the maximum norm obtained by using Implicitly Enriched Schwarz Method for 2D fourth-order problem on a Cracked Circular Domain

Degree	DOF	Number of Iteration	$\|RelErr\|_{Max}$
6	432	24	1.77E-006
7	494	32	3.33E-007
8	560	27	5.42E-008
9	630	29	1.32E-008
10	704	48	3.32E-009

annular region

$$\Omega_{sing} \cap \Omega_{reg} = \{(r, \theta) : 0 < \theta < 2\pi, \quad a \leq r \leq 1\}.$$

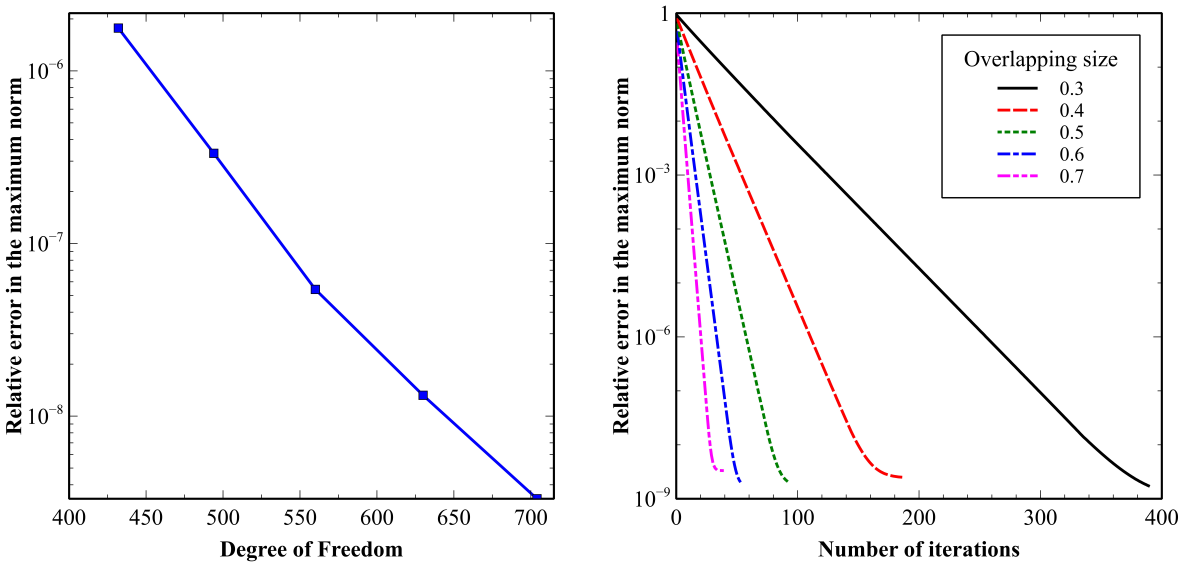

(a) (b)

Figure 19: 2D fourth-order problem on a cracked circular domain (a)Relative errors in the maximum norm for basis functions with different degrees p=6,7,8,9, and 10 for the fixed overlapping size, (b)Relation betwen number of iterations and overlapping size between subdomains for the fixed degree p=8, i.e., no extra cost is required

5.3 2D Fourth-order Problem on a Cracked Square Domain

Example 8. Consider the fourth-order equation $\Delta^2 u = f$ in the square domain $\Omega = [-2,2] \times [-2,2]$ with crack along the positive x-axis. Then imposing **homogeneous** clamped BC along the crack faces and **non-homogeneous** clamped BC along other parts of $\partial\Omega$,

$$\begin{aligned} u(r,\theta) =& 0.5r^{1.5}\Big(\sin(1.5\theta) - 3\sin(0.5\theta)\Big) + 0.7r^{1.5}\Big(\cos(1.5\theta) - \cos(0.5\theta)\Big) \\ &+ r^{2.5}\Big(\sin(2.5\theta) - 5\sin(0.5\theta)\Big) + r^{2.5}\Big(\cos(2.5\theta) - \cos(0.5\theta)\Big) \end{aligned}$$

, which is constucted by the Grisvard Theorem (21), solves this biharmonic equation with respect to $f(r,\theta) = \Delta^2 u = 0$.

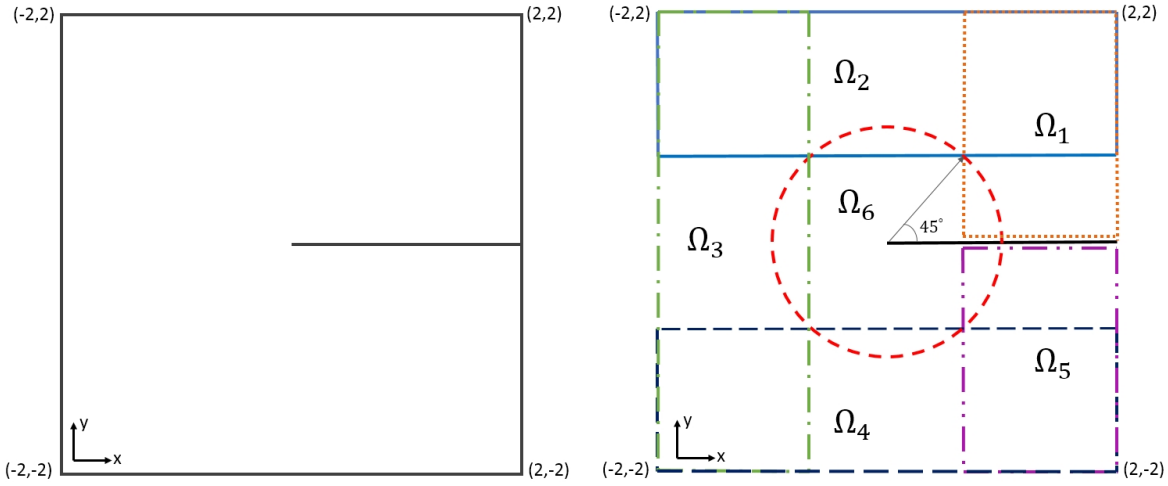

Figure 20: Cracked Square domain Ω and its partition into six subdomains $\Omega_i, i = 1, 2, ..., 6$.

PU-IGA with Mapping Method

We partition the physical domain into six subdomains as shown in Figure 20 We construct five geometric mappings G_1, G_2, G_3, G_4, and G_5 onto Ω_1, Ω_2, Ω_3, Ω_4, and Ω_5 respectively. In order to capture the singularities around the crack tip in

subdomain Ω_6, we divide the subdomain into singular zone $\Omega_{6_{sing}} = \{(r,\theta) : 0 < \theta < 2\pi, \quad 0 \le r \le 0.4\}$ and non-singular zone $\Omega_{6_{reg}} = \{(r,\theta) : 0 < \theta < 2\pi, \quad 0.3 \le r \le 1\}$. We consider F-mapping to generate singular functions resembling the singularities on a singular zone $\Omega_{6_{sing}}$ and G_6-mapping to build regular basis functions on a regular zone $\Omega_{6_{reg}}$.

[G_1-mapping]: $G_1 : \hat{\Omega} = [0,1] \times [0,1] \to \Omega_1 = [\frac{1}{\sqrt{2}}, 2] \times [0,2]$

$$G_1(\xi,\eta) = \begin{cases} x(\xi,\eta) = \frac{1}{\sqrt{2}} + (2 - \frac{1}{\sqrt{2}})\xi, \\ y(\xi,\eta) = 2\eta \end{cases}$$

where

$$J(G_1) = \begin{bmatrix} 2 - \frac{1}{\sqrt{2}} & 0 \\ 0 & 2 \end{bmatrix}, \quad |J(G_1)| = 4 - \frac{2}{\sqrt{2}}$$

[G_2-mapping]: $G_2 : \hat{\Omega} = [0,1] \times [0,1] \to \Omega_2 = [-2,2] \times [\frac{1}{\sqrt{2}}, 2]$

$$G_2(\xi,\eta) = \begin{cases} x(\xi,\eta) = -2 + 4\xi, \\ y(\xi,\eta) = \frac{1}{\sqrt{2}} + (2 - \frac{1}{\sqrt{2}})\eta \end{cases}$$

where

$$J(G_2) = \begin{bmatrix} 4 & 0 \\ 0 & 2 - \frac{1}{\sqrt{2}} \end{bmatrix}, \quad |J(G_2)| = 8 - \frac{4}{\sqrt{2}}$$

[G_3-mapping]: $G_3 : \hat{\Omega} = [0,1] \times [0,1] \to \Omega_3 = [-2, -\frac{1}{\sqrt{2}}] \times [-2, 2]$

$$G_3(\xi,\eta) = \begin{cases} x(\xi,\eta) = -2 + (2 - \frac{1}{\sqrt{2}})\xi, \\ y(\xi,\eta) = -2 + 4\eta \end{cases}$$

where

$$J(G_3) = \begin{bmatrix} 2 - \frac{1}{\sqrt{2}} & 0 \\ 0 & 4 \end{bmatrix}, \quad |J(G_3)| = 8 - \frac{4}{\sqrt{2}}$$

[G_4-mapping]: $G_4 : \hat{\Omega} = [0,1] \times [0,1] \to \Omega_4 = [-2, 2] \times [-2, -\frac{1}{\sqrt{2}}]$

$$G_4(\xi,\eta) = \begin{cases} x(\xi,\eta) = -2 + 4\xi, \\ y(\xi,\eta) = -2 + (2 - \frac{1}{\sqrt{2}})\eta \end{cases}$$

where

$$J(G_4) = \begin{bmatrix} 4 & 0 \\ 0 & 2 - \frac{1}{\sqrt{2}} \end{bmatrix}, \quad |J(G_4)| = 8 - \frac{4}{\sqrt{2}}$$

[G_5-mapping]: $G_5 : \hat{\Omega} = [0,1] \times [0,1] \to \Omega_5 = [\frac{1}{\sqrt{2}}, 2] \times [-2, 0]$

$$G_5(\xi,\eta) = \begin{cases} x(\xi,\eta) = \frac{1}{\sqrt{2}} + (2 - \frac{1}{\sqrt{2}})\xi, \\ y(\xi,\eta) = -2 + 2\eta \end{cases}$$

where

$$J(G_5) \;=\; \begin{bmatrix} 2-\dfrac{1}{\sqrt{2}} & 0 \\ 0 & 2 \end{bmatrix}, \quad |J(G_3)| = 4 - \frac{2}{\sqrt{2}}$$

[G_6-mapping]: $G_6 : \hat{\Omega} = [0,1]\times[0,1] \longrightarrow \Omega_{6_{reg}}$

$$G_6(\xi,\eta) = (0.3+0.7\eta)\Big(\cos 2\pi(1-\xi), \sin 2\pi(1-\xi)\Big) \tag{41}$$

where $\Omega_{6_{reg}}$ has a crack along the positive x-axis. Then we have

$$G_6^{-1}(x,y) \;=\; (\xi(x,y),\eta(x,y))$$

$$\xi(x,y) \;=\; \begin{cases} \dfrac{1}{2\pi}\cos^{-1}(\dfrac{x}{r}) & \text{if } y<0 \\ 1-\frac{1}{2\pi}\cos^{-1}(\frac{x}{r}) & \text{if } 0\le y \end{cases}, \qquad \eta(x,y) = \frac{(r-0.3)}{0.7}$$

$$J(G_6) \;=\; \begin{bmatrix} 2\pi(0.3+0.7\eta)\sin 2\pi(1-\xi), & -2\pi(0.3+0.7\eta)\cos 2\pi(1-\xi) \\ 0.7\cos 2\pi(1-\xi), & 0.7\sin 2\pi(1-\xi) \end{bmatrix}$$

$$|J(G_6)| = 1.4\pi\Big(0.3+0.7\eta\Big)$$

[F-mapping]: Next, define a mapping to deal with singularities

$$F : \hat{\Omega} = [0,1]\times[0,1] \longrightarrow \Omega_{6_{sing}}$$

that maps polynomials to singular functions as follows:

$$F(\xi,\eta) = 0.4\eta^2\Big(\cos 2\pi(1-\xi), \sin 2\pi(1-\xi)\Big)$$

Then

$$F^{-1}(x,y) = (\xi(x,y), \eta(x,y))$$

where

$$\xi(x,y) = \begin{cases} \frac{1}{2\pi}\cos^{-1}(\frac{x}{r}) & \text{if } y < 0 \\ 1 - \frac{1}{2\pi}\cos^{-1}(\frac{x}{r}) & \text{if } 0 \le y \end{cases}, \qquad \eta(x,y) = \frac{r^{1/2}}{\sqrt{0.4}}$$

$$J(F) = \begin{bmatrix} 0.8\pi\eta^2 \sin 2\pi(1-\xi), & -0.8\pi\eta^2 \cos 2\pi(1-\xi) \\ 0.8\eta \cos 2\pi(1-\xi), & 0.8\eta \sin 2\pi(1-\xi) \end{bmatrix}, \quad |J(F)| = 0.64\pi\eta^3$$

$\mathcal{C}^1$-continuous flat-top PU functions: We define the following $\mathcal{C}^1$-continuous flat-top PU functions on the physical domain Ω:

$$\begin{aligned} \psi_R(r,\theta) &= \begin{cases} 1 & \text{if } 0 \le r \le 0.3 \\ \Big(4-10r\Big)^2\Big(20r-5\Big) & \text{if } 0.3 \le r \le 0.4 \\ 0 & \text{if } 0.4 \le r \le 1 \end{cases} \\ \hat{\psi}_R(\xi,\eta) &= \psi_R \circ F \\ &= \begin{cases} 1 & \text{if } 0 \le \eta \le \sqrt{0.75} \\ \Big(4-4\eta^2\Big)^2\Big(8\eta^2-5\Big) & \text{if } \sqrt{0.75} \le \eta \le 1 \\ 0 & \text{if } 1 \le \eta \end{cases} \end{aligned} \tag{42}$$

$$\begin{aligned} \psi_L(r,\theta) &= 1 - \psi_R(r,\theta) \\ \hat{\psi}_L(\xi,\eta) &= \psi_L \circ G_6 \\ &= \begin{cases} 0 & \text{if } \eta \le 0 \\ -49\eta^2(14\eta-3) & \text{if } 0 \le \eta \le 1/7 \\ 1 & \text{if } 1/7 \le \eta \end{cases} \end{aligned} \tag{43}$$

Note that $\psi_L(r,\theta)+\psi_R(r,\theta)=1$ for all $(r,\theta)\in\Omega$, but $\hat{\psi}_L(\xi,\eta)+\hat{\psi}_R(\xi,\eta)\neq 1$.

Construction of $\mathcal{C}^1$ basis functions

Basis functions on $\Omega_1,\Omega_2,\cdots,\Omega_5$:

We assume for $p,q\geq 4$, $\hat{N}^1_{k,p+1}(\xi),\ldots,\hat{N}^5_{k,p+1}(\xi), k=1,2,\ldots,2p+1$, and $\hat{M}^1_{l,q+1}(\eta),\ldots,\hat{M}^5_{l,q+1}(\eta), l=1,2,\ldots,2q+1, l=1,2,\ldots,2q+1$ are $\mathcal{C}^{p-1}$ and $\mathcal{C}^{q-1}$-continuous B-splines, respectively, corresponding to an open knot vectors

$$\begin{aligned}
S^1_\xi=S^3_\xi=S^5_\xi &= \{\underbrace{0\ldots0}_{p+1},0.1,0.2,\ldots,0.8,0.9,\underbrace{1\cdots1}_{p+1}\}.\\
S^2_\xi=S^4_\xi &= \{\underbrace{0\ldots0}_{p+1},0.05,0.1,\ldots,0.9,0.95,\underbrace{1\cdots1}_{p+1}\}.\\
S^1_\eta=S^2_\eta=S^4_\eta=S^5_\eta &= \{\underbrace{0\ldots0}_{q+1},0.1,0.2,\ldots,0.8,0.9,\underbrace{1\cdots1}_{q+1}\}.\\
S^3_\eta &= \{\underbrace{0\ldots0}_{q+1},0.05,0.1,\ldots,0.9,0.95,\underbrace{1\cdots1}_{q+1}\}.
\end{aligned}$$

Define basis functions on the reference domain for the corresponding geometric mappings as follows:

$$\hat{\mathcal{V}}_{G_1}=\{\hat{N}^1_{i,p+1}(\xi)\cdot\hat{M}^1_{j,q+1}(\eta): i=1,\ldots,p+10; j=3,\cdots,q+10\}.$$

$$\hat{\mathcal{V}}_{G_2}=\{\hat{N}^2_{i,p+1}(\xi)\cdot\hat{M}^2_{j,q+1}(\eta): i=1,\ldots,p+20; j=1,\cdots,q+10\}.$$

$$\hat{\mathcal{V}}_{G_3}=\{\hat{N}^3_{i,p+1}(\xi)\cdot\hat{M}^3_{j,q+1}(\eta): i=1,\ldots,p+10; j=1,\cdots,q+20\}.$$

$$\hat{\mathcal{V}}_{G_4}=\{\hat{N}^4_{i,p+1}(\xi)\cdot\hat{M}^4_{j,q+1}(\eta): i=1,\ldots,p+20, j=1,\cdots,q+10\}.$$

$$\hat{\mathcal{V}}_{G_5}=\{\hat{N}^5_{i,p+1}(\xi)\cdot\hat{M}^5_{j,q+1}(\eta): i=1,\ldots,p+10; j=1,\cdots,q+8\}.$$

The corresponding approximation functions on the physical subspaces are as follows:

$$\begin{aligned} \mathcal{V}_{G_1} &= (\hat{\mathcal{V}}_{G_1} \circ G_1^{-1}) \\ &= \left\{ \left(\hat{N}^1_{i,p+1}(\xi) \cdot \hat{M}^1_{j,q+1}(\eta) \right) \circ G_1^{-1} : 1 \leq i \leq p+10; 3 \leq j \leq q+10 \right\} \end{aligned} \tag{44}$$

On Ω_1, the first two among $\hat{M}^1_{i,q+1}(\eta), 1 \leq i \leq q+10$, were discarded in the η-direction to satisfy the clamped boundary condition on the crack. In the ξ-direction, the first two basis functions were modified to satisfy non-homgeneous artificial boundary condition on the interface, and the last two were modified to satisfy non-homogeneous clamped boundary conditions.

$$\begin{aligned} \mathcal{V}_{G_2} &= (\hat{\mathcal{V}}_{G_2} \circ G_2^{-1}) \\ &= \left\{ \left(\hat{N}^2_{i,p+1}(\xi) \cdot \hat{M}^2_{j,q+1}(\eta) \right) \circ G_2^{-1} : 1 \leq i \leq p+20; 1 \leq j \leq q+10 \right\} \end{aligned} \tag{45}$$

On Ω_2, the first two and the last two basis functions were modified in the ξ-direction to satisfy non-homogeneous clamped boundary condition. In the η-direction, the first two basis functions were modified to satisfy non-homgeneous artificial boundary condition on the interface, and the last two were modified to satisfy non-homogeneous clamped boundary conditions.

$$\begin{aligned} \mathcal{V}_{G_3} &= (\hat{\mathcal{V}}_{G_3} \circ G_3^{-1}) \\ &= \left\{ \left(\hat{N}^3_{i,p+1}(\xi) \cdot \hat{M}^3_{j,q+1}(\eta) \right) \circ G_3^{-1} : 1 \leq i \leq p+10; 1 \leq j \leq q+20 \right\} \end{aligned} \tag{46}$$

On Ω_3, the first two and the last two basis functions in the η-direction are modified to satisfy non-homogeneous clamped boundary condition. In the ξ-direction, the first two were modified to satisfy non-homogeneous clamped boundary conditions, and the

last two basis functions were modified to satisfy non-homgeneous artificial boundary condition on the interface.

$$\begin{aligned} \mathcal{V}_{G_4} &= (\hat{\mathcal{V}}_{G_4} \circ G_4 - 1) \\ &= \left\{ \left(\hat{N}^4_{i,p+1}(\xi) \cdot \hat{M}^4_{j,q+1}(\eta) \right) \circ G_4^{-1} : 1 \le i \le p+20; 1 \le j \le q+10 \right\} \end{aligned} \tag{47}$$

On Ω_4, the first two and the last two basis functions were modified in the ξ-direction to satisfy non-homogeneous clamped boundary condition. In the η-direction, the first two were modified to satisfy non-homogeneous clamped boundary conditions, and the last two basis functions were modified to satisfy non-homgeneous artificial boundary condition on the interface.

$$\begin{aligned} \mathcal{V}_{G_5} &= (\hat{\mathcal{V}}_{G_5} \circ G_5^{-1}) \\ &= \left\{ \left(\hat{N}^5_{i,p+1}(\xi) \cdot \hat{M}^5_{j,q+1}(\eta) \right) \circ G_5^{-1} : 1 \le i \le p+10; 1 \le j \le q+8 \right\} \end{aligned} \tag{48}$$

On Ω_5, the last two among $\hat{M}_{i,q+1}, 1 \le i \le q+10$, were discarded in the η-direction to satisfy the clamped boundary condition on the crack, and the first two were modified. In the ξ-direction, the first two basis functions were modified to satisfy non-homgeneous artificial boundary condition on the interface, and the last two were modified to satisfy non-homogeneous clamped boundary conditions.

Basis functions on $\Omega_{6_{sing}}$

We assume $p \ge 4$. $\hat{N}^6_{k,p+1}(\xi), k = 1, 2, \ldots, p+19$, are $\mathcal{C}^{p-1}$-continuous B-splines of degree p, corresponding to an open knot vector

$$S^6_\xi = \{\underbrace{0 \ldots 0}_{p+1}, 0.05, 0.1, \ldots, 0.9, 0.95, \underbrace{1 \cdots 1}_{p+1}\}$$

We removed the first two and the last two B-spline functions among $\hat{N}_{i,p+1}(\xi), 1 \leq i \leq p+19$, so that the homogeneous clamped boundary conditions are satisfied at both ends. We define basis functions on the reference domain for the mapping F as follows:

$$\hat{\mathcal{V}}_F = \{\hat{N}^6_{i,p+1}(\xi)(\eta\sqrt{0.4})^l : i = 3, \ldots, p+17; l = 3, 5\}.$$

Then the set $\hat{\mathcal{V}}_F \circ F^{-1}$ generates the crack singularity $r^{1.5}, r^{2.5}$ in the radial direction, where $r^2 = x^2 + y^2$.

Using the PU function ψ_R, we construct basis functions defined on $\Omega_{6_{sing}}$ as follows:

$$\begin{aligned} \mathcal{V}_F &= (\hat{\mathcal{V}}_F \circ F^{-1}) \cdot \psi_R \\ &= \left\{ \left(\hat{N}^6_{i,p+1}(\xi) \cdot (\eta\sqrt{0.4})^l \cdot \hat{\psi}_R(\xi, \eta) \right) \circ F^{-1} : i = 3, \ldots, p+17; l = 3, 5 \right\} \quad (49) \end{aligned}$$

Basis functions on $\Omega_{6_{reg}}$

We define basis functions on the reference domain for the mapping G_6 as follows:

$$\hat{\mathcal{V}}_{G_6} = \{\hat{N}^6_{i,p+1}(\xi) \cdot \hat{M}^6_{j,q+1}(\eta) : i = 3, \ldots, p+18; j = 1, \cdots, q+5\},$$

where $\hat{N}_{i,p+1}(\xi), i = 3, 2, \ldots, p+17$, and $\hat{M}_{j,q+1}(\eta), j = 1, 2, \ldots, q+5$ are $\mathcal{C}^{p-1}$ and $\mathcal{C}^{q-1}$-continuous B-splines, respectively, corresponding to an open knot vectors

$$\begin{aligned} S^6_\xi &= \{\underbrace{0 \ldots 0}_{p+1}, 0.05, 0.1, \ldots, 0.9, 0.95, \underbrace{1 \cdots 1}_{p+1}\} \\ S^6_\eta &= \{\underbrace{0 \ldots 0}_{q+1}, 0.2, 0.4, 0.6, 0.8, \underbrace{1 \cdots 1}_{q+1}\}. \end{aligned}$$

We construct basis functions defined on $\Omega_{6_{reg}}$ by using the PU function ψ_L as follows:

$$\begin{aligned} \mathcal{V}_{G_6} &= (\hat{\mathcal{V}}_{G_6} \circ G_6^{-1}) \cdot \psi_L \qquad (50) \\ &= \left\{ \left(\hat{N}^6_{i,p+1}(\xi) \cdot \hat{M}^6_{j,q+1}(\eta) \cdot \hat{\psi}_L(\xi,\eta) \right) \circ G_6^{-1} : 3 \le i \le p+17; 1 \le j \le q+5 \right\} \end{aligned}$$

On $\Omega_{6_{reg}}$, the last two among $\hat{M}_{j,q+1}, 1 \le i \le q+5$, were modified in the η-direction to satisfy the non-homogeneous cramped boundary condition on the boundary. The first two and the last two among $\hat{N}_{i,p+1}, 1 \le i \le p+19$, were removed in the ξ-direction to safisfy homogeneous clamped boundary conditions on the crack.

Approximation Space on Ω

Approximation space to deal with fourth-order partial differential equation on a cracked square domain Ω is

$$\mathcal{V}_\Omega = \mathcal{V}_{G_1} \cup \mathcal{V}_{G_2} \cup \mathcal{V}_{G_3} \cup \mathcal{V}_{G_4} \cup \mathcal{V}_{G_5} \cup \mathcal{V}_{G_6} \cup \mathcal{V}_F$$

- The total number of the degree of freedom is

$$\begin{aligned} \text{card}(\mathcal{V}_\Omega) &= \text{card}(\mathcal{V}_{G_1}) + \cdots + \text{card}(\mathcal{V}_{G_6}) + \text{card}(\mathcal{V}_F) \\ &= \Big(2 * (p+10) * (q+8)\Big) + \Big(2 * (p+20) * (q+10)\Big) \\ &+ \Big((p+10) * (q+20)\Big) + \Big((p+16)(2+q+5)\Big) \end{aligned}$$

- The intersections of basis functions in $\mathcal{V}_F$ and those in $\mathcal{V}_{G_6}$ occur only in the annular region

$$\Omega_{sing} \cap \Omega_{reg} = \{(r,\theta) : 0 < \theta < 2\pi, \quad 0.3 \le r \le 0.4\}.$$

For $u, v \in \mathcal{V}_{G_6}$, we implement this mapping method calculating the bilinear form $\mathcal{B}(u,v)$ and load vector $\mathcal{F}(v)$ as follows. Let $\triangle_{xy} = \dfrac{\partial^2}{\partial x^2} + \dfrac{\partial^2}{\partial y^2}$

Case 1: $\forall u, v \in \mathcal{V}_F$

$$\begin{aligned}
\mathcal{B}(u,v) &= \int_0^{2\pi}\int_0^{0.4} (\Delta_{xy}u)(\Delta_{xy}v)dxdy \\
&= \Big(\int_0^1\int_0^{F^{-1}(0.3)} + \int_0^1\int_{F^{-1}(0.3)}^1\Big)(\Delta_{xy}u)\circ F \cdot (\Delta_{xy}v)\circ F \cdot |J(F)|d\xi d\eta \\
\mathcal{F}(v) &= \Big(\int_0^1\int_0^{F^{-1}(0.4)} + \int_0^1\int_{F^{-1}(0.4)}^1\Big) f(F(\xi,\eta))\cdot \hat{v}\cdot |J(F)|d\xi d\eta
\end{aligned}$$

Case 2: $\forall u, v \in \mathcal{V}_{G_6}$

$$\begin{aligned}
\mathcal{B}(u,v) &= \Big(\int_0^1\int_0^{G_6^{-1}(0.4)} + \int_0^1\int_{G_6^{-1}(0.4)}^1\Big)(\Delta_{xy}u)\circ G_6 \cdot (\Delta_{xy}v)\circ G_6 \cdot |J(G_6)|d\xi d\eta \\
\mathcal{F}(v) &= \Big(\int_0^1\int_0^{G_6^{-1}(0.4)} + \int_0^1\int_{G_6^{-1}(0.4)}^1\Big) f(G_6(\xi,\eta))\cdot \hat{v}\cdot |J(G_6)|d\xi d\eta
\end{aligned}$$

Case 3: $\forall u \in \mathcal{V}_F$ **and** $\forall v \in \mathcal{V}_{G_6}$

$$\begin{aligned}
\mathcal{B}(u,v) &= \int_0^{2\pi}\int_0^{0.4} (\Delta_{xy}u)(\Delta_{xy}v)dxdy \\
&= \int_0^{2\pi}\int_{0.3}^{0.4} \Delta_{xy}(\hat{u}\circ F^{-1})\Delta_{xy}(\hat{v}\circ G_6^{-1})\circ G_6 \circ G_6^{-1} dxdy \\
&= \int_0^{2\pi}\int_{0.3}^{0.4} \Big(\Delta_{xy}(\hat{u}\circ F^{-1})\circ G_6 \cdot \Delta_{xy}(\hat{v}\circ G_6^{-1})\circ G_6\Big)\circ G_6^{-1} dxdy \\
&= \int_0^1\int_{F^{-1}(0.3)}^1 \Big((\Delta_{xy}(\hat{u}\circ F^{-1})\circ G_6 \cdot \Delta_{xy}(\hat{v}\circ G_6^{-1})\circ G\Big)\circ \\
&\quad (G_6^{-1}\circ F)\cdot |J(F)|d\xi d\eta \\
&= \int_0^1\int_{F^{-1}(0.3)}^1 \Big(\Delta_{xy}(\hat{u}\circ F^{-1})\circ F\Big)\cdot\Big(\Delta_{xy}(\hat{v}\circ G_6^{-1})\circ G_6\Big)\circ \\
&\quad (G_6^{-1}\circ F)\cdot |J(F)|d\xi d\eta
\end{aligned}$$

where

$$(G_6^{-1} \circ F)(\xi, \eta) = (\xi, \quad \frac{0.4\eta^2 - 0.3}{0.7}).$$

Note that the second part of the last integral is actually $\Delta_{xy}(\hat{v} \circ G_6^{-1}) \circ F$. However, the simple relation $\nabla_{xy}(\hat{v} \circ G_6^{-1}) \circ G = J(G_6)^{-1} \cdot \nabla_{\xi\eta}(\hat{v})$ is not applicable to that form.

The pullback of the Laplacian on the physical domain onto the reference domain for the stiffness matrix calculation is calculated as shown in the previous section.

Iteration Algorithm

The proposed iterative method for fourth-order problem on a square domain containing crack singularity is as follows:

Step 0: (Initializing)

(i) Find an approximate solutions $u_2^{(0)}$, $u_4^{(0)}$, and $u_6^{(0)}$ by taking initial guesses 0 on artificial boundaries of subdomains Ω_2, Ω_4, and Ω_6 using the k-refinement of B-spline basis functions with fixed p-degree ($p = 8$).

(ii) Taking the values of the approximate solution $u_2^{(0)}$, $u_4^{(0)}$, and $u_6^{(0)}$ as artificial boundary conditions along corresponding interfaces, find $u_1^{(0)}$, $u_3^{(0)}$, and $u_5^{(0)}$ solving each subproblem independently.

Step II: Update approximate solutions in the following order:

- Find $u_2^{(k+1)}$ by updating corresponding artificial boundary conditions with $u_1^{(k)}$, $u_3^{(k)}$, and $u_6^{(k)}$.
- Find $u_4^{(k+1)}$ by updating corresponding artificial boundary conditions with $u_3^{(k)}$, $u_5^{(k)}$, and $u_6^{(k)}$.

Table 8: Relative errors in the maximum norm obtained by using Implicitly Enriched Schwarz Method for 2D fourth-order problem on a Cracked Square Domain

Degree	DOF	Iterations	$\|RelErr\|_{Max}$
4	1564	1590	8.67E-004
5	1767	3370	8.50E-006
6	1982	3490	4.97E-006
7	2209	3541	7.65E-007
8	2448	4436	9.98E-008

- Find $u_1^{(k+1)}$ by updating corresponding artificial boundary conditions with $u_2^{(k+1)}$ and $u_6^{(k)}$.
- Find $u_3^{(k+1)}$ by updating corresponding artificial boundary conditions with $u_2^{(k+1)}$, $u_4^{(k+1)}$, and $u_6^{(k)}$.
- Find $u_5^{(k+1)}$ by updating corresponding artificial boundary conditions with $u_4^{(k+1)}$ and $u_6^{(k)}$.
- Find $u_6^{(k+1)}$ by updating corresponding artificial boundary conditions with $u_1^{(k+1)}$, $u_2^{(k+1)}$, $u_3^{(k+1)}$, $u_4^{(k+1)}$, and $u_5^{(k+1)}$.

Let $Error = \|u_{true} - u^{k+1}\|_{\infty,rel} = \dfrac{\|u_{true} - u^{k+1}\|_\infty}{\|u_{true}\|_\infty}$ be the relative error in the maximum norm and TOL is a given number.

- if $Error \leq TOL = 10^{-8}$ or the iteration number ≥ 4500 , then stop the iteration steps. An approximate solution is $u_h = u^{(k+1)}$.
- if $Error \geq TOL$, go to Step II.

To decrease required number of iterations in Example 8, we increase overlapping size with a new partition shown in Figure 21. Table 9 shows that new partition

Table 9: Relative errors in the maximum norm obtained by using Implicitly Enriched Schwarz Method for 2D fourth-order problem on a Cracked Square Domain with Larger Overlapping Size

Degree	DOF	Iterations	$\|RelErr\|_{Max}$
4	1564	46	1.58E-004
5	1767	224	6.70E-006
6	1982	229	4.04E-007
7	2209	261	2.64E-007
8	2448	329	9.90E-008

provides almost same accuracy with less number of iterations. The larger overlapping parts among subdomain, the faster the Schwarz Alternating method converges. However, if the subdomains are close to the crack tip, the local solutions on the subdomains are influenced by the singularity. Hence, we choose subdomains which are away from the singularity zone, $\{(r, \theta) : 0 < \theta < 2\pi, \quad 0 \leq r \leq 0.4\}$

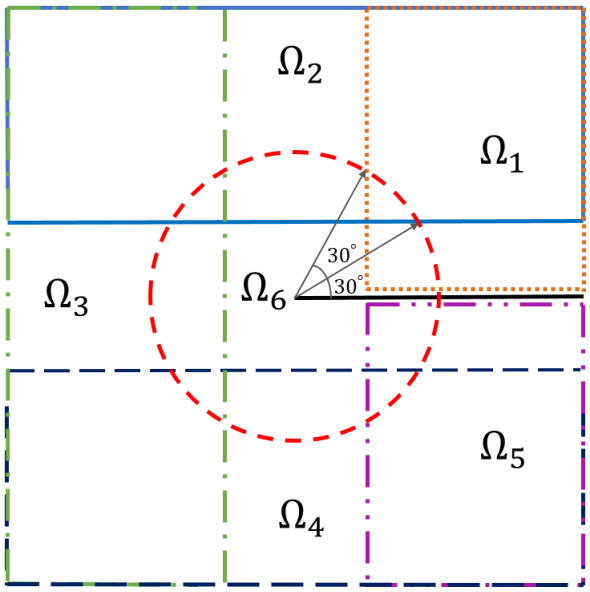

Figure 21: Cracked square domain with larger overlapping subdomains

5.3.1 Supplemental Subdomain Method

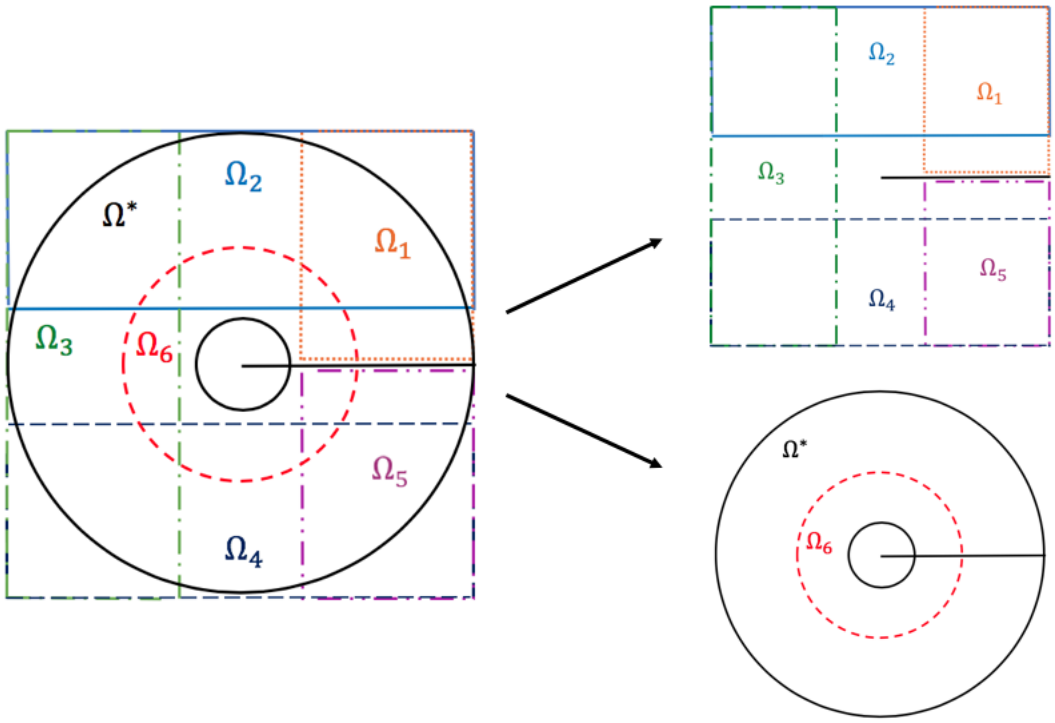

Figure 22: Cracked square domain with Supplemental Subdomain Method for b=0.4

In the master patch approach used IGA, calculations are carried out on the master patch no matter how large the physical domains are. Under the fixed degree of freedom, increasing overlapping parts of subdomains as long as it is not excessively large amount of increment nor do not contain singularities, does not drop the accuracy.

In the previous section, we could reduce the iteration numbers by one order of magnitude by increasing the overlapping parts of subdomains, and subdomains have almost a maximal amount of overlapping sizes. However, the number of iterations is still several hundred. In order to obtain a further reduction of the number of iterations, we can take advantage of the following known information of the given problem:

- At those points $p_i \in \Omega$ near $\partial\Omega$, the values $u(p_i)$ are influenced by the clamped BC.

- On a neighborhood of the crack singularity, $u(x,y) \approx \mathcal{O}(r^{1.5} \cdot (\sin(1.5\theta) - 3\sin(0.5\theta) + \cos(1.5\theta) - \cos(0.5\theta)))$.

For this end, we construct an additional subdomain with crack along $y = 0$:

$$\Omega^* = \{(x,y) : b^2 < x^2 + y^2 < 2^2\}, \quad 0.1 < b \leq 0.4$$

whose inner boundary is close to the crack tip and the outer boundary is as close as the physical boundary as shown in Figure 22. Since we use the master element approach, the number of basis functions to approximate the solution on Ω^* is independent of the size of Ω^*. Now we define a geometric mapping $G^* : \hat{\Omega} = [0,1] \times [0,1] \to \Omega^*$ as follows:

[G^***-mapping]:**.

$$G^* = \Big(x(\xi,\eta), y(\xi,\eta)\Big) = \Big((b + (2-b)\eta)\cos 2\pi(1-\xi), (b + (2-b)\eta)\sin 2\pi(1-\xi)\Big).$$

Then, we have

$$(G^*)^{-1}(x,y) \;\; = \;\; (\xi(x,y), \eta(x,y))$$

$$\xi(x,y) \;\; = \;\; \begin{cases} \dfrac{1}{2\pi}\cos^{-1}(\dfrac{x}{r}) & \text{if } y < 0 \\ 1 - \frac{1}{2\pi}\cos^{-1}(\frac{x}{r}) & \text{if } 0 \leq y \end{cases}, \qquad \eta(x,y) = \frac{(r - 0.5)}{1.5}$$

$$J(G^*) = \begin{bmatrix} 2\pi(0.5+1.5\eta)\sin 2\pi(1-\xi), & -2\pi(0.5+1.5\eta)\cos 2\pi(1-\xi) \\ 1.5\cos 2\pi(1-\xi), & 1.5\sin 2\pi(1-\xi) \end{bmatrix}$$

$$|J(G^*)| = 3\pi\Big(0.5+1.5\eta\Big)$$

Since the artificial boundary $r = 1$ of the subdomain Ω_6 locates inside the supplemental subdomain Ω^*, we could have more accurate BC along $r = 1$ than that of the previous section. Hence, for $j = 1, \ldots, 6$, we have more accurate u_j^k at fewer iterations.

The supplemental subdomain method for fourth-order problem on a square domain containing crack singularity is as follows:

Step I: (Initializing)

(i) Find approximate solutions $u_2^{(0)}$, $u_4^{(0)}$, and $u_6^{(0)}$ by taking initial guesses 0 on artificial boundaries of subdomains Ω_2, Ω_4, and Ω_6 using the k-refinement of B-spline basis functions with fixed p-degree ($p = 8$).

(ii) Taking the values of the approximate solution $u_2^{(0)}$, $u_4^{(0)}$, and $u_6^{(0)}$ as artificial boundary conditions along corresponding interfaces, find $u_1^{(0)}$, $u_3^{(0)}$, and $u_5^{(0)}$ solving each subproblem independently.

(iii) Find an approximate solution $u_*^{(0)}$ with respect to the following BC:

- along the outer boundary $r = 2$, $u_*(2, \theta)$ can be obtained by using $u_1^{(0)}$, $u_2^{(0)}$, $u_3^{(0)}$, $u_4^{(0)}$, and $u_5^{(0)}$.
- along the inner boundary $r = b$, $u_*(b, \theta) = b^{1.5} \cdot \Big(\sin(1.5\theta) - 3\sin(0.5\theta) +$

$$\cos(1.5\theta) - \cos(0.5\theta)\Big)$$

Step II: For $k \geq 0$, update approximate solutions on each subdomain in the following order:

(a) Find $u_6^{(k+1)}$ by updating boundary condition along $r = 1$ with $u_*^{(k)}$.

(b) Find $u_2^{(k+1)}$ by updating corresponding artificial boundary conditions with $u_1^{(k)}$, $u_3^{(k)}$, and $u_6^{(k+1)}$.

(c) Find $u_4^{(k+1)}$ by updating corresponding artificial boundary conditions with $u_3^{(k)}$, $u_5^{(k)}$, and $u_6^{(k+1)}$.

(d) Find $u_1^{(k+1)}$ by updating corresponding artificial boundary conditions with $u_2^{(k+1)}$ and $u_6^{(k+1)}$.

(e) Find $u_3^{(k+1)}$ by updating corresponding artificial boundary conditions with $u_2^{(k+1)}$, $u_4^{(k+1)}$, and $u_6^{(k+1)}$.

(f) Find $u_5^{(k+1)}$ by updating corresponding artificial boundary conditions with $u_4^{(k+1)}$ and $u_6^{(k+1)}$.

(g) Find $u_*^{(k+1)}$ with the following BC:

- use $u_1^{(k+1)}$, $u_2^{(k+1)}$, $u_3^{(k+1)}$, $u_4^{(k+1)}$, and $u_5^{(k+1)}$ along the outer boundary $r = 2$,
- use $u_6^{(k+1)}$ along the inner boundary $r = b$.

Step III: Update approximate solutions $u_6^{(k+1)}$ and $u_*^{(k+1)}$ by iterating them as follows:

1. Find $u_6^{(k+1)}$ by updating boundary condition along $r = 1$ with $u_*^{(k+1)}$.

Table 10: Relative errors in the maximum norm obtained by using Implicitly Enriched Schwarz Method and Supplemental Subdomain Method with b=0.4 for 2D fourth-order problem on a Cracked Square Domain with Larger Overlapping Size

Degree	DOF	Iterations	$\|RelErr\|_{Max}$
4	1844	10	3.52E-006
5	2082	14	3.10E-007
6	2334	17	3.73E-008
7	2600	19	7.07E-009
8	2880	19	6.40E-009

2. Find an approximate solution $u_*^{(k+1)}$ by using $u_*^{(previous)}$ along the boundary $r = 2$, and by using $u_6^{(previous)}$ along the boundary $r = b$. Apply Step III 2 times.

   Let $Error = \|u_{true} - u^{k+1}\|_{\infty,rel} = \dfrac{\|u_{true} - u^{k+1}\|_\infty}{\|u_{true}\|_\infty}$ be the relative error in the maximum norm and TOL is a given number.

   - if $Error \leq TOL$, then stop the iteration steps. An approximate solution is $u_h = u^{(k+1)}$.
   - if $Error \geq TOL$, go to Step II.

Numerical results obtained by Implicitly Enriched Schwarz Alternating method along with Supplemental Subdomain method are shown in Table 10. The results in Table 10 show that the Supplemental Subdomain method reduces the number of iterations by on order of magnitude without losing the accuracy.

Moreover, the results in Table 10 can be also compared with Table 4 of [5] that are obtained without using enrichment.

5.4 2D Fourth-order Problem on an L-shaped Domain

Example 9. Consider the fourth-order equation $\Delta^2 u = f$ on an L-shaped domain Ω containing corner singularity with **non-homogeneous** clamped boundary conditions whose true solution is constucted as follows:

$$u(r,\theta) = r^{\lambda}\Big(\sin(2\theta/3) - (1/3)\sin(2\theta)\Big)$$

where $\lambda = 1.54448373678$. Then

$$f(r,\theta) = -(6.583208901846914sin(2t) + 8.164403894229210sin((2t)/3))/r^{2.45552}$$

Note that $\lambda_1 = 1.54448373678$ and $\lambda_2 = 1.908529189846$ are the roots of the characteristic equation $sin^2((z-1)3\pi/2) - (z-1)^2 sin^2(3\pi/2) = 0$ [3].

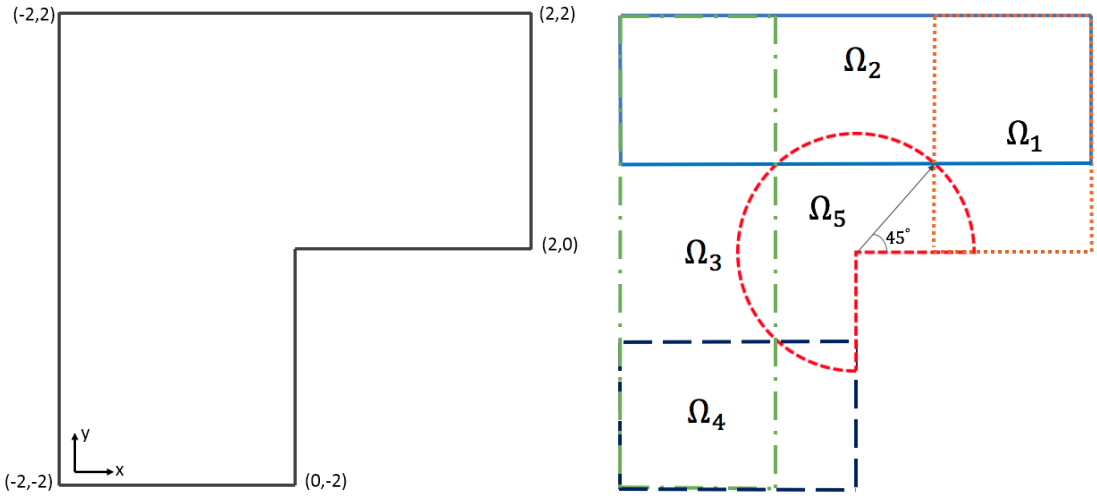

Figure 23: L-shaped domain and its domain decomposition

Geometric Mappings:

We partition the physical domain into five subdomains as shown in Figure 23.

[G_1-mapping]: $G_1 : \hat{\Omega} = [0,1] \times [0,1] \to \Omega_1 = [\frac{1}{\sqrt{2}}, 2] \times [0,2]$

$$G_1(\xi,\eta) = \begin{cases} x(\xi,\eta) = \frac{1}{\sqrt{2}} + (2 - \frac{1}{\sqrt{2}})\xi, \\ y(\xi,\eta) = 2\eta \end{cases}$$

where

$$J(G_1) = \begin{bmatrix} 2 - \frac{1}{\sqrt{2}} & 0 \\ 0 & 2 \end{bmatrix}, \quad |J(G_1)| = 4 - \frac{2}{\sqrt{2}}$$

[G_2-mapping]: $G_2 : \hat{\Omega} = [0,1] \times [0,1] \to \Omega_2 = [-2,2] \times [\frac{1}{\sqrt{2}}, 2]$

$$G_2(\xi,\eta) = \begin{cases} x(\xi,\eta) = -2 + 4\xi, \\ y(\xi,\eta) = \frac{1}{\sqrt{2}} + (2 - \frac{1}{\sqrt{2}})\eta \end{cases}$$

where

$$J(G_2) = \begin{bmatrix} 4 & 0 \\ 0 & 2 - \frac{1}{\sqrt{2}} \end{bmatrix}, \quad |J(G_2)| = 8 - \frac{4}{\sqrt{2}}$$

[G_3-mapping]: $G_3 : \hat{\Omega} = [0,1] \times [0,1] \to \Omega_3 = [-2, -\frac{1}{\sqrt{2}}] \times [-2,2]$

$$G_3(\xi,\eta) = \begin{cases} x(\xi,\eta) = -2 + (2 - \frac{1}{\sqrt{2}})\xi, \\ y(\xi,\eta) = -2 + 4\eta \end{cases}$$

where

$$J(G_3) = \begin{bmatrix} 2 - \frac{1}{\sqrt{2}} & 0 \\ 0 & 4 \end{bmatrix}, \quad |J(G_3)| = 8 - \frac{4}{\sqrt{2}}$$

[G_4-mapping]: $G_4 : \hat{\Omega} = [0,1] \times [0,1] \to \Omega_4 = [-2,0] \times [-2, -\frac{1}{\sqrt{2}}]$

$$G_4(\xi,\eta) = \begin{cases} x(\xi,\eta) = -2 + 2\xi, \\ y(\xi,\eta) = -2 + (2 - \frac{1}{\sqrt{2}})\eta \end{cases}$$

where

$$J(G_4) = \begin{bmatrix} 2 & 0 \\ 0 & 2 - \frac{1}{\sqrt{2}} \end{bmatrix}, \quad |J(G_4)| = 4 - \frac{2}{\sqrt{2}}$$

In order to generate re-entrant corner singularity in the radial direction of the subdomain Ω_5, we divide the subdomain into singular zone $\Omega_{5_{sing}} = \{(r,\theta) : 0 \leqslant r \leqslant 0.4, 0 \leqslant \theta \leqslant 1.5\pi\}$ and non-singular zone $\Omega_{5_{reg}} = \{(r,\theta) : 0.3 \leqslant r \leqslant 1, 0 \leqslant \theta \leqslant 1.5\pi\}$. We consider F-mapping to generate the corner singularity $r^{1.54448}$ on a singular zone $\Omega_{5_{sing}}$ and G_5-mapping to build regular basis functions on a regular zone $\Omega_{5_{reg}}$.

[G_5-mapping]: $G_5 : \hat{\Omega} = [0,1] \times [0,1] \longrightarrow \Omega_{5_{reg}} = \{(r,\theta) : 0.3 \leqslant r \leqslant 1, 0 \leqslant \theta \leqslant 1.5\pi\}$

$$G_5(\xi,\eta) = (0.3 + 0.7\eta)\Big(\cos 1.5\pi(1-\xi), \sin 1.5\pi(1-\xi)\Big) \tag{51}$$

where $\Omega_{5_{reg}}$ has a corner along the positive x-axis. Then we have

$$G_5^{-1}(x,y) = (\xi(x,y),\eta(x,y))$$

$$\xi(x,y) = \begin{cases} \frac{1}{1.5\pi}\cos^{-1}(\frac{x}{r}) - \frac{1}{3} & \text{if } y < 0 \\ 1.5\pi - \frac{1}{1.5\pi}\cos^{-1}(\frac{x}{r}) & \text{if } 0 \leq y \end{cases}, \qquad \eta(x,y) = \frac{(r-0.3)}{0.7}$$

$$J(G_5) = \begin{bmatrix} (1.5\pi(0.3+0.7\eta)\sin 1.5\pi(1-\xi), & -1.5\pi(0.3+0.7\eta)\cos 1.5\pi(1-\xi) \\ 0.7\cos 1.5\pi(1-\xi), & 0.7\sin 1.5\pi(1-\xi) \end{bmatrix}$$

$$|J(G_5)| = \frac{2.1}{2}\pi\Big(0.3+0.7\eta\Big)$$

[F-mapping]: Next, define a mapping to deal with singularities

$$F : \hat{\Omega} = [0,1]\times[0,1] \longrightarrow \Omega_{5_{sing}} = \{(r,\theta) : r \leqslant 0.4, 0 \leqslant \theta \leqslant 1.5\pi\}$$

that maps polynomials to singular functions as follows:

$$F(\xi,\eta) = 0.4\eta^2\Big(\cos 1.5\pi(1-\xi), \sin 1.5\pi(1-\xi)\Big)$$

Then

$$F^{-1}(x,y) = (\xi(x,y),\eta(x,y))$$

where

$$\xi(x,y) = \begin{cases} \frac{1}{1.5\pi}\cos^{-1}(\frac{x}{r}) - \frac{1}{3} & \text{if } y < 0 \\ 1.5\pi - \frac{1}{1.5\pi}\cos^{-1}(\frac{x}{r}) & \text{if } 0 \leq y \end{cases}, \qquad \eta(x,y) = \frac{r^{1/2}}{\sqrt{0.4}}$$

$$J(F) = \begin{bmatrix} 0.6\pi\eta^2 \sin 1.5\pi(1-\xi), & -0.6\pi\eta^2 \cos 1.5\pi(1-\xi) \\ 0.8\eta \cos 1.5\pi(1-\xi), & 0.8\eta \sin 1.5\pi(1-\xi) \end{bmatrix}, \quad |J(F)| = 0.48\pi\eta^3$$

Construction of Approximation Space

We assume for $p, q \geq 4, \hat{N}^1_{k,p+1}(\xi), \ldots, \hat{N}^4_{k,p+1}(\xi), k = 1, 2, \ldots, 2p+1$, and $\hat{M}^1_{l,q+1}(\eta), \ldots, \hat{M}^4_{l,q+1}(\eta), l = 1, 2, \ldots, 2p+1, l = 1, 2, \ldots, 2q+1$ are $\mathcal{C}^{p-1}$ and $\mathcal{C}^{q-1}$-continuous B-splines, respectively, corresponding to an open knot vectors

$$\begin{aligned} S^1_\xi = S^3_\xi = S^4_\xi &= \{\underbrace{0 \ldots 0}_{p+1}, 0.1, 0.2, \ldots, 0.8, 0.9, \underbrace{1 \cdots 1}_{p+1}\}. \\ S^2_\xi &= \{\underbrace{0 \ldots 0}_{p+1}, 0.05, 0.1, \ldots, 0.9, 0.95, \underbrace{1 \cdots 1}_{p+1}\}. \\ S^1_\eta = S^2_\eta = S^4_\eta &= \{\underbrace{0 \ldots 0}_{q+1}, 0.1, 0.2, \ldots, 0.8, 0.9, \underbrace{1 \cdots 1}_{q+1}\}. \\ S^3_\eta &= \{\underbrace{0 \ldots 0}_{q+1}, 0.05, 0.1, \ldots, 0.9, 0.95, \underbrace{1 \cdots 1}_{q+1}\}. \end{aligned}$$

Define basis functions on the reference domain for the corresponding geometric mappings as follows:

$$\hat{\mathcal{V}}_{G_1} = \{\hat{N}^1_{i,p+1}(\xi) \cdot \hat{M}^1_{j,q+1}(\eta) : i = 1, \ldots, p+10; j = 1, \cdots, q+10\}.$$

$$\hat{\mathcal{V}}_{G_2} = \{\hat{N}^2_{i,p+1}(\xi) \cdot \hat{M}^2_{j,q+1}(\eta) : i = 1, \ldots, p+20; j = 1, \cdots, q+10\}.$$

$$\hat{\mathcal{V}}_{G_3} = \{\hat{N}^3_{i,p+1}(\xi) \cdot \hat{M}^3_{j,q+1}(\eta) : i = 1, \ldots, p+10; j = 1, \cdots, q+20\}.$$

$$\hat{\mathcal{V}}_{G_4} = \{\hat{N}^4_{i,p+1}(\xi) \cdot \hat{M}^4_{j,q+1}(\eta) : i = 1, \ldots, p+10, j = 1, \cdots, q+10\}.$$

where the first two and the last two basis functions in the ξ- direction as well as in the η- direction on subdomains $\Omega_1, \cdots, \Omega_4$ are modified as defined in (26) to satisfy non-homogeneous artificial and clamped boundary conditions.

The corresponding approximation functions on the physical subspaces are as follows:

$$\begin{aligned}\mathcal{V}_{G_1} &= (\hat{\mathcal{V}}_{G_1} \circ G_1^{-1}) \qquad (52)\\ &= \left\{\left(\hat{N}^1_{i,p+1}(\xi)\cdot\hat{M}^1_{j,q+1}(\eta)\right)\circ G_1^{-1} : 1\le i\le p+10; 1\le j\le q+10\right\}\end{aligned}$$

$$\begin{aligned}\mathcal{V}_{G_2} &= (\hat{\mathcal{V}}_{G_2} \circ G_2^{-1}) \qquad (53)\\ &= \left\{\left(\hat{N}^2_{i,p+1}(\xi)\cdot\hat{M}^2_{j,q+1}(\eta)\right)\circ G_2^{-1} : 1\le i\le p+20; 1\le j\le q+10\right\}\end{aligned}$$

$$\begin{aligned}\mathcal{V}_{G_3} &= (\hat{\mathcal{V}}_{G_3} \circ G_3^{-1}) \qquad (54)\\ &= \left\{\left(\hat{N}^3_{i,p+1}(\xi)\cdot\hat{M}^3_{j,q+1}(\eta)\right)\circ G_3^{-1} : 1\le i\le p+10; 1\le j\le q+20\right\}\end{aligned}$$

$$\begin{aligned}\mathcal{V}_{G_4} &= (\hat{\mathcal{V}}_{G_4} \circ G_4{-}1) \qquad (55)\\ &= \left\{\left(\hat{N}^4_{i,p+1}(\xi)\cdot\hat{M}^4_{j,q+1}(\eta)\right)\circ G_4^{-1} : 1\le i\le p+10; 1\le j\le q+10\right\}\end{aligned}$$

We consider the following two open knot vectors that correspond to the k-refinement in the ξ- direction and η- direction, respectively, to construct B-spline basis functions on the subdomain Ω_5

$$\begin{aligned}S^5_\xi &= \{\underbrace{0\ldots0}_{p+1}, \frac{1}{12}, \frac{2}{12}, \ldots, \frac{10}{12}, \frac{11}{12}, \underbrace{1\cdots1}_{p+1}\}.\\ S^5_\eta &= \{\underbrace{0\ldots0}_{q+1}, 0.2, 0.4, 0.6, 0.8, \underbrace{1\cdots1}_{q+1}\}. \qquad (56)\end{aligned}$$

Then we have $\mathcal{C}^{p-1}$-continuous B-spline basis functions $\hat{N}^5_{k,p+1}(\xi), k = 1, 2, \ldots, p+12$ and $\mathcal{C}^{q-1}$-continuous B-splines basis functions $\hat{M}^5_{l,q+1}(\eta), l = 1, 2, \ldots, q+5$, respectively. We choose the corresponding approximation space on the reference domain

for the mapping G_5 as follows:

$$\hat{\mathcal{V}}_{G_5} = \{\hat{N}^5_{i,p+1}(\xi) \cdot \hat{M}^5_{j,q+1}(\eta) : i = 3, \ldots, p+10; j = 1, \cdots, q+5\}.$$

where the last two of $\hat{M}^5_{l,q+1}(\eta), l = 1, 2, \ldots, q+5$ are modified as defined in (26). We also remove the first two and the last two B-spline basis functions among $\hat{N}^5_{k,p+1}(\xi), k = 1, 2, \ldots, p+12$ so that the clamped boundary conditions are satisfied at both ends. We construct basis functions defined on $\Omega_{5_{reg}}$ by using the PU function ψ_L (43) as follows:

$$\begin{aligned} \mathcal{V}_{G_5} &= (\hat{\mathcal{V}}_{G_5} \circ G_5^{-1}) \cdot \psi_L \qquad (57) \\ &= \left\{ \left(\hat{N}^5_{i,p+1}(\xi) \cdot \hat{M}^6_{j,q+1}(\eta) \cdot \hat{\psi}_L(\xi, \eta) \right) \circ G_5^{-1} : 3 \leq i \leq p+10; 1 \leq j \leq q+5 \right\} \end{aligned}$$

We define basis functions on the reference domain for the mapping F as follows:

$$\hat{\mathcal{V}}_F = \{\hat{N}^5_{i,p+1}(\xi)(\eta\sqrt{0.4})^{(2*1.54448373678)} : i = 3, \ldots, p+10\}.$$

Then the set $\hat{\mathcal{V}}_F \circ F^{-1}$ generates the re-entrant corner singularity $r^{1.54448}$ in the radial direction where $r^2 = x^2 + y^2$. Note that the strength of singularity at the re-entrant corner of L-shaped domain is $\lambda = 1.544483736782464$. However, for simplicity, we choose $\lambda = 1.54448$ that makes the fourth derivatives of the true solution simple. Using the PU function ψ_R (42), we construct basis functions defined on $\Omega_{5_{sing}}$ as follows:

$$\begin{aligned} \mathcal{V}_F &= (\hat{\mathcal{V}}_F \circ F^{-1}) \cdot \psi_R \\ &= \left\{ \left(\hat{N}^5_{i,p+1}(\xi) \cdot (\eta\sqrt{0.4})^{(2*1.54448)} \cdot \hat{\psi}_R(\xi, \eta) \right) \circ F^{-1} : i = 3, \ldots, p+10 \right\} \qquad (58) \end{aligned}$$

Table 11: Relative errors in the maximum norm obtained by using Implicitly Enriched Schwarz Method for 2D fourth-order problem on an L-shaped Domain

Degree	DOF	Iterations	$\|RelErr\|_{Max}$
4	1228	1607	4.95E-005
5	1392	3199	1.96E-005
6	1566	2409	4.16E-006
7	1750	3730	3.35E-006
8	1944	3561	9.96E-007

Approximation space to deal with fourth-order partial differential equation on an L-shaped domain Ω is

$$\mathcal{V}_\Omega = \mathcal{V}_{G_1} \cup \mathcal{V}_{G_2} \cup \mathcal{V}_{G_3} \cup \mathcal{V}_{G_4} \cup \mathcal{V}_{G_5} \cup \mathcal{V}_F \tag{59}$$

The total number of the degree of freedom is

$$\begin{aligned} \text{card}(\mathcal{V}_\Omega) &= \text{card}(\mathcal{V}_{G_1}) + \cdots + \text{card}(\mathcal{V}_{G_5}) + \text{card}(\mathcal{V}_F) \\ &= \Big(2 * (p+10) * (q+10)\Big) + \Big((p+20) * (q+10)\Big) \\ &+ \Big((p+10) * (q+20)\Big) + \Big((p+8)(1+q+5)\Big) \end{aligned}$$

By increasing overlapping size with a new partition shown in Figure 24, we reduce the required number of iterations in Example 9. Table 12 shows that new partition provides almost same accuracy with less number of iterations.

In order to obtain a further reduction of the number of iterations, we can take advantage of the Supplemental Subdomain Method. We construct an additional subdomain:

$$\Omega^* = \{(x, y) : b^2 < x^2 + y^2 < 2^2\}, \quad 0.1 < b \leq 0.4$$

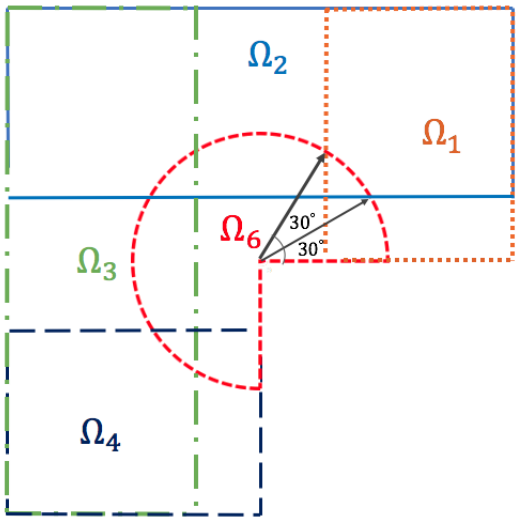

Figure 24: L-shaped domain with large overlapping subdomains

Table 12: Relative errors in the maximum norm obtained by using Implicitly Enriched Schwarz Method for 2D fourth-order problem on an L-shaped Domain with larger overlapping size

Degree	DOF	Iterations	$\|RelErr\|_{Max}$
4	1228	95	5.15E-005
5	1392	103	2.13E-005
6	1566	120	5.47E-006
7	1750	182	4.12E-006
8	1944	188	9.96E-007

whose inner boundary is close to the crack tip and the outer boundary is as close as the physical boundary as shown in Figure 22. Since we use the mater element approach, the number of basis functions to approximate the solution on Ω^* is independent of the size of Ω^*. Now we define a geometric mapping $G^* : \hat{\Omega} = [0,1] \times [0,1] \to \Omega^* = \{(r,\theta) : b \leqslant r \leqslant 2, 0 \leqslant \theta \leqslant 1.5\pi\}$ as follows:

[G^*-mapping]:

$$G^* = \Big(x(\xi,\eta), y(\xi,\eta)\Big) = \Big((b+(2-b)\eta)\cos 1.5\pi(1-\xi), (b+(2-b)\eta)\sin 1.5\pi(1-\xi)\Big).$$

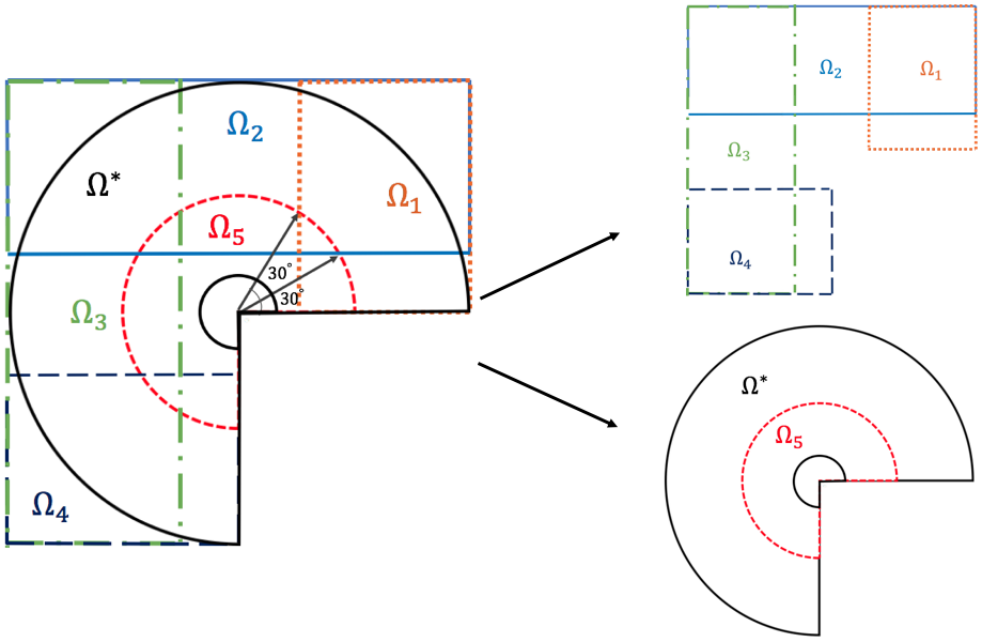

Figure 25: L-shaped domain with Supplemental Subdomain Method for b=0.4

Then, we have

$$(G^*)^{-1}(x,y) \;=\; (\xi(x,y),\eta(x,y))$$

$$\xi(x,y) \;=\; \begin{cases} \dfrac{1}{1.5\pi}\cos^{-1}(\dfrac{x}{r}) - \frac{1}{3} & \text{if } y<0 \\ 1.5\pi - \dfrac{1}{1.5\pi}\cos^{-1}(\dfrac{x}{r}) & \text{if } 0\le y \end{cases}, \qquad \eta(x,y) = \frac{(r-b)}{2-b}$$

$$J(G^*) \;=\; \begin{bmatrix} 1.5\pi(b+(2-b)\eta)\sin 1.5\pi(1-\xi), & -1.5\pi(b+(2-b)\eta)\cos 1.5\pi(1-\xi) \\ (2-b)\cos 1.5\pi(1-\xi), & (2-b)\sin 1.5\pi(1-\xi) \end{bmatrix}$$

$$|J(G^*)| = -\Big(1.5\pi(b-(b-2)\eta)(b-2)\Big)$$

Since the artificial boundary $r=1$ of the subdomain Ω_6 locates inside the supplemental subdomain Ω^*, we could have more accurate BC along $r=1$ than that of the

previous section. Hence, for $j = 1, \ldots, 5$, we have more accurate u_j^k at less iterations.

The supplemental subdomain method for fourth-order problem on an L-shaped domain containing crack singularity is as follows:

Step 0: (Initializing)

(i) Find an approximate solutions $u_2^{(0)}$, $u_4^{(0)}$, and $u_5^{(0)}$ by taking initial guesses 0 on artificial boundaries of subdomains Ω_2, Ω_4, and Ω_5 using the k-refinement of B-spline basis functions with fixed p-degree ($p = 8$).

(ii) Taking the values of the approximate solution $u_2^{(0)}$, $u_4^{(0)}$, and $u_5^{(0)}$ as artificial boundary conditions along corresponding interfaces, find $u_1^{(0)}$ and $u_3^{(0)}$ solving each subproblem independently.

(iii) Find an approximate solution $u_*^{(0)}$ with respect to the following BC:

- along the outer boundary $r = 2$, $u_*(2, \theta)$ can be obtained by using $u_1^{(0)}$, $u_2^{(0)}$, $u_3^{(0)}$, and $u_4^{(0)}$.
- along the inner boundary $r = b$, $u_*(b, \theta) = b^{1.54448373678}$

Step II: For $k \geq 0$, update approximate solutions on each subdomain in the following order:

(a) Find $u_5^{(k+1)}$ by updating boundary condition along $r = 1$ with $u_*^{(k)}$.

(b) Find $u_2^{(k+1)}$ by updating corresponding artificial boundary conditions with $u_1^{(k)}$, $u_3^{(k)}$, and $u_5^{(k+1)}$.

(c) Find $u_4^{(k+1)}$ by updating corresponding artificial boundary conditions with $u_3^{(k)}$ and $u_5^{(k+1)}$.

(d) Find $u_1^{(k+1)}$ by updating corresponding artificial boundary conditions with $u_2^{(k+1)}$ and $u_5^{(k+1)}$.

(e) Find $u_3^{(k+1)}$ by updating corresponding artificial boundary conditions with $u_2^{(k+1)}$, $u_4^{(k+1)}$, and $u_5^{(k+1)}$.

(f) (i) compute the stress intensity factors λ_1 and λ_2 by using $u_5^{(k+1)}$.

(ii) Find $u_*^{(k+1)}$ with the following BC:

- use $u_1^{(k+1)}$, $u_2^{(k+1)}$, $u_3^{(k+1)}$, and $u_4^{(k+1)}$ along the outer boundary $r = 2$,
- use $u_5^{(k+1)}$ along the inner boundary $r = b$.

Step III: Update approximate solutions $u_5^{(k+1)}$ and $u_*^{(k+1)}$ by iterating them as follows:

1. Find $u_5^{(k+1)}$ by updating boundary condition along $r = 1$ with $u_*^{(k+1)}$.

2. Find an approximate solution $u_*^{(k+1)}$ by using $u_*^{(previous)}$ along the boundary $r = 2$, and by using $u_5^{(previous)}$ along the boundary $r = b$. Apply Step III 2 times.

   Let $Error = \|u_{true} - u^{k+1}\|_{\infty,rel} = \dfrac{\|u_{true} - u^{k+1}\|_\infty}{\|u_{true}\|_\infty}$ be the relative error in the maximum norm and TOL is a given number.

   - if $Error \leq TOL$, then stop the iteration steps. An approximate solution is $u_h = u^{(k+1)}$.
   - if $Error \geq TOL$, go to Step II.

Numerical results obtained by Implicitly Enriched Schwarz Method along with Supplemental Subdomain method are shown in Table 13. Comparing Table 12 and Table

Table 13: Relative errors in the maximum norm obtained by using Implicitly Enriched Schwarz Method and Supplemental Subdomain Method with b=0.4 for 2D fourth-order problem on an L-shaped Domain with larger overlapping size

Degree	DOF	Iterations	$\|RelErr\|_{Max}$
4	1352	15	3.08E-005
5	1538	16	1.35E-005
6	1736	18	4.19E-006
7	1946	21	7.60E-007
8	2168	25	6.16E-008

13, we observe that the Supplemental Subdomain method makes for the iteration number to be reduced by one order of magnitude without sacrificing accuracy.

CHAPTER 6: CONCLUDING REMARKS AND FUTURE WORK

In this dissertation, in order to alleviate difficulties arising in analysis of fourth-order probems on non-convex polygonal domains, we introduced new numerical methods and justified them. First, we constructed the approximation spaces consisting of B-spline basis functions, whose members are smooth up to any desired order and are modified to satisfy complex boundary conditions. Secondly, we developed an implicit mapping method to introduce singular functions resembling the singularities due to the corners and/ or the cracks in the solution domains. Unlike the existing enrichment methods such as X-FEM, G-FEM, and PUFEM, our enrichment method does not require any extra precautions such as handling the singular integrals in calculation of stiffness matrices and load vectors. Thirdly, we combined Domain Decomposition method(DDM) with Isogeometric Analysis(IGA) to handle complexity of solution domains.

There has been limitations for solving fourth-order problems on non-convex domains with cracks or corners and complex boundaries since it is difficult to obtain $\mathcal{C}^1$-continuous global mapping from the reference domain onto such irregular shaped domains. Thus, we develop and implement Implicitly Enriched Schwarz Methods for localized treatments and less computational complexity. We tested the proposed method to the fourth-order problems on a triangle, a cracked disk, a cracked square, and an L-shaped domain.

Once we showed that we could get highly accurate approximate solutions for these fourth-order problems containing singularities, we took a step towards reducing the number of iterations required for the desired accuracy of the approximate solution. By increasing the overlapping parts of subdomains, we could reduce the iteration numbers by one order of magnitude, but it was still several hundred. In order to obtain a further reduction of the number of iterations, we introduced a Supplemental Subdomain Method and tested this method in fourth-order problems cracked square and L-shaped problems. This approach allowed us to derive same accuracy of results with much smaller number of iterations.

In the future research work, those methods proposed in this dissertation may be expanded to analyze thin plates (Kirchhoff-Love plate model) subjected to loadings and satisfying various boundary conditions such as clamped, simple support, free, and so on. Analysis of thin plates (i.e., finding stresses and deformations in the plates) under loading and boundary conditions requires solving fourth-order partial differential equations [14], [31]. Our proposed method for handling the fourth-order problems will be extended to the analysis of Kirchhoff-Love plates which have irregular shapes more and satisfy various combination of boundary conditions.

REFERENCES

[1] Bazilevs, Y., Beirao Da Veiga, L., Cottrell, J. A., Hughes, T. J. R., Sangalli, G., *Isogeometric analysis: Approximation, stability and error estimates for h-refined meshes*, Mathematical Models and Methods in Applied Sciences **16** (2006), 1031–1090.

[2] Bazilevs, Y., Calo, V., Cottrell, J., Evans, J., Hughes, T., Lipton, S., Scott, M., Sederberg, T., *Isogeometric analysis using T-splines*, Comput. Methods Appl. Mech. Engrg. 199 (5-8)(2010), 229-263.

[3] Blumn, H., and Rannacher, R., *On the Boundary Value Problem of the Biharmonic Operator on Domain with Angular Corners*, Math. Mech. in the Appl. Sci. 2 (1980) 556-581.

[4] Borden, M.J., Scott, M.A., Evans, J.A., Hughes, T.J. R., *Isogeometric finite element data structures based on Bézier extration of NURBS*, Int. J. Numer. Meth. Engng **87** (2010), 15-47.

[5] Brenner, S. C., Davis, C., Snug, L., *A two-level additive Schwarz domain decomposition pre-conditioned for a flat-top partition of unity method*, Meshfree Methods for Partial Differential Equations VIII, Lecture Notes in Computational Science and Engineering 115, M. Griebel and M. A. Schweitzer ed., Springer, 2017, pp. 1-16.

[6] Cai, X., *Overlapping Domain Decomposition Methods*, In: Langtangen H.P., Tveito A. (eds) Advanced Topics in Computational Partial Differential Equations. Lecture Notes in Computational Science and Engineering (2003), vol 33. Springer, Berlin, Heidelberg.

[7] Ciarlet, P. G., *Basic error estimates for elliptic problems*, Handbook of Numerical Analysis, Vol. II, North-Holland, 1991.

[8] Cottrell, J. A., Hughes, T. J. R., Bazilevs, Y., *Isogeometric analysis: Toward integration of CAD and FEM*, Wiley, 2009.

[9] De Luycker, E., Benson, D. J., Belytschko, T., Bazilevs, Y. and Hsu, M. C.,*X-FEM in isogeometric analysis for linear fracture mechanics*, International Journal for Numerical Methethod in Engrg **87** (2011), 541–565.

[10] Dorfel, M. R., Juttler, B., Simeon, B., *Adaptive isogeometric analysis by local h-refinement with T-splines*, Comput. Methods Appl. Mech. Engrg. 199 (5-8) (2010), 264-275.

[11] Evans, D.J., Li-Shan, K., Jian-Ping, S., and Yu-Ping, C., *The convergence rate of the Schwarz alternating procedure (I): For one-dimensional problems,* International Journal for Computer Mathematics20.2 (1986), pp. 157–170.

[12] Evans, D.J., Li-Shan, K., Jian-Ping, S., and Yu-Ping, C., *The convergence rate of the Schwarz alternating procedure (II): For two-dimensional problems,* International Journal for Computer Mathematics20.3–4 (1986), pp. 325–339.

[13] Li-Shan, K. and Evans, D.J., *The convergence rate of the Schwarz alternating procedure (V): For morethan two domains,* International Journal for Computer Mathematics23.3–4 (1988), pp. 295–313.

[14] Gdoutos, E. E., *Fracture Mechanics*, Criteria and Applications Kluwer Academic Publishers, 1990.

[15] Grisvard, P., *Elliptic Problems in Nonsmooth domains*, SIAM, 2011.

[16] Han, W., Meng, X., *Error analysis of reproducing kernel particle method*, Comput. Meth. Appl. Mech. Engrg. 190 (2001) 6157-6181.

[17] Hughes, T. J. R., Cottrell, J. A., Bazilevs, Y., *Isogeometric analysis: CAD, finite elements, NURBS, exact geometry and mesh refinement*, Comput. Meth. Appl. Mech. Engrg. **194** (2005), 4135–4195.

[18] Jeong, J. W., Oh, H.-S., Kang, S., Kim, H., *Mapping Techniques in Isogeometric Analysis for elliptic boundary value problems containing singularities,* Comput. Meth. Appl. Mech. Engrg. 254 (2013) 334-352.

[19] Kim, S., Oh, H.-S., Palta, B., Kim, H., *Implicitly enriched Galerkin methods for numerical solutions of fourth-order partial differential equations containing singularities*, Numer. Methods Partial Differential Eq., 34 (2018), 2079-2112.

[20] Kim, S., Palta, B., Oh, H.-S., *Extraction Formulas of Stress Intensity Factors for fourth-order problems containing crack singularities*, submitted(2018).

[21] Lions, Pierre-Louis, *On the Schwarz alternating method*, I. In First InternationalSymposium on Domain Decomposition Methods for Partial Differential Equations (Paris, 1987), pages 1–42. SIAM, Philadelphia, PA, 1988.

[22] Lions, Pierre-Louis, *On the Schwarz alternating method*, II. In Tony Chan, Roland Glowinski, Jacques Periaux, and Olof Widlund, editors, Domain Decomposition Methods. Second International Symposium on Domain Decomposition Methods, pages 47-70, Philadelphia, PA, 1989. SIAM. Los Angeles, California, January 14-16, 1988.

[23] Lions, Pierre-Louis, *On the Schwarz alternating method*, III. A variant fornonoverlapping subdomains. In Third International Symposium on Domain Decomposition Methods for Partial Differential Equations (Houston, TX, 1989), pages 202–223. SIAM, Philadelphia, PA, 1990.

[24] Mota, A., Tezaur, I. , Alleman ,C., *The Schwarz alternating method in solid mechanics* Computer Methods in Applied Mechanics and Engineering, ISSN: 0045-7825, Vol: 319, Page: 19-51.

[25] Melenk, J. M., Babuška, I., *The partition of unity finite element method:Theory and application* , Comput. Methods Appl. Mech. Engr. 139 (1996) 239-314.

[26] Mousavi, S.E., Sukumar, N., *Generalized Duffy Transformation for integrating vertex singularities*, Comput. Mech. (2010) 45:127-140.

[27] Oh, H.-S., Kim, J. G., Hong, W.T., *The Piecewise Polynomial Partition of Unity Shape Functions for the Generalized Finite Element Methods,* Comput. Methods Appl. Mech. Engrg. 197 (2008) 3702-3711.

[28] Oh, H.-S., Kim, H., Jeong, J. W., *Enriched isogeometric analysis of elliptic boundary value problems in domains with crackes and/or corners*, Int. J. Numer. Meth. Engrg 97 (2014) 149-180.

[29] Oliger, J., Shamarock, W., and Tang, W., *Convergence analysis and acceleration of the Schwarz alternating method*, Technical report, Stanford Univ., Center for Large Scale Scientific Computation, 1986.

[30] Piegl, L. and Tiller, W., *The NURBS Book,* 2nd ed, Springer, 1997.

[31] Reddy, J. N., *Theory and Analysis of Elastic Plates and Shells*, CRC Press, 1999.

[32] Rogers, D. F., *An introduction to NURBS*, Academic Press, 2001.

[33] Schwarz, H.A., *uber einen grenzbergang durch alternierendes verfahren*, Vierteljahrsschrift der Naturforschenden Gesellschaft in Zurich, 15: pp. 272-286, 1870.

[34] Xu, G., Mourrain, B., Duvigneau, R. , Galligo, A., *A New Error Assessment method in isogeometric analysis of 2D heat conduction problems*, Advanced Science Letters, American Scientific Publishers, 2012, 10(1) pp. 508-512.